**Distribution Agreement**

In presenting this thesis or dissertation as a partial fulfillment of the requirements for an advanced degree from Emory University, I hereby grant to Emory University and its agents the non-exclusive license to archive, make accessible, and display my thesis or dissertation in whole or in part in all forms of media, now or hereafter known, including display on the world wide web. I understand that I may select some access restrictions as part of the online submission of this thesis or dissertation. I retain all ownership rights to the copyright of the thesis or dissertation. I also retain the right to use in future works (such as articles or books) all or part of this thesis or dissertation.

Signature:

_____ _____

Joshua Wayne Francis Date

A Novel Role for the ARL2 GTPase in Cofactor-mediated Tubulin Folding

By

Joshua Wayne Francis
Doctor of Philosophy

Graduate Division of Biological and Biomedical Science
Biochemistry, Cell, and Developmental Biology

_____
Richard A. Kahn, Ph.D.
Advisor

_____
Graeme L. Conn, Ph.D.
Committee Member

_____
John R. Hepler, Ph.D.
Committee Member

_____
Eric A. Ortlund, Ph.D.
Committee Member

_____
Winfield S. Sale, Ph.D.
Committee Member

Accepted:

_____
Lisa A. Tedesco, Ph.D.
Dean of the James T. Laney School of Graduate Studies

_____
Date

# A Novel Role for the ARL2 GTPase in Cofactor-mediated Tubulin Folding

By

Joshua Wayne Francis
B. S., Kennesaw State University, 2011

Advisor: Richard A. Kahn, Ph.D.

An abstract of
a dissertation submitted to the Faculty of the
James T. Laney School of Graduate Studies of Emory University
in partial fulfillment of the requirements for the degree of
Doctor of Philosophy
in the Graduate Division of Biological and Biomedical Sciences
Biochemistry, Cell, and Developmental Biology
2017

## ABSTRACT

A Novel Role for the ARL2 GTPase in Cofactor-mediated Tubulin Folding

By Joshua W. Francis

Microtubules are dynamic, filamentous polymers composed of αβ-tubulin and are essential cytoskeletal components of all eukaryotic cells. Microtubules are required for a variety of essential cellular functions, including cell morphogenesis, motility, mitosis, intracellular traffic, and formation of both primary cilia and flagella. Highlighting their cellular importance, microtubules are also the primary target for many cancer therapeutics. In addition to post-translational modifications and selective expression of tubulin isotypes, the functions of microtubules are strongly regulated by the dynamics of the individual microtubule polymers. Dynamic instability is a term that describes the process by which microtubules stochastically alternate between polymerization and depolymerization, which is largely controlled by the binding and hydrolysis of tubulin-bound guanine nucleotide. Despite our understanding of the many levels of microtubule regulation, one fundamental aspect of microtubule biology remains poorly understood: the biogenesis and assembly of the αβ-tubulin heterodimer. Tubulin is composed of α- and β-subunits, whose folding and assembly require a set of tubulin-specific chaperones, or cofactors, that form a series of folding intermediates in the eventual production of native αβ-tubulin dimer. Described herein is a novel role for the small, regulatory GTPase ARL2 in the cofactor-mediated tubulin folding and heterodimer assembly pathway. ARL2 is shown to strongly interact with the tubulin-specific chaperone D (TBCD), forming a complex that I argue is integral to the tubulin folding pathway. In contrast to previous models, I also propose that the cycling of guanine nucleotides on ARL2 is a key regulatory mechanism that is required for the folding and formation of native αβ-tubulin heterodimers.

# A Novel Role for the ARL2 GTPase in Cofactor-mediated Tubulin Folding

By

Joshua Wayne Francis
B. S., Kennesaw State University, 2011

Advisor: Richard A. Kahn, Ph.D.

A dissertation submitted to the Faculty of the
James T. Laney School of Graduate Studies of Emory University
in partial fulfillment of the requirements for the degree of
Doctor of Philosophy
in the Graduate Division of Biological and Biomedical Sciences
Biochemistry, Cell, and Developmental Biology
2017

**TABLE OF CONTENTS**

## Abbreviations

| | |
|---|---|
| ADP | Adenine diphosphate |
| ANT1 | Adenine nucleotide transporter 1 |
| ARL2 | ADP-ribosylation factor-like 2; or ARF-like 2 |
| ATP | Adenine triphosphate |
| BART | Binder of ARL2 |
| BN-PAGE | Blue native polyacrylamide gel electrophoresis |
| CCT | Cytosolic chaperonin containing T-complex polypeptide 1 |
| Dscam | Down syndrome cell adhesion molecule |
| E-site | Exchangeable site (β-tubulin) |
| GAP | GTPase activating protein |
| GDP | Guanosine diphosphate |
| GEF | Guanine-nucleotide exchange factor |
| Gpp(NH)p | 5'-Guanylyl [β, γ-imido]triphosphate |
| GST | Glutahione S-transferase |
| GTP | Guanosine triphosphate |
| GTPγS | Guanosine 5'-3-*O*-(thio)triphosphate |
| HDX-MS | Hydrogen/deuterium exchange coupled with mass spectrometry |
| HEK | Human embryonic kidney |
| Mant | Methylmanthraniloyl |

| | |
|---|---|
| MAPs | Microtubule-associated proteins |
| miRNA | microRNA |
| PD | Pulldown |
| PTMs | Post-translational modifications |
| SMA | Spinal muscular atrophy |
| STAT3 | Signal transducer and activator of transcription 3 |
| TBCA | Tubulin-specific chaperone A; also termed Cofactor A |
| TBCB | Tubulin-specific chaperone B; also termed Cofactor B |
| TBCC | Tubulin-specific chaperone C; also termed Cofactor C |
| TBCD | Tubulin-specific chaperone D; also termed Cofactor D |
| TBCE | Tubulin-specific chaperone E; also termed Cofactor E |
| TEV | Tobacco etch virus |
| TriC | TCP-1 ring complex (same as CCT) |
| N-site | Nonexchangeable site (α-tubulin) |

# CHAPTER 1

## Introduction

**Microtubules**

Microtubules are dynamic, filamentous polymers that are essential ultrastructural components of almost all eukaryotic cells. Though first observed by electron microscopy in the early 1950's (Manton and Clarke, 1952; Fawcett and Porter, 1954), it was a decade later that the term "microtubule" was coined (Slautterback, 1963) and these structures thought to be a ubiquitous component of the eukaryotic cytoskeleton. In the last half-century, microtubules have been shown to be required for a diverse set of essential cellular functions, including cell morphogenesis, motility, division, intracellular traffic, and ciliogenesis. To accomplish these tasks, microtubules form specific assemblies inside the cell, such as the stable axonemes of cilia/flagella. They also form more transient structures, such as the mitotic spindle of a dividing cell, where chromosome positioning and segregation are largely controlled by microtubule polymerization and depolymerization, respectively (Rieder and Salmon, 1994; Desai and Mitchison, 1997; McIntosh et al., 2010). Highlighting this critical role, the disruption of microtubule dynamics has been the primary target of many anticancer therapeutics, including the taxanes and Vinca alkaloids (Jordan and Wilson, 2004; Dumontet and Jordan, 2010).

Microtubules are polymers of tubulin, a protein heterodimer comprised of α- and β-tubulin subunits. α- and β-tubulin are each ~55 kDa (forming a ~110 kDa dimer) and share 40% sequence identity. Both tubulins are also highly conserved throughout eukaryotic evolution, highlighting their essential nature. The αβ-tubulin dimers assemble in a head-to-tail fashion to form individual protofilaments that interact laterally to create a hollow, cylindrical structure. The αβ-tubulin dimer was first purified by its ability to bind colchicine, another antimitotic drug, and shown to have two kinetically distinct sites of guanine-nucleotide binding (Weisenberg et al., 1968). The nonexchangeable site (N-site) is located on the α-subunit and is buried within the binding interface between α- and β-tubulin (Nogales et al., 1998). The N-site is constitutively bound by GTP and provides structural stability to the tubulin dimer (Menendez et al., 1998). The exchangeable site (E-site), located on the β-subunit, is exposed to solvent in the unpolymerized dimer (Nogales, 2000)

and freely exchanges GTP for bound GDP, readying the tubulin dimer for assembly into a growing microtubule. The E-site is also exposed at the plus end of polymerized microtubules (Mitchison, 1993), though the bound GTP becomes hydrolyzed as polymerization progresses (Weisenberg et al., 1976; David-Pfeuty et al., 1977; MacNeal and Purich, 1978).

The exchange and hydrolysis of guanine nucleotides on β-tubulin is the driving force behind a fundamental aspect of microtubule function called dynamic instability, an intrinsic mechanism by which microtubules stochastically alternate between periods of polymerization and depolymerization (Mitchison and Kirschner, 1984). There are a multitude of factors known to regulate the dynamics and/or function of microtubules. For example, there are many microtubule-associated proteins (MAPs) that interact with polymerized microtubules to regulate their stability, connect them with other cellular structures, or generate forces (*i.e.*, motor proteins). There are also proteins that interact with unpolymerized tubulin dimers in order to influence microtubule dynamics. For example, stathmin proteins inhibit microtubule polymerization by binding and sequestering αβ-tubulin (Curmi et al., 1997; Jourdain et al., 1997). Another layer of microtubule regulation originates from the composition of the microtubules themselves. The expression of multiple tubulin isotypes (nine genes each for mammalian α- and β-tubulin) and a host of post-translational modifications (PTMs) gives rise to a highly complex internal programming system referred to as the "tubulin code." The large number of permutations of different tubulin isotypes and PTM combinations enables microtubule function to be fine-tuned for particular cell types or even for specific localized activities within a cell, as nicely described in detail in a recent review (Gadadhar et al., 2017). Despite extensive knowledge of both extrinsic and intrinsic facets of regulation of microtubule dynamics, however, relatively little is known regarding one fundamental aspect of microtubule biology: the biogenesis and assembly of the αβ-tubulin heterodimer.

**Tubulin Folding**

Much of what we understand about the process of tubulin folding, *i.e.*, the formation of nascent αβ-tubulin heterodimers, comes from the pioneering work of Nicholas Cowan (NYU Medical Center), who developed a series of biochemical studies using *in vitro* tubulin folding assays (Cowan, 1998) to generate the first model of tubulin folding and dimer formation that has been the prevailing (and only) model for close to two decades (Figure 1-1). In fact, it has only been within the last couple of years that any challenges to the Cowan model have been proposed, as discussed in detail in the following chapters. To begin the process of tubulin folding, newly synthesized α- and β-tubulin polypeptides first interact with the heterohexameric chaperone prefoldin (Vainberg et al., 1998). Prefoldin then transfers the tubulin subunits to the Cytosolic Chaperonin containing T-complex Polypeptide 1 (CCT); also termed TCP-1 Ring Complex (TriC). CCT is a large, multi-subunit complex that, like all chaperonins, relies on the cycling and hydrolysis of ATP to regulate the interaction, folding and release of its substrate proteins (Valpuesta et al., 2002; Spiess et al., 2004), including actin (Gao et al., 1992). Unlike actin, however, interaction with CCT alone is insufficient for formation of the native tubulin proteins (Gao et al., 1993). Instead, α- and β-tubulin interact with several cofactors, termed tubulin-specific chaperones A-E (TBCA-E; also termed Cofactors A-E), which form a series of folding intermediates that facilitate the assembly and production of native αβ-tubulin heterodimers (Tian et al., 1996; Lewis et al., 1997). According to the Cowan model, after interaction with CCT, α- and β-tubulin are transferred to the cofactors TBCB and TBCA, respectively (forming dimers TBCB/α-tubulin and TBCA/β-tubulin). Free exchange then enables transfer to TBCE and TBCD, resulting in formation of TBCE/α-tubulin and TBCD/β-tubulin complexes. These complexes are then thought to associate, bringing together the tubulin subunits in the penultimate tetrameric complex in αβ-tubulin dimer production (*i.e.*, TBCD/TBCE/α-tubulin/β-tubulin). TBCC then binds to form

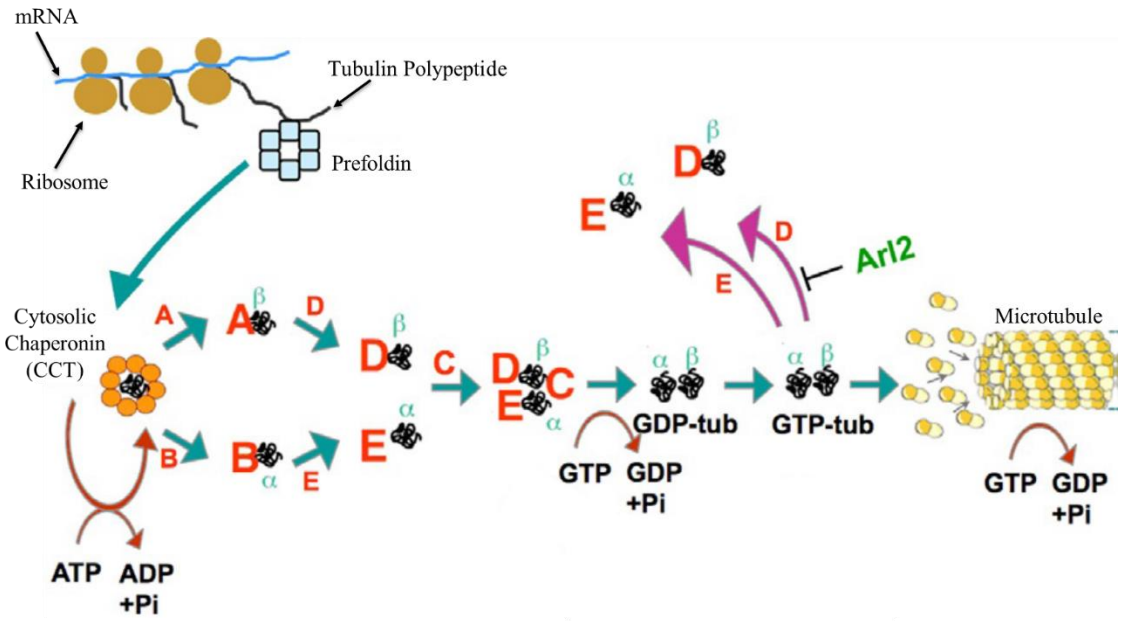


**Figure 1-1. The Cowan model for cofactor-mediated tubulin folding and αβ-tubulin heterodimer assembly (Tian and Cowan, 2013).** Newly translated α- and β-tubulin polypeptides first interact with the chaperone prefoldin, which transfers the tubulin subunits to the cytosolic chaperonin (CCT). Multiple rounds of ATP hydrolysis produce quasi-native conformations of α- and β-tubulin, which then interact with TBCB and TBCA, respectively. From here, the tubulins freely exchange to form the TBCD/β-tubulin and TBCE/α-tubulin dimers, which associate to form the penultimate complex in tubulin dimer production. Finally, TBCC associates with this complex and stimulates hydrolysis of GTP at the E-site (on β-tubulin), resulting in dissociation of the cofactors and production of nascent αβ-tubulin heterodimers. After exchange of GTP for bound GDP, the tubulin dimers are competent for incorporation into a polymerizing microtubule. TBCD and TBCE can also disrupt this pathway by interacting with, and dissociating, the native heterodimer (purple arrows), though the regulatory GTPase ARL2 inhibits this activity for TBCD. (Reprinted with minor adaptation from Methods in Cell Biology, Vol. 115, Guoling Tian and Nicholas J. Cowan, Tubulin-Specific Chaperones: Components of a Molecular Machine That Assembles the α/β Heterodimer, Pages 155-171, Copyright 2013, with permission from Elsevier (License No. 4103130621838)).

the pentameric complex, resulting in disassembly of the cofactors and release of the native αβ-tubulin heterodimer. Cowan's work and subsequent model suggest that TBCC, along with the other cofactors, act as a GTPase activating protein (GAP) for β-tubulin, and hydrolysis of the E-site GTP stimulates dissociation of the cofactors (Tian et al., 1999). Although consistent with earlier studies showing a requirement for GTP hydrolysis in tubulin dimer formation (Fontalba et al., 1993), challenges to the specificity of the TBCC-stimulated GAP activity have been proposed by more recent work (Mori and Toda, 2013; Nithianantham et al., 2015), and will be discussed in more detail in the following chapters.

Cowan's model also accounts for the possible reversal of dimer formation, in a process he terms the "back-reaction." Through *in vitro* and *in vivo* studies, TBCD and TBCE have been suggested to play an inhibitory role in tubulin dimer formation and microtubule polymerization by interacting with, and dissociating, the αβ-dimer (Bhamidipati et al., 2000; Martin et al., 2000; Kortazar et al., 2006; Kortazar et al., 2007; Tian et al., 2010; Serna et al., 2015). It is also proposed that the tubulin dissociation activity of TBCD can be modulated via interaction with the small, regulatory GTPase ADP-ribosylation factor-like 2 (ARL2), which is assumed to compete for TBCD binding with β-tubulin (Bhamidipati et al., 2000; Tian et al., 2010). However, this putative tubulin destruction pathway is based largely on overexpression studies, with little direct evidence of such a process occurring naturally in cells. Furthermore, the primary focus of this dissertation is the study of the novel, trimeric complex TBCD/ARL2/β-tubulin, the existence of which directly challenges tenets of the TBCD-mediated tubulin destruction hypothesis. Additionally, based on the purification and characterization of this complex (described in detail in the following chapters), I propose a more integral role for ARL2 in the tubulin biogenesis pathway than that portrayed by the Cowan model.

**Tubulin-specific Chaperone D (TBCD)**

The earliest evidence of TBCD involvement in aspects of microtubule regulation came from screens in the model genetic system *S. cerevisiae*. Screens for altered sensitivity to benomyl, a microtubule destabilizing drug, identified mutations in the budding yeast ortholog of TBCD, *CIN1* (Hoyt et al., 1990; Stearns et al., 1990). Similar screens for microtubule and cell cycle defects in other model organisms later identified mutations in *Alp1* (Hirata et al., 1998; Radcliffe et al., 1999) and *TTN1* (Liu and Meinke, 1998), the TBCD orthologs in *S. pombe* and *A. thaliana*, respectively. The essential role of TBCD in tubulin/microtubule dynamics was confirmed when the first mammalian ortholog was discovered by Cowan and colleagues through purification of its *in vitro* tubulin folding activity (*i.e.*, interaction with β-tubulin) from bovine testis lysates (Tian et al., 1996). Since its initial discovery, TBCD has been studied using a variety of approaches and shown to have several cellular functions distinct from its tubulin folding activity.

TBCD localizes to centrosomes where it recruits other centrosomal proteins, including the γ-tubulin ring complex that is required for nucleation of microtubule growth (Cunningham and Kahn, 2008). It is even suggested that TBCD plays a role in centriologenesis itself (Fanarraga et al., 2010). Several studies also implicate TBCD in different mitotic processes. Knockdown of TBCD in HeLa cells causes centrosome fragmentation and multipolar mitotic spindles (Cunningham and Kahn, 2008). TBCD also localizes to the midbody during late-stage cytokinesis, where it is ostensibly required for proper abscission of dividing cells (Fanarraga et al., 2010). In *S. pombe*, mutations in the TBCD ortholog *Alp1* lead to chromosome segregation defects, resulting from perturbed kinetochore-microtubule interactions (Fedyanina et al., 2006). These examples serve to highlight the essential role of TBCD in mitosis and cell cycle progression, though these activities are perhaps distinct from its role in tubulin folding.

In a recent study focusing on mechanisms of neuronal morphogenesis, mutations in TBCD were shown to disrupt the microtubule network in *Drosophila* projection neurons, resulting in reduced axonal branching and neuron degradation (Okumura et al., 2015). The same study also

showed a direct interaction between TBCD and the intracellular domain of the neuronal receptor Down syndrome cell adhesion molecule (Dscam), which is involved in the regulation of neuronal development (Hattori et al., 2008). Other reports have provided additional links between TBCD and activities at the cell surface. In endothelial cells, laminar shear stress appears to directly influence TBCD mRNA and protein expression levels (Schubert et al., 2000). TBCD is also important for proper cell-cell adhesion of epithelial cells, where it regulates the assembly/disassembly of the apical junctional complex (Shultz et al., 2008). These studies demonstrate a potential for TBCD to function as a bridge between microtubules and activities at the cell surface, again seemingly independent of its role in tubulin folding.

Based upon its size (133 kDa) and predicted, predominantly modular alpha-helical, structure (Grynberg et al., 2003), TBCD is often presumed to serve a scaffolding role for assembly of the tubulin subunits and other cofactors in the tubulin folding pathway. It has also been proposed to act as a scaffold during ciliogenesis, recruiting proteins to the basal bodies of developing cilia (Fanarraga et al., 2010). Therefore, if the predominant cellular role of TBCD is to function as a scaffold for assembly or recruitment of other proteins, then identifying and investigating binding partners is of particular importance to understanding the biological mechanisms of TBCD cellular activities. Aside from the other TBCs and tubulin, the first binding partner identified for TBCD was the GTPase ARL2 (Bhamidipati et al., 2000).

**ARF-like 2 (ARL2)**

While TBCD was being identified as a central player in the regulation of microtubules and cell cycle-dependent processes, strong links were also consistently being found with the regulatory GTPase ARL2. The same genetic screens that identified mutations in TBCD orthologs also identified mutations in *CIN4 (Hoyt et al., 1990; Stearns et al., 1990)*, *Alp41* (Hirata et al., 1998; Radcliffe et al., 1999), and *TTN5* (Liu and Meinke, 1998), the orthologs of ARL2 in *S. cerevisiae*, *S. pombe*, and *A. thaliana*, respectively. Studies using other model genetic systems found similar

microtubule-related roles for the orthologs of ARL2 in *C. elegans* (Antoshechkin and Han, 2002), *T. brucei* (Price et al., 2010), and *D. melanogaster* (Chen et al., 2016). Collectively, these data provide compelling evidence for the involvement of ARL2 in microtubule and/or tubulin-related processes and for a closer linkage between ARL2 and TBCD. However, one aspect of ARL2 biology that makes its study more complicated, though undoubtedly more interesting and important, is the increasing evidence that this single GTPase is required for the proper regulation of several other essential cellular functions (Francis et al., 2016).

ARL2 is highly conserved across eukaryotic evolution and is predicted to have existed in the last eukaryotic common ancestor (Li et al., 2004). It is also ubiquitous among eukaryotes, and has been proven essential to all organisms in which it has been studied, with the exception of *S. cerevisiae*. ARL2 is a member of the ARF family, within the RAS superfamily, of regulatory GTPases. The members of the RAS superfamily are predominantly small (~20 kDa) proteins that consist of a single GTPase domain of ~180 amino acids. Despite their size and relatively simple domain composition, the members of the RAS superfamily are found in the midst of almost every essential cellular process. Increasing evidence also suggests that even a single one of these GTPases (*e.g.*, ARL2) can be involved in the regulation of multiple cellular pathways (Francis et al., 2016).

The cellular activity of regulatory GTPases, like ARL2, is predominantly controlled by the binding of guanine nucleotides. Often referred to as “molecular switches,” the binding of GTP or GDP induces different conformational states that result in the GTPase being active or inactive, respectively. Additional cellular factors, termed guanine-nucleotide exchange factors (GEFs) and GTPase activating proteins (GAPs), regulate the switching between the different nucleotide-bound states and provide a means for cells to regulate GTPase activity. GEFs facilitate the exchange of GTP for bound GDP, thereby switching the GTPase to the active (“on”) state. The active, GTP-bound, conformation is then capable of interacting with effector proteins that mediate downstream cellular responses. GAPs function by stimulating GTP hydrolysis, effectively turning “off” the GTPase. A single GTPase can have several different GAPs and GEFs, providing a means by which

cells can spatially and temporally fine-tune the activity of a particular GTPase. The GTPase cycle can also be artificially manipulated through point mutations to provide us with tools for studying GTPase cellular activities. The dominant-active mutant (Q70L for ARL2) locks the GTPase into the active state by mutating the residue required for GTP hydrolysis. The dominant-inactive mutant (T30N for ARL2) decreases the overall affinity for guanine nucleotide and causes a dominant effect by binding and sequestering GEFs, thus preventing the activation of even the endogenous GTPase. The use of these tools has proven invaluable for the identification and characterization of the signaling pathways of many GTPases, including ARL2 (Francis, et al., 2016).

In addition to influencing its GTPase cycle, cells also control ARL2 cellular activity through direct regulation of its expression levels. Several studies have identified microRNAs (miRNAs) that target ARL2, leading to decreased cellular mRNA and protein levels. In rat cardiomyocytes, miRNA-15b regulates ATP levels and mitochondria morphology (Nishi et al., 2010). ARL2-targeting miRNAs also influence cell cycle progression in many cultured cell types (Wang et al., 2011), including neural progenitor cells (Zhou et al., 2013). Additionally, miRNAs that reduce ARL2 expression levels influence the progression of human colon and cervical cancers (Long et al., 2015; Peng et al., 2017). ARL2 expression levels have also been correlated with aggressivity and chemosensitivity of human breast cancer cells (Beghin et al., 2007; Beghin et al., 2008; Beghin et al., 2009), though it is not currently known if miRNAs directly modulate ARL2 levels in these cells.

A growing body of evidence has begun to outline roles for ARL2 in regulating several aspects of mitochondrial biology. Characterization of the first ARL2-specific antibody revealed its localization to mitochondria (Sharer et al., 2002), where it was also shown to form a complex with its effector Binder of ARL2 (BART) and the mitochondrial ADP/ATP transporter, adenine nucleotide translocase 1 (ANT1). The same study showed that deletion of ANT1 resulted in increased localization, but not overall cellular abundance, of ARL2 to mitochondria. A more recent study from our lab also demonstrated an increase in levels of mitochondrial ARL2 as a result of

several metabolic stressors, as well as in cells with a perturbed mitochondrial fusion pathway (Newman et al., 2017). Underscoring its mitochondrial importance, knockdown of ARL2 results in mitochondrial fragmentation, decreased mitochondrial motility, and a reduction in cellular ATP levels (Newman et al., 2014). Expression of the dominant-inactive ARL2[T30N] phenocopies ARL2 knockdown, with the exception of the drop in ATP levels, perhaps indicating mitochondrial actions of ARL2 occur via two distinct, though related, pathways.

In addition to mitochondria, ARL2 also localizes to the nucleus, where a single study reports its involvement in the nuclear retention of the signal transducer and activator of transcription 3 (STAT3), a transcriptional activator (Muromoto et al., 2008). ARL2 is also found at centrosomes along with TBCD (Zhou et al., 2006; Cunningham and Kahn, 2008), though it is uncertain whether these proteins are in direct interaction at this site. Despite its presence at several cellular locations, however, the vast majority (estimated at ~90%) of ARL2 is found in cytosol. Unlike the other ARF family members, which predominantly exist as monomers, ARL2 fractionates as a ~200 kDa species from cell and tissue lysates (Shern et al., 2003; Francis et al., 2017), where it is found in a complex with TBCD (as discussed in detail in Chapter 2). Due to their interaction in cytosol, and close association at centrosomes, it is perhaps unsurprising that many ARL2 phenotypes closely resemble those seen in studies of TBCD. For example, expression of the dominant-active ARL2[Q70L] (Zhou et al., 2006) or overexpression of TBCD (Bhamidipati et al., 2000; Cunningham and Kahn, 2008) both result in the loss of polymerized microtubules. ARL2[Q70L] expression also results in centrosome fragmentation and cell cycle arrest (Zhou et al., 2006), similar to siRNA-mediated knockdown of TBCD (Cunningham and Kahn, 2008). In addition to the several genetic screens implicating both ARL2 and TBCD in microtubule and cell cycle-dependent processes, these cell-based studies serve to further highlight the strong link between the cellular functions of these two proteins.

**TBCs in Disease**

Due to the essential nature of proper αβ-tubulin folding and dimer assembly, and the critical roles that the tubulin-specific chaperones play in this pathway, it is unsurprising that each of these cofactors have been individually studied and shown to be important for a variety of cellular processes, with strong links to several disease states. For example, TBCA expression is essential for viability of cultured mammalian cells, with knockdown resulting in decreased tubulin levels and cell cycle arrest (Nolasco et al., 2005). TBCA expression levels, in both mice and cultured cells, have also been correlated with progression and metastasis of a renal cell carcinoma (Zhang et al., 2013). TBCC levels in human breast cancer cells have been implicated in influencing tumor growth and sensitivity to chemotherapeutics (Hage-Sleiman et al., 2010; Hage-Sleiman et al., 2011).

Though cancer is perhaps the most obvious disease relevance for the tubulin cofactors, based upon the involvement of microtubules in mitosis and cell cycle progression, the most common phenotypes resulting from aberrant cofactor expression or function are neurological in nature. The most striking example of this, and the most highly reported, is the connection between neurological disorders and mutations in TBCE. Several mutations in TBCE have been linked to disorders characterized by congenital hypoparathyroidism, mental retardation, facial dysmorphism, and extreme growth failure, such as Sanjad-Sakadi Syndrome (Hellani et al., 2004; Tian et al., 2006; Padidela et al., 2009) and the related Kenney-Caffey Syndrome (Parvari et al., 2002). TBCE mutations also result in a progressive motor neuronopathy in mice (Bommel et al., 2002; Martin et al., 2002), which appears to be a result of reduced Golgi-anchored axonal microtubules that is caused by decreased localization of TBCE to the *cis*-Golgi (Schaefer et al., 2007). Additionally, TBCE is required for the proper development and function of neuromuscular synapses in *Drosophila* (Jin et al., 2009). In human patients, mutations in TBCE cause the motor neuron disease spinal muscular atrophy (SMA), as well as early-onset encephalopathy (Sferra et al., 2016). Although TBCE has been the most well-documented cofactor involved in neurological disorder, a

spate of recent studies within the last couple years have also linked several mutations in TBCD with early-onset encephalopathy (Edvardson et al., 2016; Flex et al., 2016; Miyake et al., 2016), infantile atypical SMA (Ikeda et al., 2016), and intractable seizures (Pode-Shakked et al., 2017). The highly documented disease relevance of the TBCs, as well as ARL2, demonstrates that the continued study of these proteins will not only advance our understanding of essential, basic cellular processes, but will also provide insight into the molecular mechanisms underlying several human pathologies.

**Focus of this Dissertation**

The aim of this current project is to specifically investigate the functional significance of interaction between TBCD and ARL2, particularly as it applies to tubulin biogenesis. According to the Cowan model (Figure 1-1), the main role for ARL2 in the tubulin folding pathway is as an inhibitor of TBCD-mediated tubulin destruction (*i.e.*, αβ-dimer dissociation; Bhamidipati et al., 2000). More specifically, this model suggests that ARL2 and β-tubulin compete for binding to TBCD. However, recent evidence has begun to challenge this well-established model for tubulin folding. Bacterial expression of yeast orthologs showed that a complex of TBCD, TBCE, and ARL2 was the minimal stable cofactor complex capable of interacting with purified αβ-tubulin (Nithianantham et al., 2015). My work using mammalian cells and tissues has shown that the predominant species of ARL2 and TBCD appears to be a trimeric complex of TBCD/ARL2/β-tubulin (Francis et al., 2017). Based on this and the other work described in the following chapters, I propose that the TBCD/ARL2/β-tubulin complex is an essential intermediate complex in the tubulin folding pathway, and that the exchange and hydrolysis of GTP on ARL2 is a regulatory mechanism in the progression of β-tubulin folding, assembly of the α- and β-tubulin subunits, and production of the native αβ-tubulin heterodimer.

**References**

Antoshechkin, I. and Han, M. (2002). The C. elegans evl-20 gene is a homolog of the small GTPase ARL2 and regulates cytoskeleton dynamics during cytokinesis and morphogenesis. Dev Cell 2, 579-591.

Beghin, A., Belin, S., Hage-Sleiman, R., Brunet Manquat, S., Goddard, S., Tabone, E., Jordheim, L.P., Treilleux, I., Poupon, M.F., Diaz, J.J. and Dumontet, C. (2009). ADP ribosylation factor like 2 (Arl2) regulates breast tumor aggressivity in immunodeficient mice. PLoS One 4, e7478.

Beghin, A., Honore, S., Messana, C., Matera, E.L., Aim, J., Burlinchon, S., Braguer, D. and Dumontet, C. (2007). ADP ribosylation factor like 2 (Arl2) protein influences microtubule dynamics in breast cancer cells. Exp Cell Res 313, 473-485.

Beghin, A., Matera, E.L., Brunet-Manquat, S. and Dumontet, C. (2008). Expression of Arl2 is associated with p53 localization and chemosensitivity in a breast cancer cell line. Cell Cycle 7, 3074-3082.

Bhamidipati, A., Lewis, S.A. and Cowan, N.J. (2000). ADP ribosylation factor-like protein 2 (Arl2) regulates the interaction of tubulin-folding cofactor D with native tubulin. J Cell Biol 149, 1087-1096.

Bommel, H., Xie, G., Rossoll, W., Wiese, S., Jablonka, S., Boehm, T. and Sendtner, M. (2002). Missense mutation in the tubulin-specific chaperone E (Tbce) gene in the mouse mutant progressive motor neuronopathy, a model of human motoneuron disease. J Cell Biol 159, 563-569.

Chen, K., Koe, C.T., Xing, Z.B., Tian, X., Rossi, F., Wang, C., Tang, Q., Zong, W., Hong, W.J., Taneja, R., Yu, F., Gonzalez, C., Wu, C., Endow, S. and Wang, H. (2016). Arl2- and Msps-dependent microtubule growth governs asymmetric division. J Cell Biol 212, 661-676.

Cowan, N.J. (1998). Mammalian cytosolic chaperonin. Methods Enzymol 290, 230-241.

Cunningham, L.A. and Kahn, R.A. (2008). Cofactor D functions as a centrosomal protein and is required for the recruitment of the gamma-tubulin ring complex at centrosomes and organization of the mitotic spindle. J Biol Chem 283, 7155-7165.

Curmi, P.A., Andersen, S.S., Lachkar, S., Gavet, O., Karsenti, E., Knossow, M. and Sobel, A. (1997). The stathmin/tubulin interaction in vitro. J Biol Chem 272, 25029-25036.

David-Pfeuty, T., Erickson, H.P. and Pantaloni, D. (1977). Guanosinetriphosphatase activity of tubulin associated with microtubule assembly. Proc Natl Acad Sci U S A 74, 5372-5376.

Desai, A. and Mitchison, T.J. (1997). Microtubule polymerization dynamics. Annu Rev Cell Dev Biol 13, 83-117.

Dumontet, C. and Jordan, M.A. (2010). Microtubule-binding agents: a dynamic field of cancer therapeutics. Nat Rev Drug Discov 9, 790-803.

Edvardson, S., Tian, G., Cullen, H., Vanyai, H., Ngo, L., Bhat, S., Aran, A., Daana, M., Da'amseh, N., Abu-Libdeh, B., Cowan, N.J., Heng, J.I. and Elpeleg, O. (2016). Infantile neurodegenerative disorder associated with mutations in TBCD, an essential gene in the tubulin heterodimer assembly pathway. Hum Mol Genet 25, 4635-4648.

Fanarraga, M.L., Bellido, J., Jaen, C., Villegas, J.C. and Zabala, J.C. (2010). TBCD links centriologenesis, spindle microtubule dynamics, and midbody abscission in human cells. PLoS One 5, e8846.

Fawcett, D.W. and Porter, K.R. (1954). A Study of the Fine Structure of Ciliated Epithelia. Journal of Morphology 94, 221-282.

Fedyanina, O.S., Mardanov, P.V., Tokareva, E.M., McIntosh, J.R. and Grishchuk, E.L. (2006). Chromosome segregation in fission yeast with mutations in the tubulin folding cofactor D. Curr Genet 50, 281-294.

Flex, E., Niceta, M., Cecchetti, S., Thiffault, I., Au, M.G., Capuano, A., Piermarini, E., Ivanova, A.A., Francis, J.W., Chillemi, G., Chandramouli, B., Carpentieri, G., Haaxma, C.A., Ciolfi, A., Pizzi, S., Douglas, G.V., Levine, K., Sferra, A., Dentici, M.L., Pfundt, R.R., Le Pichon,

J.B., Farrow, E., Baas, F., Piemonte, F., Dallapiccola, B., Graham, J.M., Jr., Saunders, C.J., Bertini, E., Kahn, R.A., Koolen, D.A. and Tartaglia, M. (2016). Biallelic Mutations in TBCD, Encoding the Tubulin Folding Cofactor D, Perturb Microtubule Dynamics and Cause Early-Onset Encephalopathy. Am J Hum Genet 99, 962-973.

Fontalba, A., Paciucci, R., Avila, J. and Zabala, J.C. (1993). Incorporation of tubulin subunits into dimers requires GTP hydrolysis. J Cell Sci 106 ( Pt 2), 627-632.

Francis, J.W., Newman, L.E., Cunningham, L.A. and Kahn, R.A. (2017). A Trimer Consisting of the Tubulin-specific Chaperone D (TBCD), Regulatory GTPase ARL2, and beta-Tubulin Is Required for Maintaining the Microtubule Network. J Biol Chem 292, 4336-4349.

Francis, J.W., Turn, R.E., Newman, L.E., Schiavon, C. and Kahn, R.A. (2016). Higher order signaling: ARL2 as regulator of both mitochondrial fusion and microtubule dynamics allows integration of 2 essential cell functions. Small GTPases 7, 188-196.

Gadadhar, S., Bodakuntla, S., Natarajan, K. and Janke, C. (2017). The tubulin code at a glance. J Cell Sci 130, 1347-1353.

Gao, Y., Thomas, J.O., Chow, R.L., Lee, G.H. and Cowan, N.J. (1992). A cytoplasmic chaperonin that catalyzes beta-actin folding. Cell 69, 1043-1050.

Gao, Y., Vainberg, I.E., Chow, R.L. and Cowan, N.J. (1993). Two cofactors and cytoplasmic chaperonin are required for the folding of alpha- and beta-tubulin. Mol Cell Biol 13, 2478-2485.

Grynberg, M., Jaroszewski, L. and Godzik, A. (2003). Domain analysis of the tubulin cofactor system: a model for tubulin folding and dimerization. BMC Bioinformatics 4, 46.

Hage-Sleiman, R., Herveau, S., Matera, E.L., Laurier, J.F. and Dumontet, C. (2010). Tubulin binding cofactor C (TBCC) suppresses tumor growth and enhances chemosensitivity in human breast cancer cells. BMC Cancer 10, 135.

Hage-Sleiman, R., Herveau, S., Matera, E.L., Laurier, J.F. and Dumontet, C. (2011). Silencing of tubulin binding cofactor C modifies microtubule dynamics and cell cycle distribution and enhances sensitivity to gemcitabine in breast cancer cells. Mol Cancer Ther 10, 303-312.

Hattori, D., Millard, S.S., Wojtowicz, W.M. and Zipursky, S.L. (2008). Dscam-mediated cell recognition regulates neural circuit formation. Annu Rev Cell Dev Biol 24, 597-620.

Hellani, A., Aqueel, A., Jaroudi, K., Ozand, P. and Coskun, S. (2004). Pregnancy after preimplantation genetic diagnosis for Sanjad-Sakati syndrome. Prenat Diagn 24, 302-306.

Hirata, D., Masuda, H., Eddison, M. and Toda, T. (1998). Essential role of tubulin-folding cofactor D in microtubule assembly and its association with microtubules in fission yeast. EMBO J 17, 658-666.

Hoyt, M.A., Stearns, T. and Botstein, D. (1990). Chromosome instability mutants of Saccharomyces cerevisiae that are defective in microtubule-mediated processes. Mol Cell Biol 10, 223-234.

Ikeda, T., Nakahara, A., Nagano, R., Utoyama, M., Obara, M., Moritake, H., Uechi, T., Mitsui, J., Ishiura, H., Yoshimura, J., Doi, K., Kenmochi, N., Morishita, S., Nishino, I., Tsuji, S. and Nunoi, H. (2016). TBCD may be a causal gene in progressive neurodegenerative encephalopathy with atypical infantile spinal muscular atrophy. J Hum Genet.

Jin, S., Pan, L., Liu, Z., Wang, Q., Xu, Z. and Zhang, Y.Q. (2009). Drosophila Tubulin-specific chaperone E functions at neuromuscular synapses and is required for microtubule network formation. Development 136, 1571-1581.

Jordan, M.A. and Wilson, L. (2004). Microtubules as a target for anticancer drugs. Nat Rev Cancer 4, 253-265.

Jourdain, L., Curmi, P., Sobel, A., Pantaloni, D. and Carlier, M.F. (1997). Stathmin: a tubulin-sequestering protein which forms a ternary T2S complex with two tubulin molecules. Biochemistry 36, 10817-10821.

Kortazar, D., Carranza, G., Bellido, J., Villegas, J.C., Fanarraga, M.L. and Zabala, J.C. (2006). Native tubulin-folding cofactor E purified from baculovirus-infected Sf9 cells dissociates tubulin dimers. Protein Expr Purif 49, 196-202.

Kortazar, D., Fanarraga, M.L., Carranza, G., Bellido, J., Villegas, J.C., Avila, J. and Zabala, J.C. (2007). Role of cofactors B (TBCB) and E (TBCE) in tubulin heterodimer dissociation. Exp Cell Res 313, 425-436.

Lewis, S.A., Tian, G. and Cowan, N.J. (1997). The alpha- and beta-tubulin folding pathways. Trends Cell Biol 7, 479-484.

Li, Y., Kelly, W.G., Logsdon, J.M., Jr., Schurko, A.M., Harfe, B.D., Hill-Harfe, K.L. and Kahn, R.A. (2004). Functional genomic analysis of the ADP-ribosylation factor family of GTPases: phylogeny among diverse eukaryotes and function in C. elegans. FASEB J 18, 1834-1850.

Liu, C.M. and Meinke, D.W. (1998). The titan mutants of Arabidopsis are disrupted in mitosis and cell cycle control during seed development. Plant J 16, 21-31.

Long, L.M., He, B.F., Huang, G.Q., Guo, Y.H., Liu, Y.S. and Huo, J.R. (2015). microRNA-214 functions as a tumor suppressor in human colon cancer via the suppression of ADP-ribosylation factor-like protein 2. Oncol Lett 9, 645-650.

MacNeal, R.K. and Purich, D.L. (1978). Stoichiometry and role of GTP hydrolysis in bovine neurotubule assembly. J Biol Chem 253, 4683-4687.

Manton, I. and Clarke, B. (1952). An Electron Microscope Study of the Spermatozoid of Sphagnum. Journal of Experimental Botany 3, 265-&.

Martin, L., Fanarraga, M.L., Aloria, K. and Zabala, J.C. (2000). Tubulin folding cofactor D is a microtubule destabilizing protein. FEBS Lett 470, 93-95.

Martin, N., Jaubert, J., Gounon, P., Salido, E., Haase, G., Szatanik, M. and Guenet, J.L. (2002). A missense mutation in Tbce causes progressive motor neuronopathy in mice. Nat Genet 32, 443-447.

McIntosh, J.R., Volkov, V., Ataullakhanov, F.I. and Grishchuk, E.L. (2010). Tubulin depolymerization may be an ancient biological motor. J Cell Sci 123, 3425-3434.

Menendez, M., Rivas, G., Diaz, J.F. and Andreu, J.M. (1998). Control of the structural stability of the tubulin dimer by one high affinity bound magnesium ion at nucleotide N-site. J Biol Chem 273, 167-176.

Mitchison, T. and Kirschner, M. (1984). Dynamic instability of microtubule growth. Nature 312, 237-242.

Mitchison, T.J. (1993). Localization of an exchangeable GTP binding site at the plus end of microtubules. Science 261, 1044-1047.

Miyake, N., Fukai, R., Ohba, C., Chihara, T., Miura, M., Shimizu, H., Kakita, A., Imagawa, E., Shiina, M., Ogata, K., Okuno-Yuguchi, J., Fueki, N., Ogiso, Y., Suzumura, H., Watabe, Y., Imataka, G., Leong, H.Y., Fattal-Valevski, A., Kramer, U., Miyatake, S., Kato, M., Okamoto, N., Sato, Y., Mitsuhashi, S., Nishino, I., Kaneko, N., Nishiyama, A., Tamura, T., Mizuguchi, T., Nakashima, M., Tanaka, F., Saitsu, H. and Matsumoto, N. (2016). Biallelic TBCD Mutations Cause Early-Onset Neurodegenerative Encephalopathy. Am J Hum Genet 99, 950-961.

Mori, R. and Toda, T. (2013). The dual role of fission yeast Tbc1/cofactor C orchestrates microtubule homeostasis in tubulin folding and acts as a GAP for GTPase Alp41/Arl2. Mol Biol Cell 24, 1713-1724, S1711-1718.

Muromoto, R., Sekine, Y., Imoto, S., Ikeda, O., Okayama, T., Sato, N. and Matsuda, T. (2008). BART is essential for nuclear retention of STAT3. Int Immunol 20, 395-403.

Newman, L.E., Schiavon, C.R., Zhou, C. and Kahn, R.A. (2017). The abundance of the ARL2 GTPase and its GAP, ELMOD2, at mitochondria are modulated by the fusogenic activity of mitofusins and stressors. PLoS One 12, e0175164.

Newman, L.E., Zhou, C.J., Mudigonda, S., Mattheyses, A.L., Paradies, E., Marobbio, C.M. and Kahn, R.A. (2014). The ARL2 GTPase is required for mitochondrial morphology, motility, and maintenance of ATP levels. PLoS One 9, e99270.

Nishi, H., Ono, K., Iwanaga, Y., Horie, T., Nagao, K., Takemura, G., Kinoshita, M., Kuwabara, Y., Mori, R.T., Hasegawa, K., Kita, T. and Kimura, T. (2010). MicroRNA-15b modulates cellular ATP levels and degenerates mitochondria via Arl2 in neonatal rat cardiac myocytes. J Biol Chem 285, 4920-4930.

Nithianantham, S., Le, S., Seto, E., Jia, W., Leary, J., Corbett, K.D., Moore, J.K. and Al-Bassam, J. (2015). Tubulin cofactors and Arl2 are cage-like chaperones that regulate the soluble alphabeta-tubulin pool for microtubule dynamics. Elife 4.

Nogales, E. (2000). Structural insights into microtubule function. Annu Rev Biochem 69, 277-302.

Nogales, E., Wolf, S.G. and Downing, K.H. (1998). Structure of the alpha beta tubulin dimer by electron crystallography. Nature 391, 199-203.

Nolasco, S., Bellido, J., Goncalves, J., Zabala, J.C. and Soares, H. (2005). Tubulin cofactor A gene silencing in mammalian cells induces changes in microtubule cytoskeleton, cell cycle arrest and cell death. FEBS Lett 579, 3515-3524.

Okumura, M., Sakuma, C., Miura, M. and Chihara, T. (2015). Linking cell surface receptors to microtubules: tubulin folding cofactor D mediates Dscam functions during neuronal morphogenesis. J Neurosci 35, 1979-1990.

Padidela, R., Kelberman, D., Press, M., Al-Khawari, M., Hindmarsh, P.C. and Dattani, M.T. (2009). Mutation in the TBCE gene is associated with hypoparathyroidism-retardation-dysmorphism syndrome featuring pituitary hormone deficiencies and hypoplasia of the anterior pituitary and the corpus callosum. J Clin Endocrinol Metab 94, 2686-2691.

Parvari, R., Hershkovitz, E., Grossman, N., Gorodischer, R., Loeys, B., Zecic, A., Mortier, G., Gregory, S., Sharony, R., Kambouris, M., Sakati, N., Meyer, B.F., Al Aqeel, A.I., Al Humaidan, A.K., Al Zanhrani, F., Al Swaid, A., Al Othman, J., Diaz, G.A., Weiner, R.,

Khan, K.T., Gordon, R., Gelb, B.D. and Consortium, H.R.A.R.K.-C.S. (2002). Mutation of TBCE causes hypoparathyroidism-retardation-dysmorphism and autosomal recessive Kenny-Caffey syndrome. Nat Genet 32, 448-452.

Peng, R., Men, J., Ma, R., Wang, Q., Wang, Y., Sun, Y. and Ren, J. (2017). miR-214 down-regulates ARL2 and suppresses growth and invasion of cervical cancer cells. Biochem Biophys Res Commun 484, 623-630.

Pode-Shakked, B., Barash, H., Ziv, L., Gripp, K.W., Flex, E., Barel, O., Carvalho, K.S., Scavina, M., Chillemi, G., Niceta, M., Eyal, E., Kol, N., Ben-Zeev, B., Bar-Yosef, O., Marek-Yagel, D., Bertini, E., Duker, A.L., Anikster, Y., Tartaglia, M. and Raas-Rothschild, A. (2017). Microcephaly, intractable seizures and developmental delay caused by biallelic variants in TBCD: further delineation of a new chaperone-mediated tubulinopathy. Clin Genet 91, 725-738.

Price, H.P., Peltan, A., Stark, M. and Smith, D.F. (2010). The small GTPase ARL2 is required for cytokinesis in Trypanosoma brucei. Mol Biochem Parasitol 173, 123-131.

Radcliffe, P.A., Hirata, D., Vardy, L. and Toda, T. (1999). Functional dissection and hierarchy of tubulin-folding cofactor homologues in fission yeast. Mol Biol Cell 10, 2987-3001.

Rieder, C.L. and Salmon, E.D. (1994). Motile kinetochores and polar ejection forces dictate chromosome position on the vertebrate mitotic spindle. J Cell Biol 124, 223-233.

Schaefer, M.K., Schmalbruch, H., Buhler, E., Lopez, C., Martin, N., Guenet, J.L. and Haase, G. (2007). Progressive motor neuronopathy: a critical role of the tubulin chaperone TBCE in axonal tubulin routing from the Golgi apparatus. J Neurosci 27, 8779-8789.

Schubert, A., Cattaruzza, M., Hecker, M., Darmer, D., Holtz, J. and Morawietz, H. (2000). Shear stress-dependent regulation of the human beta-tubulin folding cofactor D gene. Circ Res 87, 1188-1194.

Serna, M., Carranza, G., Martin-Benito, J., Janowski, R., Canals, A., Coll, M., Zabala, J.C. and Valpuesta, J.M. (2015). The structure of the complex between alpha-tubulin, TBCE and TBCB reveals a tubulin dimer dissociation mechanism. J Cell Sci 128, 1824-1834.

Sferra, A., Baillat, G., Rizza, T., Barresi, S., Flex, E., Tasca, G., D'Amico, A., Bellacchio, E., Ciolfi, A., Caputo, V., Cecchetti, S., Torella, A., Zanni, G., Diodato, D., Piermarini, E., Niceta, M., Coppola, A., Tedeschi, E., Martinelli, D., Dionisi-Vici, C., Nigro, V., Dallapiccola, B., Compagnucci, C., Tartaglia, M., Haase, G. and Bertini, E. (2016). TBCE Mutations Cause Early-Onset Progressive Encephalopathy with Distal Spinal Muscular Atrophy. Am J Hum Genet 99, 974-983.

Sharer, J.D., Shern, J.F., Van Valkenburgh, H., Wallace, D.C. and Kahn, R.A. (2002). ARL2 and BART enter mitochondria and bind the adenine nucleotide transporter. Mol Biol Cell 13, 71-83.

Shern, J.F., Sharer, J.D., Pallas, D.C., Bartolini, F., Cowan, N.J., Reed, M.S., Pohl, J. and Kahn, R.A. (2003). Cytosolic Arl2 is complexed with cofactor D and protein phosphatase 2A. J Biol Chem 278, 40829-40836.

Shultz, T., Shmuel, M., Hyman, T. and Altschuler, Y. (2008). Beta-tubulin cofactor D and ARL2 take part in apical junctional complex disassembly and abrogate epithelial structure. FASEB J 22, 168-182.

Slautterback, D.B. (1963). Cytoplasmic Microtubules. I. Hydra. J Cell Biol 18, 367-388.

Spiess, C., Meyer, A.S., Reissmann, S. and Frydman, J. (2004). Mechanism of the eukaryotic chaperonin: protein folding in the chamber of secrets. Trends Cell Biol 14, 598-604.

Stearns, T., Kahn, R.A., Botstein, D. and Hoyt, M.A. (1990). ADP ribosylation factor is an essential protein in Saccharomyces cerevisiae and is encoded by two genes. Mol Cell Biol 10, 6690-6699.

Tian, G., Bhamidipati, A., Cowan, N.J. and Lewis, S.A. (1999). Tubulin folding cofactors as GTPase-activating proteins. GTP hydrolysis and the assembly of the alpha/beta-tubulin heterodimer. J Biol Chem 274, 24054-24058.

Tian, G. and Cowan, N.J. (2013). Tubulin-specific chaperones: components of a molecular machine that assembles the alpha/beta heterodimer. Methods Cell Biol 115, 155-171.

Tian, G., Huang, M.C., Parvari, R., Diaz, G.A. and Cowan, N.J. (2006). Cryptic out-of-frame translational initiation of TBCE rescues tubulin formation in compound heterozygous HRD. Proc Natl Acad Sci U S A 103, 13491-13496.

Tian, G., Huang, Y., Rommelaere, H., Vandekerckhove, J., Ampe, C. and Cowan, N.J. (1996). Pathway leading to correctly folded beta-tubulin. Cell 86, 287-296.

Tian, G., Thomas, S. and Cowan, N.J. (2010). Effect of TBCD and its regulatory interactor Arl2 on tubulin and microtubule integrity. Cytoskeleton (Hoboken) 67, 706-714.

Vainberg, I.E., Lewis, S.A., Rommelaere, H., Ampe, C., Vandekerckhove, J., Klein, H.L. and Cowan, N.J. (1998). Prefoldin, a chaperone that delivers unfolded proteins to cytosolic chaperonin. Cell 93, 863-873.

Valpuesta, J.M., Martin-Benito, J., Gomez-Puertas, P., Carrascosa, J.L. and Willison, K.R. (2002). Structure and function of a protein folding machine: the eukaryotic cytosolic chaperonin CCT. FEBS Lett 529, 11-16.

Wang, K., Li, P., Dong, Y., Cai, X., Hou, D., Guo, J., Yin, Y., Zhang, Y., Li, J., Liang, H., Yu, B., Chen, J., Zen, K., Zhang, J., Zhang, C.Y. and Chen, X. (2011). A microarray-based approach identifies ADP ribosylation factor-like protein 2 as a target of microRNA-16. J Biol Chem 286, 9468-9476.

Weisenberg, R.C., Borisy, G.G. and Taylor, E.W. (1968). The colchicine-binding protein of mammalian brain and its relation to microtubules. Biochemistry 7, 4466-4479.

Weisenberg, R.C., Deery, W.J. and Dickinson, P.J. (1976). Tubulin-nucleotide interactions during the polymerization and depolymerization of microtubules. Biochemistry 15, 4248-4254.

Zhang, P., Ma, X., Song, E., Chen, W., Pang, H., Ni, D., Gao, Y., Fan, Y., Ding, Q., Zhang, Y. and Zhang, X. (2013). Tubulin cofactor A functions as a novel positive regulator of ccRCC progression, invasion and metastasis. Int J Cancer 133, 2801-2811.

Zhou, C., Cunningham, L., Marcus, A.I., Li, Y. and Kahn, R.A. (2006). Arl2 and Arl3 regulate different microtubule-dependent processes. Mol Biol Cell 17, 2476-2487.

Zhou, Y., Jiang, H., Gu, J., Tang, Y., Shen, N. and Jin, Y. (2013). MicroRNA-195 targets ADP-ribosylation factor-like protein 2 to induce apoptosis in human embryonic stem cell-derived neural progenitor cells. Cell Death Dis 4, e695.

# CHAPTER 2

## A Trimer Consisting of the Tubulin-Specific Chaperone TBCD, Regulatory GTPase ARL2, and β-tubulin is Required for Maintaining the Microtubule Network

Joshua W. Francis, Laura E. Newman, Leslie A. Cunningham and Richard A. Kahn

The Department of Biochemistry, Emory University School of Medicine,

Atlanta, GA 30322

This research was originally published in The Journal of Biological Chemistry.

Francis, JW, Newman, LE, Cunningham, LA, Kahn RA. A Trimer Consisting of the Tubulin-Specific Chaperone TBCD, Regulatory GTPase ARL2, and β-tubulin is Required for Maintaining the Microtubule Network. *J Biol Chem.* 2017; 292:4336-4349. 

**Abstract**

Microtubule dynamics involves the polymerization and depolymerization of tubulin dimers and is an essential and highly regulated process required for cell viability, architecture, and division. The regulation of the microtubule network also depends upon the maintenance of a pool of αβ-tubulin heterodimers. These dimers are the end result of complex folding and assembly events, requiring the TriC/CCT chaperonin and five tubulin-specific chaperones, TBCA-E. However, models of the actions of these chaperones are incomplete or inconsistent. We previously purified TBCD from bovine tissues and showed that it tightly binds the small GTPase ARL2, yet appears to be inactive. Here, in an effort to identify the functional form of TBCD and using non-denaturing gels and immunoblotting, we analyzed lysates from a number of mouse tissues and cell lines to identify the quaternary state(s) of TBCD and ARL2. We found that both proteins co-migrated in native gels in a complex of ~200 kDa that also contained β-tubulin. Using human embryonic kidney cells enabled the purification of the TBCD/ARL2/β-tubulin trimer found in cell and tissue lysates, as well as two other novel TBCD complexes. Characterization of ARL2 point mutants that disrupt binding to TBCD suggested that the ARL2-TBCD interaction is critical for proper maintenance of microtubule densities in cells. We conclude that the TBCD/ARL2/β-tubulin trimer represents a functional complex whose activity is fundamental to microtubule dynamics.

**Introduction**

Microtubules are highly dynamic polymers that are best known for their roles as the central cytoskeletal structure in cells and in mitotic spindles during cell division. They are also the tracks on which organelles traffic, particularly important in polarized cells that generate great distances between parts of the cell. Additionally, they are the core of sensory and motile cilia or flagella. The formation and destruction of microtubules and microtubule bundles are orchestrated by a large number of proteins that include the microtubule associated proteins, or MAPs. Microtubules are polymers of the αβ-tubulin dimer, with several genes encoding each α- or β-tubulin subunit (*e.g.*,

see Lewis et al., 1987), resulting in some diversity in composition. Tubulins can also be modified by post-translational modifications, including acetylation, tyrosination and phosphorylation, which can alter the dynamics of the polymerization and depolymerization reactions. Because of the essential role of microtubules in cell division, they have also been the target of many anti-tumor therapies, *e.g.*, the taxanes and Vinca alkaloids (Jordan and Wilson, 2004). Yet despite their importance to cells and in the clinic, and decades of research, we still lack a complete molecular level understanding of the biosynthesis and regulation of the formation of αβ-tubulin.

Tubulins are typically the most abundant proteins in mammalian cells, yet the generation of the αβ-tubulin dimer requires a complex series of biosynthetic steps to support proper folding and dimer assembly. Newly synthesized α- and β-tubulin, as well as other proteins (Gao et al., 1993; Spiess et al., 2004), first interact with the TriC/CCT complex upon exiting the ribosome. The tubulins then interact with the five tubulin-specific co-chaperones, termed cofactors A-E, in a series of interactions first described by Tian et al. (Tian et al., 1996; Tian et al., 1997), using native gels to monitor the formation of different inferred complexes of *in vitro* translated tubulin. Because of the complexities involved in αβ-tubulin dimer assembly, there is currently no recombinant system capable of generating pure populations of milligram amounts of unmodified tubulin dimers. The development of a molecular model for tubulin folding would reveal the roles played by each of the required components, allow the generation of key biochemical reagents for multiple studies, and is predicted to generate a number of opportunities for therapeutic development. Such a model requires the ability to generate each component in a functional state that would then allow reconstitution of the formation of the αβ-tubulin dimer from parts. Perhaps the largest roadblock to this goal is that one of the required chaperones, Cofactor D (TBCD), is insoluble when expressed in bacteria and poorly expressed or unstable in other expression systems, and thus is not readily available. This is in marked contrast to the other four cofactors, A-C and E (Tian and Cowan, 2013).

The earliest evidence that TBCD is important to microtubule biology came from genetic screens in model genetic systems. In *S. cerevisiae*, screens for altered sensitivity to drugs acting on

microtubules identified mutations in the yeast TBCD ortholog, *CIN1* (Hoyt et al., 1990; Stearns et al., 1990). Mutations in TBCD orthologs were later identified in similar screens performed in *S. pombe* (*Alp1*) (Hirata et al., 1998; Radcliffe et al., 1999), and in *A. thaliana* (*TTN1*). Along with these compelling genetic data, the identification of TBCD as one of the five tubulin-specific cofactors required for *in vitro* folding of tubulin (Tian et al., 1996) confirmed a central role of TBCD in tubulin biosynthesis. More recently, however, TBCD has been implicated in additional cellular roles, including actions at centrosomes (Fedyanina et al., 2006; Cunningham and Kahn, 2008; Fanarraga et al., 2010) and at the cell surface (Shultz et al., 2008; Okumura et al., 2015). Several recent studies have identified a number of point mutations in TBCD found in patients with links to early-onset encephalopathy (Edvardson et al., 2016; Flex et al., 2016; Miyake et al., 2016) and intractable seizures (Pode-Shakked et al., 2016). Throughout the time that roles for TBCD in microtubule biology were being identified, there also have been strong functional links to the ARL2 GTPase, a member of the ARF family of regulatory GTPases. The same genetic screens that identified mutations in *CIN1/Alp1/TTN1 (TBCD orthologs)* that altered microtubules also identified mutations in *CIN4/Alp41/TTN5*, the orthologs of ARL2 in *S. cerevisiae*, *S. pombe*, and *A. thaliana*, respectively (Hoyt et al., 1990; Stearns et al., 1990). Genetic screening similarly identified effects of mutations in ARL2 orthologs in *C. elegans* (Antoshechkin and Han, 2002), *T. brucei* (Price et al., 2010), and *D. melanogaster* (Chen et al., 2016). Thus, there is strong evidence that ARL2 orthologs play essential roles in tubulin and microtubule biology. However, ARL2 has other essential regulatory roles in cells that both complicate analyses and increase its overall importance to cell biology (Francis et al., 2016).

While other members of the ARF family are predominantly present in cytosol as monomers, fractionating as 20 kDa species, we found that the vast majority of ARL2 fractionates with an apparent molecular weight of ≥200 kDa (Shern et al., 2003). This is in marked contrast to human ARL2 purified from bacteria or HEK cells overexpressing human ARL2, which are stable monomeric proteins (Clark et al., 1993). Upon purification from bovine tissues, we found that

ARL2 remained tightly bound as a heterodimer with TBCD. However, that heterodimer was inactive in the tubulin folding assay and displayed highly unusual guanine-nucleotide binding properties in failing to bind the activating ligands, GTP or GTPγS (Shern et al., 2003). Because the ARL2/TBCD heterodimer purified from bovine tissues appeared to be inactive in key respects, required more than one week to purify, and yielded only small (μg) amounts of protein, we sought other means of assessing the quaternary state of TBCD and ARL2 in cells and tissues.

The model for tubulin folding, first proposed by the Cowan group (Tian et al., 1997), includes the TBCD/TBCE/α-tubulin/β-tubulin tetramer as the penultimate complex to which TBCC binds, resulting in release of the folded αβ-tubulin heterodimer. Prior to this, the unfolded α- and β-tubulin monomers are thought to be maintained in their unfolded states by binding to cofactors B and A, respectively. A recent publication that used recombinant expression of yeast orthologs argues, instead, that the basal complex for tubulin folding consists of a trimer of TBCD/TBCE/ARL2 (Nithianantham et al., 2015). To test these models and further the ultimate goal of reconstitution of tubulin folding as a formal demonstration of the roles of each component, we began by assessing the quaternary state of TBCD and ARL2 in freshly prepared cell or tissue lysates. We found evidence of a very stable and novel complex consisting of TBCD, ARL2, and β-tubulin, as well as two other multi-subunit protein complexes that are described here for the first time.

**Results**

*TBCD and ARL2 are present in animal cells and tissues in a complex with an apparent molecular weight of ~200 kDa:* In order to identify the predominant form of ARL2 that exists in mammalian cells, we re-examined the nature of ARL2 complex(es) found in mammalian cells and tissues. We began by analyzing the elution profile of ARL2 by immunoblotting fractions from a size exclusion column (Superdex 200), used to resolve proteins from a clarified lysate of HeLa cells

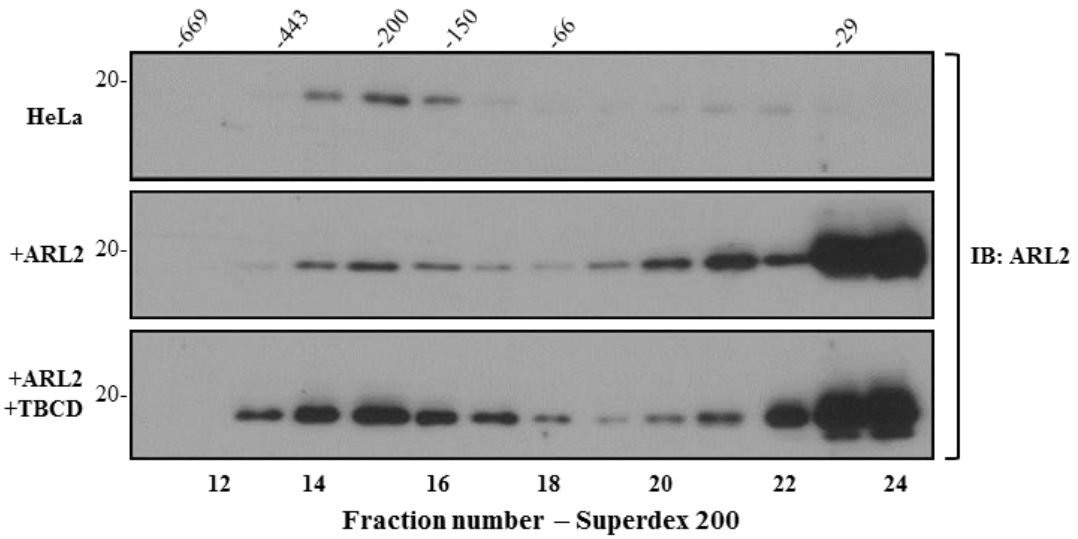


**Figure 2-1. ARL2 is predominantly present in HeLa cells in a high molecular weight complex that is increased in abundance only when TBCD levels are also increased.** The quaternary structure of ARL2 was monitored using gel filtration of HeLa cell lysates (top panel), after ARL2 overexpression alone (middle panel), or with TBCD co-expression (bottom panel), as described under Experimental Procedures. Cells were lysed 24 hours after transfection and clarified by centrifugation at 100,000x*g* before loading equal amounts of protein onto a Superdex 200 gel filtration column (fractions 12-24 shown here). Equal volumes of each fraction were analyzed by immunoblot using our rabbit polyclonal antibody to ARL2. Gel filtration standards from a parallel run are shown above, and the 20 kDa size marker for the SDS gels to the left.

(Figure 1, top panel). The overwhelming majority (estimated at ~90%) of ARL2 eluted as a single peak, in the fractions corresponding to an apparent molecular weight of ~200 kDa (peaking in fraction 15 in Figure 1, top panel). Consistent with our previous work (Shern et al., 2003), little or no ARL2 was evident in fractions corresponding to a 20 kDa monomer (fractions 23-24 in Figure 1, top panel). A faint peak of ARL2 signal was seen at slightly higher apparent molecular weights, corresponding to an estimated size of ~40 kDa (fractions 21-22 in Figure 1, top panel). In contrast, when human ARL2 is expressed in bacteria it purifies as a soluble, stable monomer, with no evidence of any species greater than 20 kDa (Clark et al., 1993). While the larger, ~200 kDa species was previously observed and proved to be abundant in animal cells/tissues (see below), the intermediate, ~40 kDa species was not observed in our earlier study of Sf295 cell lysates (Shern et al., 2003) or in several other instances, so was not pursued further at this time.

HeLa cells were then transfected with a plasmid directing the overexpression of human ARL2, prior to repeating the gel filtration analysis (Figure 1, middle panel). No evident increase in the abundance of the ~200 kDa species was seen. However, there was a clear increase in the ~40 kDa species that includes ARL2 and a vast increase in the amount of ARL2 in fractions 23-24, corresponding to monomer. This suggests that ARL2 expressed in mammalian cells can migrate as a monomer and that the larger species represent homo- or hetero-oligomers. Because ARL2 is known to bind TBCD, we then overexpressed both human ARL2 and TBCD in HeLa cells and repeated the analysis. This time there was a considerable increase in the amount of ARL2 migrating in the range of the ~200 kDa species, consistent with the presence of both ARL2 and TBCD in these fractions (Figure 1, bottom panel). These results prompted us to examine the nature of the ARL2/TBCD complex in mammalian cells and tissues.

Despite the fact that we have previously purified from mammalian tissue, over the course of several days, a stable complex that includes ARL2 and TBCD, we were concerned about the possibility of subunit dissociation during analysis altering our conclusions as to the composition of different ARL2 complexes. Therefore, we sought a method that both uses distinct characteristics

for separation and is more rapid in resolving TBCD and ARL2 complexes under native conditions. We used Blue Native Polyacrylamide Gel Electrophoresis (BN-PAGE) to analyze freshly prepared cell lysates as it is more rapid, yields higher resolution of proteins and complexes over a broad range of apparent molecular weights, allows simultaneous and parallel analyses of multiple samples, and has been used previously in analyses of tubulin and related proteins (Fanarraga et al., 2010). Cell and tissue lysates were prepared as described in Experimental Procedures, and the resulting soluble fractions (S100) were analyzed by BN-PAGE and immunoblotting for ARL2 and TBCD. Figure 2A summarizes the results obtained from human embryonic kidney (HEK), mouse Neuro 2A (N2A) neuroblastoma, mouse embryonic fibroblast (NIH-3T3), and human neuroblastoma (SH-SY5Y) cells. While multiple bands were observed in most cases, the most abundant species of ARL2 and TBCD in each sample shown, with the exception of SH-SY5Y, is a band migrating just below the 242 kDa size marker, and thus quite close to the predicted ~200 kDa species observed after gel filtration. A few other cell lines were also analyzed in this way and yielded more complex patterns with bands of different apparent sizes being more prominent than that at 200 kDa (data not shown). Thus, while the complex migrating just below the 242 kDa marker is the predominant and even sole immunoreactive band in some cell lines, this is not true in all cell lines tested. A graph of the migration distance versus the log of the molecular mass, with comparison to molecular weight markers, yielded an apparent molecular weight of 200 kDa, so we will use this size in our discussions of this complex hereafter.

We also examined the quaternary structure of TBCD in several animal tissues. Immunoblots of human, bovine, and murine brain, as well as murine liver and kidney tissue lysates, were probed with our rabbit polyclonal antibody to TBCD (Figure 2B). In each of these murine tissues, the predominant species is again migrating at ~200 kDa. In contrast, the human and bovine brain lysates contain predominantly a single band of TBCD immunoreactivity migrating at ~400 kDa, very similar in electrophoretic mobility to the predominant species seen in human SH-SY5Y cells (Figure 2A). Immunoblotting of these samples was also performed from BN-PAGE using our

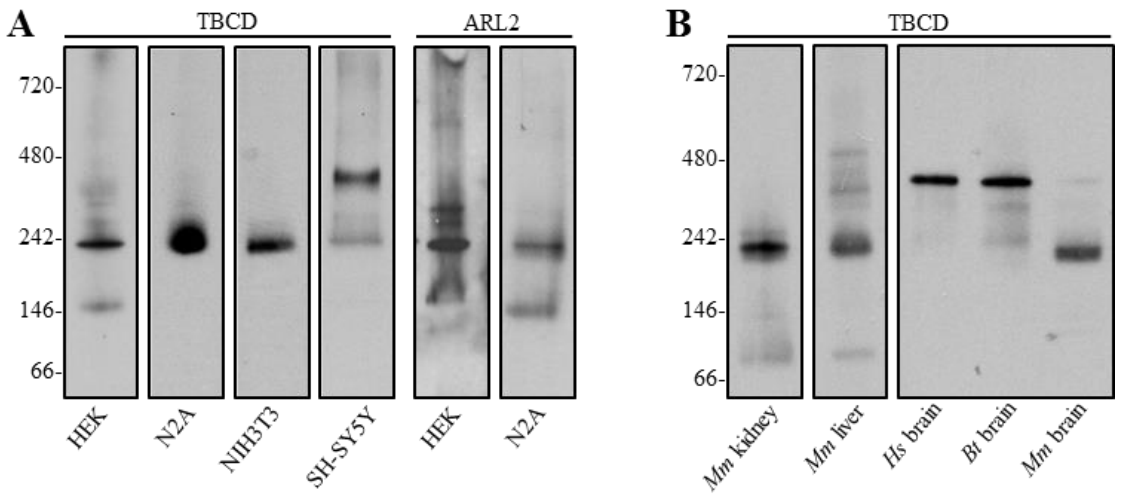


**Figure 2-2. Immunoblots of cell and tissue lysates resolved in native gels reveal endogenous TBCD and ARL2 complexes at ~200 kDa are commonly observed and can be the predominant species of each protein detected in this assay.** (**A**). Detergent extracts of HEK, N2A, NIH3T3, and SH-SY5Y cells were clarified by centrifugation at 100,000x*g*, resolved (30 µg each) in a 4-16% BN-PAGE gel and immunoblotted with antibodies specific to ARL2 or TBCD, as indicated and described under Experimental Procedures. (**B**) Murine, kidney or liver and murine, bovine, and human brain samples were homogenized and then clarified by centrifugation at 100,000x*g* for 1 hour at 4°C. Lysates (30 µg) were resolved using BN-PAGE and immunoblotted with TBCD antibodies. *Hs, Homo sapiens. Bt, Bos taurus. Mm, Mus musculus.*

ARL2 and commercial β-tubulin antibodies, but results were harder to interpret as a result of greater variability and diversity of β-tubulin containing complexes, respectively, as well as higher backgrounds in both. This issue is largely the result of immunoblotting from native gels as each antibody yielded much simpler and cleaner results when blotting from SDS-PAGE gels. The stark differences in apparent molecular weight of the TBCD complex seen in human and bovine, compared to murine, brain lysates were surprising and without explanations found in the literature. Though not pursued further in the current study, the band at ~400 kDa will likely prove to be related as we find it immunoblots positive for TBCE and ARL2 (not shown), in addition to TBCD, and thus may be related to the complex studied in the Al-Bassam laboratory (Nithianantham et al., 2015). We note that the 4-16% gradient BN-PAGE gels did a poor job of quantifying species below ~60 kDa as proteins smear, resulting in decreased sensitivity of immunoblots. These data led us to conclude that TBCD and ARL2 are present in a species migrating in native gels with an apparent molecular weight of 200 kDa that is present in almost all samples examined and the predominant, if not sole, species seen in some. This prompted a much more detailed analysis of this protein complex, including its purification from recombinant sources.

*Recombinant GST-TBCD co-purifies with αβ-tubulin:* We and others have previously found that TBCD is insoluble when expressed in bacteria. The Cowan lab has used insect cell expression for bovine TBCD, though found low yields and instability (Tian and Cowan, 2013). They later used adenoviruses to express bovine or human TBCD in HeLa cells and found β-tubulin to co-purify only with the human protein (Tian et al., 2010). We used adherent HEK cells as a mammalian expression system and transfected them with plasmids directing expression of N-terminal, GST-tagged human TBCD (GST-TBCD). Following expression, GST-TBCD was affinity purified using glutathione-conjugated Sepharose beads and eluted with glutathione. The GST tag was removed using the engineered TEV protease cleavage site between the GST tag and the TBCD open reading frame, resulting in a residual 12 amino acid extension at the N-terminus of TBCD. After optimization of time of expression, DNA/PEI ratios, and other aspects of the

expression and purification, we found that we could obtain ~1 mg of the GST-TBCD/α-tubulin/β-tubulin complex from 1 liter of adherent HEK cells (50 15-cm plates).

GST-TBCD was initially analyzed by SDS-PAGE with Coomassie blue staining after affinity purification from HEK cells expressing GST-TBCD alone (Figure 3A, lane 2) or co-expression with human ARL2 (Figure 3A, lane 3). Expression of GST alone (not shown), or co-expression with ARL2 (Figure 3A, lane 1), resulted in purification of the 28 kDa GST, as well as a band at 24 kDa (Figure 3A, all three lanes; marked by an asterisk). Note the absence of endogenous ARL2 in lanes 1 and 2. The 24 kDa contaminant is predicted to be an endogenous GST present in insect and HEK cells (Bichet et al., 2000), and is observed in all of our affinity-purified preparations using this source. The contaminant is readily removed by gel filtration or ultrafiltration using a filter with a molecular weight cut-off of 30,000 Da, and thus we are confident this protein is not a component of any of our complexes.

SDS-PAGE analysis of affinity purified GST-TBCD from HEK cells resulted in the identification of two bands, at ~160 and ~55 kDa (Figure 3A, lane 2). The larger band is GST-TBCD (28 kDa + 133 kDa), based upon prediction and confirmed by immunoblotting (data not shown). The established role of TBCD in tubulin folding, and size of the band at 55 kDa, prompted us to immunoblot for α- and β-tubulin. We found that the 55 kDa band was positive for both α- and β-tubulins, and thus conclude that the tubulin heterodimer specifically co-purifies with GST-TBCD (Figure 3B, lane 1). This is the first time that TBCD has been shown to bind directly to αβ-tubulin. Note that ARL2 was not evident in the purified preparation of GST-TBCD/α-tubulin/β-tubulin. Though ARL2 is present endogenously in HEK cells, and presumably almost all bound to endogenous TBCD (see Figure 1, top panel), we suspect there is simply not enough free ARL2 to bind the higher levels of GST-TBCD achieved in this expression system.

The TBCD/α-tubulin/β-tubulin trimer was then analyzed by both BN-PAGE and gel filtration chromatography. GST-TBCD was expressed and purified from HEK cells, and the GST tag was removed with TEV as it promotes dimerization that could confound interpretations. When

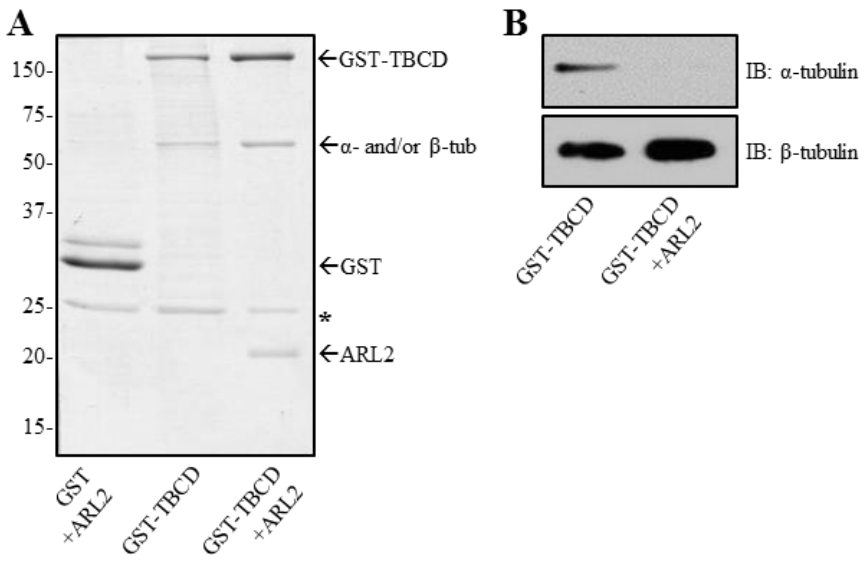


**Figure 2-3. Purification GST-TBCD +/- ARL2 from HEK cells results in the co-purification of different combinations of tubulins in novel complexes.** (**A**) GST-TBCD was expressed in HEK cells with (lane 3) or without (lane 2) ARL2 and after two days, glutathione Sepharose beads were used to affinity purify the GST-TBCD and associated proteins. GST alone (lane 1) was also co-expressed with ARL2 as a negative control and purified in the same way. Proteins (3 µg/lane) were analyzed by SDS-PAGE with Coomassie blue staining. The asterisk indicates a glutathione-binding protein contaminant. (**B**) The same samples (100 ng/lane) analyzed in lanes 2 and 3 in panel A were immunoblotted for α- or β-tubulin. Note the absence of α-tubulin when ARL2 is present.

analyzed by BN-PAGE and Coomassie blue staining, the preparation failed to reveal any distinct band(s), despite loading as much as 4 μg of purified protein. Rather, we either saw a faint haze of staining in the higher molecular weight range of the gel or, more consistently, staining that barely entered the gel (Figure 4A, left lane). Immunoblotting of BN-PAGE gels confirmed the presence of TBCD in the haze, consistent with oligomerization or aggregation (data not shown). When the same preparation was analyzed by its elution profile from a Superdex S200 column, the protein was all found in the void volume, which is again consistent with aggregation or oligomerization. Thus, when TBCD was expressed and purified from HEK cells without excess ARL2, it co-purified with α- and β-tubulin in a complex that appears to be aggregated or oligomerized. Though not shown here, when comparing the levels of αβ-tubulin co-purifying with TBCD (Figure 3B, left lane) to a purified tubulin standard, it appears that the tubulins co-purify to similar levels. However, we note that it is possible that GST-TBCD co-purifies with a combination of β-tubulin and αβ-tubulin at varying stoichiometries. Nevertheless, the finding that TBCD binds to αβ-tubulin dimers is thought to be an indication of either a residual interaction from the final step in folding/biosynthesis of the tubulin dimer or of the ability of TBCD to bind to the tubulin dimer either when free in solution or perhaps even in a microtubule. This last possibility may explain the ability of TBCD overexpression to cause the loss of cellular microtubules in cultured cells (Bhamidipati et al., 2000; Martin et al., 2000; Cunningham and Kahn, 2008; Tian et al., 2010).

*Co-expression of GST-TBCD and ARL2 results in the formation and ability to purify a TBCD/ARL2/β-tubulin trimer:* When GST-TBCD was affinity purified from HEK cells co-expressing ARL2, we observed three bands in SDS-PAGE gels corresponding to GST-TBCD at ~160 kDa, ARL2 at ~20 kDa, and again a band at ~55 kDa that appeared to co-migrate with that seen in the GST-TBCD preparation lacking ARL2 (Figure 3A). Immunoblot analyses confirmed the bands as TBCD, ARL2 and β-tubulin. However, in marked contrast to the previous trimer, the 55 kDa band was strongly immunoreactive with β-tubulin antibody but clearly negative for α-tubulin (Figure 3B, right lane). We then asked if there was specificity for any isoform of β-tubulin

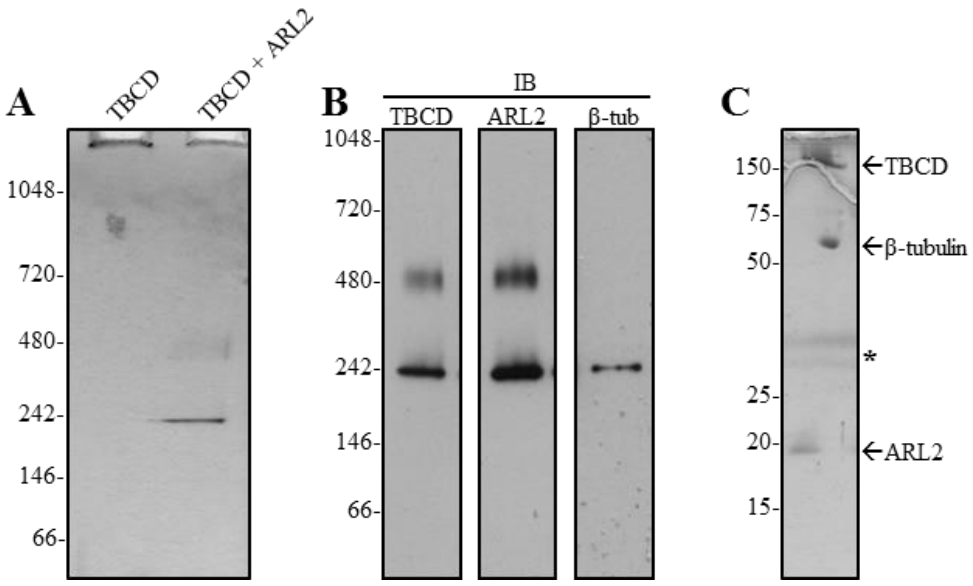


**Figure 2-4. GST-TBCD purifies as the GST-TBCD/ARL2/β-tubulin trimer from HEK cells co-expressing GST-TBCD and ARL2.** (**A**) GST-TBCD was expressed in HEK cells without (left lane) or with (right lane) ARL2 co-expression. The affinity purified products (4 μg/lane) were cleaved with TEV protease, resolved in a 4-16% BN-PAGE gel, and stained with Coomassie blue. Note that the complex(es) present in the first lane are smeared, and thus not obvious in this gel. (**B**) Immunoblot analysis of the purified complex shown in the right lane of panel A using antibodies specific to TBCD, ARL2 or β-tubulin. (**C**) Two-dimensional BN/SDS-PAGE was performed on the purified GST-TBCD complex. The sample (10 μg) was first resolved in a 4-16% acrylamide, blue native gel and stained with Coomassie blue (not shown). The band just below the 242 kDa size marker was excised and resolved in a 13% SDS-PAGE gel, and stained with Coomassie blue. The identities of the bands were confirmed by immunoblotting for each of the three components (not shown). The asterisk indicates aberrant dye bands that spanned the width of the entire gel, and are not indicative of sample staining.

by subjecting the band at 55 kDa to mass spectrometry after tryptic digestion. In two samples, we obtained over 600 spectral counts for β-tubulin peptides. Among these were multiple isoform-specific peptides derived from β-tubulins Class IIA (NP_001060.1), IIB (NP_821080.1), III (NP_006077.2), IVB (NP_006079.1), and V (NP_115914.1), with tubulin Class I (NP_821133.1) scoring the most hits but lacking any unique peptides (data not shown). Thus, we conclude that there is no *absolute* specificity for β-tubulin isoforms in the trimer purified from HEK cells. This is in agreement with results from the Cowan lab failing to find specificity for β-tubulin isoforms in different microtubules (Lewis et al., 1987). Note that because the ratios of tubulins expressed in HEK cells is unknown, we cannot exclude the possible enrichment or preference of one isoform over another. Thus, TBCD appears to bind and co-purify with αβ-tubulin heterodimers in the absence of ARL2 but with only β-tubulin when ARL2 is present.

To further confirm the composition of our TBCD/ARL2/β-tubulin complex, we removed the GST tag and analyzed the purified protein by BN-PAGE. Coomassie staining of the protein (Figure 4A, right lane) revealed a sharp band just below the 242 kDa size marker, consistent with the band observed in cell and tissue lysates (Figure 2), and in marked contrast to the TBCD/α-tubulin/β-tubulin trimer (Figure 4A, left lane). We then performed immunoblot analysis with TBCD, ARL2 and β-tubulin antibodies after resolving the sample by BN-PAGE. Figure 4B shows that all three proteins are present in the band at 200 kDa. We also note the presence of a more diffuse band at ~480 kDa that is observed by Coomassie staining and ARL2 and TBCD immunoblots of the purified TBCD/ARL2/β-tubulin complex. This band is consistently present, but highly variable in its relative abundance, and is perhaps a dimer of the trimer, or even an oligomer of TBCD and ARL2, as β-tubulin has not been observed in this band. As a final test of the composition of the TBCD/ARL2/β-tubulin trimer migrating at 200 kDa, we performed a two-dimensional gel analysis using sequential BN- and SDS-PAGE. After resolving the purified protein by BN-PAGE (first dimension; Figure 4A, right lane), the 200 kDa band was excised and minced gel pieces were loaded into the well of an SDS-PAGE gel (second dimension). Coomassie staining

of the SDS gel revealed three bands at the expected sizes, and no other bands (Figure 4C). We note that the sum of the molecular weights of TBCD (133 kDa), ARL2 (21 kDa) and β-tubulin (55 kDa) is 209 kDa and very close to our estimate of 200 kDa, based upon the electrophoretic mobility of the endogenous complex in BN gels. Similarly, the TBCD/ARL2/β-tubulin trimer eluted from the Superdex S200 column in fractions consistent with its apparent molecular weight of 200 kDa, in comparison to protein standards (data not shown). While these data are all consistent with a 1:1:1 complex, we cannot rule out the presence of two molecules of ARL2 or even a heterogeneous population with stoichiometries of 1:2:1 and 1:0:1 (TBCD/ARL2/β-tubulin), though we consider the latter unlikely. We consider it unlikely that β-tubulin is sub-stoichiometric with TBCD as the resulting difference in size should be evident in the BN-PAGE gels.

Because some differences have been noted between human and bovine TBCD (Cunningham and Kahn, 2008; Fanarraga et al., 2010; Tian et al., 2010) and their apparent affinities for tubulins, we also expressed and purified bovine GST-TBCD from HEK cells. The bovine protein behaved in all respects comparable to the human TBCD in terms of levels of expression and co-purification with other proteins, both when expressed alone or when co-expressed with human ARL2 (data not shown). Note that human and bovine ARL2 proteins are 100% identical. Thus, using recombinant preparations of TBCD purified from HEK cells, we have demonstrated its ability to bind specifically to either the αβ-tubulin dimer or to ARL2 and β-tubulin. The latter trimer displays the same electrophoretic mobility in BN-PAGE as the native complex seen in human and mouse cells and tissues; therefore, we conclude that the TBCD/ARL2/β-tubulin trimer is present in a wide array of animal cells and is the predominant form of TBCD found in many of them.

*TBCE can bind to the TBCD/ARL2/β-tubulin trimer or to TBCB/α-tubulin:* Because two different models for tubulin folding propose a central role for TBCE, acting in concert with TBCD (Tian et al., 1996; Nithianantham et al., 2015), we sought to extend our analyses of TBCD complexes using the HEK system. Thus, we next examined the effects of co-expression with

cofactor E (TBCE), cofactor B (TBCB), and cofactor C (TBCC) on complex assembly and stability. We obtained plasmids that direct the expression of untagged human TBCB, TBCC (the generous gift of Dr. Zabala, University of Cantabria, Spain), or TBCE. We also generated an expression vector, analogous to that used for GST-TBCD, to direct expression of GST-TBCE, as described under Experimental Procedures.

Expression of GST-TBCE, followed by affinity purification, yielded a single band migrating in SDS gels with an apparent molecular weight of ~85 kDa, appropriate for this 58 kDa protein fused to the ~28 kDa GST (Figure 5, lane 5). GST-TBCE expressed to the highest level of any protein or combination of proteins tested in our lab, with a yield of up to 30 mg purified protein from a liter of adherent HEK cells (~$10^9$ cells). No tubulins or other proteins co-purified with GST-TBCE, as assessed by Coomassie blue staining of the purified preparation (not shown). In contrast, when TBCB was co-expressed with GST-TBCE, the affinity purified preparation included GST-TBCE and faint bands migrating at ~28 kDa and 55 kDa that are consistent with TBCB and tubulin, respectively (Figure 5, lane 5). Immunoblotting confirmed the presence of α-, and absence of β-tubulin in this preparation (Figure 5, bottom two panels). The amounts of TBCB and α-tubulin that co-purified with GST-TBCE were more variable and always sub-stoichiometric, as judged by intensity of Coomassie blue staining. We have not performed extensive buffer optimization for this trimer or worked with it as much as the TBCD/ARL2/β-tubulin trimer but it appears to be less stable to subunit dissociation, predicted to be contributing to the variability or inconsistencies observed. Thus, co-expression in HEK cells can recapitulate the formation of the TBCE/TBCB/α-tubulin trimer described earlier and characterized, structurally and functionally, after reconstitution from components by Serna, *et al.* (Serna et al., 2015), though our preparation is not suitable for such structural analyses.

When we co-expressed GST-TBCD, ARL2, and (untagged) TBCE in the HEK system, we found that the TBCE specifically co-purified, resulting in a complex of TBCD/ARL2/β-tubulin/TBCE, again with no α-tubulin (Figure 5, lane 4). Thus, when present at comparable

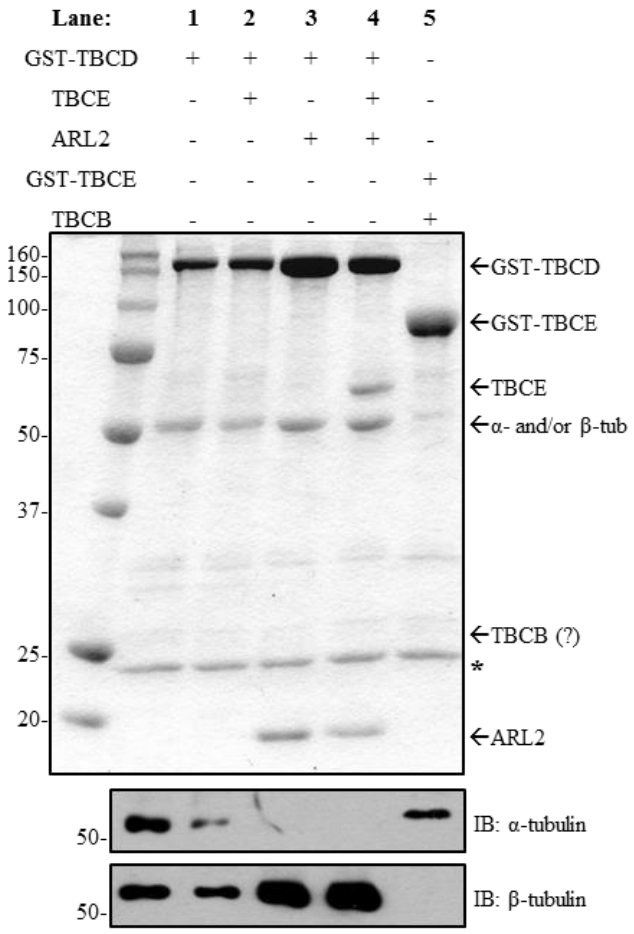


**Figure 2-5. Summary of TBCD complexes purified from HEK cells.** The indicated combinations of tubulin cofactors and ARL2 were expressed in HEK cells, followed by affinity purification. The protein complexes were isolated by batch purification, as described in Experimental Procedures, with SDS sample buffer added directly to the beads, then resolved in a 13% SDS-PAGE gel and stained with Coomassie blue. The asterisk indicates a glutathione-binding contaminant. The same samples were also diluted 1:10 in SDS sample buffer and analyzed by immunoblot for α- and β-tubulin (bottom panels). Note that TBCE is only co-purifying with TBCD when ARL2 is also present, and that TBCE specifically co-purifies with α- but not β-tubulin.

amounts, the TBCE can bind to the TBCD/ARL2/β-tubulin trimer and does so independently of α-tubulin. In contrast, co-expression of TBCD and TBCE (without ARL2) resulted in the purification of only the TBCD/α-tubulin/β-tubulin complex described above (Figure 5, lane 2). Thus, in this system, TBCE appears to require ARL2 and/or the absence of α-tubulin to bind TBCD (Figure 5, lane 4). Although the TBCE in this novel complex appears to be sub-stoichiometric, based upon Coomassie blue staining, we note that we have generated a similar complex to that argued in Nithianantham, et al (Nithianantham et al., 2015) to be the central scaffold involved in tubulin folding in yeast. However, in our case, and in contrast to that previous study, there is always β-tubulin present in the different TBCD complexes. Indeed, in each of the different combinations of protein co-expressions, summarized in Figure 5, we have never found TBCD to purify without one or both tubulins.

Because the binding of TBCC to the TBCD/TBCE/α-tubulin/β-tubulin complex is proposed to release the fully folded tubulin dimer, we also tested for effects of co-expression of human TBCC with GST-TBCD and ARL2. TBCC co-expression had no discernible effect on the complexes purified when co-expressed with (a) TBCD, (b) TBCD + TBCE, (c) TBCD + ARL2, or (d) TBCD + ARL2 + TBCE (data not shown). TBCC also did not co-purify with any of the protein combinations, despite being expressed in a soluble form in these cells.

In a separate series of experiments, we also attempted to reconstitute the TBCD/ARL2/β-tubulin trimer from purified components. Though β-tubulin has recently been shown to be stable as a monomer in solution (Montecinos-Franjola et al., 2016), it was not available to us in large quantities. Thus, we used commercially available porcine brain tubulin (Cytoskeleton, Cat. HTS03-A) as a source of the tubulin heterodimer. No combination of this tubulin preparation with recombinant, purified human ARL2 (from *E. coli* or HEK cells) and human GST-TBCD (from HEK cells) yielded assembly into any complexes (data not shown). The finding that the GST-TBCD preparation used in these studies appears to be at least partially aggregated makes interpretation of these results quite limited. Because (1) the 200 kDa complex found to be the most

abundant form of TBCD and ARL2 in a number of tissues and cell lines and (2) characterized here to be a very stable trimer containing β- but not α-tubulin and (3) was found able to bind TBCE when ARL2 was present, we believe that the TBCD/ARL2/β-tubulin trimer is likely to serve a central role as a scaffold for assembly of other cofactors, including TBCE, involved in tubulin biogenesis.

*ARL2 mutants that lose TBCD binding have reduced ability to alter microtubule densities:* Both ARL2 and TBCD have multiple actions in mammalian cells. They are each implicated in tubulin folding and microtubule dynamics, which are expected to be sensitive to the levels of tubulin dimer in cells. This makes dissection of specific functions and interactions technically challenging. To begin to assess the biological actions of one or more complexes of ARL2 with TBCD, we designed a series of mutations in ARL2 that were each predicted to compromise binding to TBCD. No structural information is currently available for TBCD so we instead based our mutants on residues shown by co-crystal structures to be involved in ARL2 binding to other known effectors, including BART and phosphodiesterase delta (PDEδ) (Hanzal-Bayer et al., 2002; Zhang et al., 2009). We focused on the residues directly involved in effector interactions that were found within the three GTP-binding, conformation-sensitive switch regions of ARL2: the amphipathic N-terminus and the canonical switch I and II regions present in all regulatory GTPases, which are known to bind effectors. Based on this information, we constructed the following ARL2 mutants: Δ1-9 (deletion of the first 9 residues), L3A, I6R and F50A. The last of these previously has been shown to disrupt interaction with TBCD (Bhamidipati et al., 2000). We also included ARL2 dominant inactivating and activating mutants, T30N and Q70L, respectively, in our binding assays. We co-expressed each of the ARL2 mutants with GST-TBCD in HEK cells, purified using glutathione-Sepharose, and analyzed the results by SDS-PAGE. Surprisingly, each of the ARL2 mutants we tested co-purified to similar levels as wild-type ARL2, with no apparent differences in the composition of the trimer (data not shown). Because our data strongly suggest that TBCD is stabilized by ARL2 binding (Figure 4A), we considered the possibility that even a mutant with

weakened affinity would still bind and co-purify with TBCD, absent an alternative. Therefore, we developed a novel "relative binding assay" in which GST-TBCD was co-expressed with ARL2 and each of the ARL2 mutants. To differentiate between the two expressed ARL2 proteins, we used C-terminal, HA-tagged ARL2 (ARL2-HA) as it migrates more slowly in SDS-PAGE and is readily distinguished from the un-tagged proteins. Thus, GST-TBCD was co-expressed with two different ARL2 constructs, purified as before, and analyzed by SDS-PAGE, followed by immunoblotting. Two examples are shown in Figure 6A. On the left we compare the levels of expression of ARL2 and ARL2-HA in the soluble fraction of the cell lysate (S14, see Experimental Procedures) and after affinity enrichment/pulldown (PD). Clearly the presence of the C-terminal HA tag does not alter the level of expression or binding to GST-TBCD as both ARL2 proteins are pulled down in equal amounts. In contrast, the F50A mutant was found to express to higher levels than wild-type ARL2 but was very poorly brought down with TBCD. To quantify the relative abilities of the different ARL2 mutants to co-purify with GST-TBCD, we immunoblotted the co-purifying ARL2 proteins and quantified by densitometry using infrared fluorescence scans from a LI-COR Odyssey imaging system, as described under Experimental Procedures. While most ARL2 mutants expressed to similar levels in HEK cells, the ARL2[T30N] and ARL2[F50A] mutants did not, with decreased and increased expression levels over wild-type, respectively. To account for any differences in protein expression, the soluble fractions (S14) from cell lysates were immunoblotted for ARL2 and the relative expression levels ($R_{exp}$) were determined for each mutant by densitometry as the ratio of ARL2-HA/ARL2 mutant. Similarly, the relative levels of ARL2 co-purifying with GST-TBCD ($R_{pur}$) were determined after small scale purifications, again from scans of immunoblots (Figure 6). Each of these values were determined for each mutant as averages from triplicates of independently transfected wells of cells. Finally, to quantify the effect of each mutant, the ratio of expression levels was divided by the ratio of purification levels ($R_{exp}/R_{pur}$), and these results were normalized to the final ratio obtained for ARL2-HA/ARL2 (Figure 6B). A result greater than 1 indicates the mutant bound preferably to the ARL2-HA, while a value of less than 1

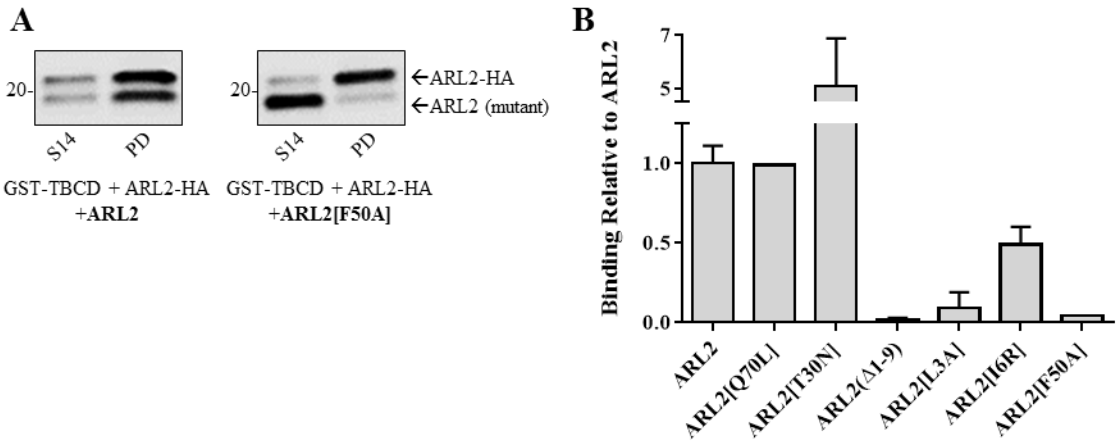


**Figure 2-6. Identification of point mutations in ARL2 that compromise binding to TBCD**. (**A**) Tagged ARL2-HA and different ARL2 mutants were co-expressed with GST-TBCD in HEK cells and purified in small scale. The clarified lysates (S14) and purified products (PD) were analyzed by a 4-20% SDS-PAGE gel and immunoblotted for ARL2 to monitor levels of expression and association with TBCD, respectively. Co-expression of GST-TBCD with ARL2-HA and either ARL2 or ARL2[F50A] are shown here as examples. (**B**) The relative level of co-purification of each ARL2 mutant was quantified, as described in Experimental Procedures. Error bars represent one standard deviation.

suggests that the mutant was less effective than ARL2-HA in binding to GST-TBCD. Results from this analysis reveal that the dominant activating mutant, ARL2[Q70L], binds comparably to ARL2 and ARL2-HA, while three of the other mutants tested (Δ1-9, L3A, F50A) displayed markedly decreased binding to GST-TBCD (0.02 ± 0.01, 0.09 ± 0.1, 0.04 ± 0.00, respectively). The I6R mutant bound more than these three but was still only about half as effective ARL2-HA. Interestingly, the dominant inactivating mutant, ARL2[T30N], showed about a 5-fold increase in co-purification compared to ARL2-HA. This result is consistent with previously published data that found this mutant more effective at reversing the effects of TBCD expression on microtubule levels in cells (Bhamidipati et al., 2000). Thus, the two point mutants, L3A or F50A, or the 9 residue N-terminal truncation mutant were each found to be clearly compromised in the ability to bind TBCD in this assay.

Expression of ARL2[Q70L] causes the loss of polymerized microtubules in cultured cells (Zhou et al., 2006) (Figure 7A). We reasoned then that combining this activating mutation with one that compromises binding to TBCD would give us correlative evidence to assess whether these two processes, ARL2 binding to TBCD and regulation of microtubule densities, are linked. We combined the loss-of-binding mutants with ARL2[Q70L] to generate the following double mutants: ARL2[L3A, Q70L], ARL2[I6R, Q70L] and ARL2[F50A, Q70L]. We expressed these mutants, as well as ARL2 and ARL2[Q70L], in HeLa cells and performed immunocytochemistry with ARL2 and α-tubulin antibodies, to mark transfected cells and microtubule arrays, respectively (Figure 7A). To quantify the effects, microtubule densities were scored in three categories: normal, intermediate loss, and severe loss (examples of each of these are shown in Figure 7B). Cells from each population were also immunoblotted with antibodies specific to ARL2 to compare relative expression levels of the ARL2 constructs (Figure 7C). We note that the expression level of each double mutant is higher than the ARL2[Q70L] positive control. Therefore, the varying expression levels of the ARL2 constructs are not expected to dramatically affect the results of the assay. Figure 7D summarizes the quantified effects of the ARL2 mutants on microtubule densities. Consistent

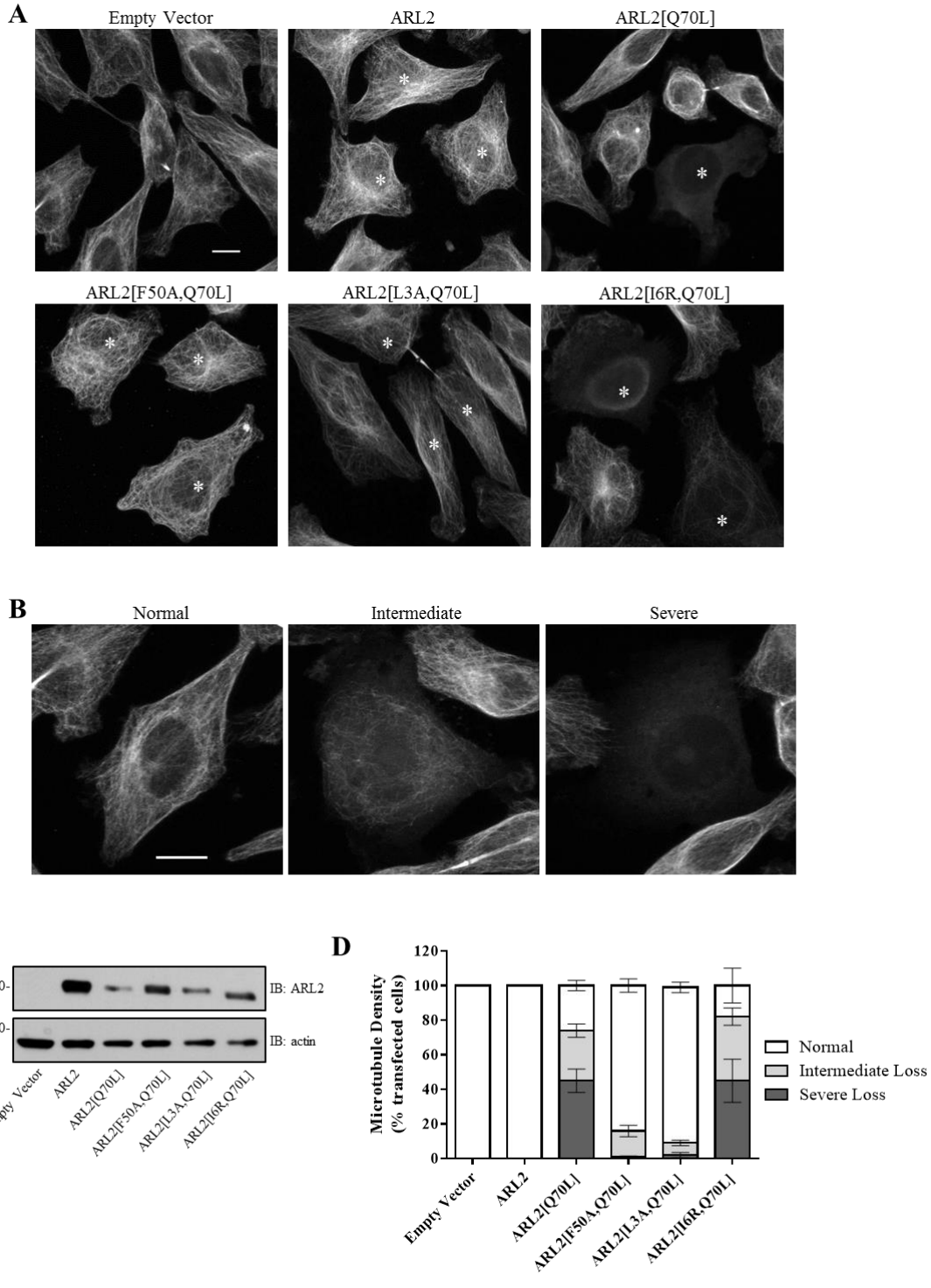
A
Empty Vector
ARL2
ARL2[Q70L]
ARL2[F50A,Q70L]
ARL2[L3A,Q70L]
ARL2[I6R,Q70L]
B
Normal
Intermediate
Severe
C
20-
50-
IB: ARL2
IB: actin
Empty Vector
ARL2
ARL2[Q70L]
ARL2[F50A,Q70L]
ARL2[L3A,Q70L]
ARL2[I6R,Q70L]
D
Microtubule Density (% transfected cells)
120
100
80
60
40
20
0
Normal
Intermediate Loss
Severe Loss
Empty Vector
ARL2
ARL2[Q70L]
ARL2[F50A,Q70L]
ARL2[L3A,Q70L]
ARL2[I6R,Q70L]

**Figure 2-7**. **ARL2 double mutants reverse the microtubule loss phenotype caused by ARL2[Q70L] expression.** (**A**) HeLa cells were transiently transfected with plasmids directing the expression of ARL2 or point mutants, fixed 3 days later, and stained for ARL2 and α-tubulin. Transfected cells were identified by increased ARL2 staining (not shown), and are indicated with an asterisk. Note the loss of the microtubule array in the one cell expressing ARL2[Q70L] in the top right panel, but its retention in others. (**B**) Representative images of cells stained with α-tubulin and scored as having normal microtubule density, intermediate microtubule loss, and severe microtubule loss, as described under Experimental Procedures. (**C**) Clarified lysates of the same cells shown in panel A were immunoblotted for ARL2, to show relative levels of expression, with actin serving as a loading control. (**D**) The effect of each ARL2 construct on microtubule density was scored, using the classifications highlighted in panel B. Error bars represent standard deviation, and the average of 3 independent experiments is shown, with N greater than 200 cells per condition. Scale bars in **A** and **B** represent 10 μm.

with earlier studies, cells expressing ARL2[Q70L] showed a dramatic loss in polymerized microtubules, with ~75% of transfected cells displaying at least partial loss of microtubule arrays (Figure 7D). However, cells expressing ARL2[L3A, Q70L] or ARL2[F50A, Q70L] showed a reversal of this microtubule loss phenotype, with <10% and <20%, respectively, of transfected cells showing only intermediate loss in microtubule densities. In contrast, the addition of the I6R mutation to the Q70L did not reverse the effects of the dominant mutant on microtubule densities. Rather, this mutation, which showed only partial loss in relative affinity for TBCD (Figure 6B), displayed only a slight increase in the percentage of cells displaying the intermediate phenotype (Figure 7D). Thus, these results show a correlation between the ability of ARL2 and ARL2 mutants to bind TBCD and to alter microtubule dynamics in a cell-based assay, though not surprisingly the two assays are not quantitatively comparable.

**Discussion**

We set out years ago to examine the roles of ARL2 and TBCD in the αβ-tubulin biosynthesis and microtubule destruction pathways. We had previously purified ARL2 from bovine tissues and found it to co-purify with TBCD, but the heterodimer was inactive in tubulin folding or GTPγS binding assays (Shern et al., 2003). In contrast, Cowan and colleagues had found that ARL2 inhibits the binding of TBCD to αβ-tubulin in their *in vitro* system, essentially competing for the binding of β-tubulin to TBCD and preventing TBCD from dissociating the αβ-tubulin heterodimer, which they termed the tubulin destruction pathway (Bhamidipati et al., 2000). We began here by monitoring the quaternary state of ARL2 and TBCD in cytosol from cultured mammalian cells and mouse tissues and found several cell lines and tissues in which the clear majority of each protein co-fractionated in both native polyacrylamide gels and gel filtration media, though this was also quite variable between tissues and even species. When TBCD and ARL2 were overexpressed in HEK cells and affinity purified, β-tubulin was shown to co-purify in a novel TBCD/ARL2/β-tubulin trimeric complex with an estimated 1:1:1 stoichiometry. The characterization of this and

related complexes revealed several features in common with results from the Cowan lab but also some clear differences that ultimately lead us to different conclusions regarding the likely roles of ARL2 in tubulin biology and the nature of the complex(es) in which it acts. Most importantly, we find that every time we purify TBCD from cultured human cells it co-purifies with at least one tubulin. Additionally, when ARL2 is present in sufficient amounts the complex includes ARL2, resulting in a more stable and homogeneous complex. TBCE can bind to the TBCD/ARL2/β-tubulin complex, even in the absence of α-tubulin. We discuss below the novel protein complexes described herein and how they are thought to relate to previously described complexes.

We found the predominant form of both ARL2 and TBCD in many cells and tissues to be a complex of ~200 kDa that co-migrates in native gels and co-purified from HEK cells as an apparent 1:1:1 complex of TBCD/ARL2/β-tubulin. This trimer has not been described before, though we speculate it was present in previous studies (Bhamidipati et al., 2000). The assays developed in the Cowan lab that identified the five tubulin co-chaperones, or cofactors A-E, used low percentage (8%) polyacrylamide gels to assess protein purity (Tian et al., 1996; Tian et al., 1997). At 20 kDa, ARL2 runs at the dye front in such gels and was likely simply not appreciated to be a partner of TBCD. This conclusion is supported by our observations that we have never found a preparation of TBCD that is mono-disperse and stable that lacks ARL2. Thus, we believe the "middle band" described in Tian, et al (Tian et al., 1996) that was identified by addition of TBCD to *in vitro* translated β-tubulin, and migrated in native gels with a size of 200-300 kDa, contains ARL2 in addition to the TBCD and β-tubulin described. And later, when ARL2 was found to bind to TBCD, they found that addition of TBCD to *in vitro* translated ARL2 resulted in the formation of a ~200 kDa complex, which was shown to contain ARL2 and TBCD but was not analyzed for β-tubulin (Bhamidipati et al., 2000). The consistent observations in multiple laboratories that gel filtration or native gels yield apparent molecular weights for TBCD in the range of 200-300 kDa has been interpreted as possible homo-dimerization, but we believe is the result of a heterotrimer that actually migrates very close to its expected size of 208 kDa. Thus, the TBCD/ARL2/β-tubulin trimer is a stable component in a

wide array of mammalian cells and tissues that we have purified in milligram amounts from HEK cells, and we speculate was present and functional in the tubulin folding assays that first identified the cofactors. This is consistent with our conclusion that TBCD/ARL2/β-tubulin is an intermediate in the folding reaction. Indeed, based upon our re-interpretation of the pioneering work of Cowan and colleagues, we propose that it is the central scaffold onto which α-tubulin is later added, in concert with TBCE and TBCB.

We also found that in the absence of ARL2, TBCD bound and co-purified with αβ-tubulin, generating the TBCD/α-tubulin/β-tubulin trimer, though as purified from HEK cells this is not stable as a monodisperse species. Addition of purified ARL2, either from bacteria or HEK cells after overexpression, to this trimer had no effect; *i.e.*, it did not bind stably or alter the amount or ratio of tubulins bound. This is in apparent contradiction to work described in Bhamidipati, *et al*. (Bhamidipati et al., 2000) in which addition of TBCD to *in vitro* translated tubulin dimers resulted in the formation of a new band in native gels that is thought to be a dimer of TBCD/β-tubulin, though α-tubulin was not monitored in that study. Addition of ARL2 in that system decreased the amount of tubulin dimers binding to TBCD, which was interpreted as ARL2 competing for the binding of TBCD and β-tubulin. They even speculate that the appearance of another band, present only when excess ARL2 was added, was the TBCD/ARL2/β-tubulin trimer. In contrast, we have never observed evidence of a TBCD/ARL2 or TBCD/β-tubulin dimer in, or coming from, the HEK cell expression system. Trivial explanations for these differences might be found in the different gel systems, protein preparations, or assays used. But another model to explain these apparent differences is that TBCD can bind to tubulin dimers, perhaps even in both dimeric and polymerized (microtubule) states. Thus, the band generated upon addition of TBCD to *in vitro* translated αβ-tubulin dimers could be the same as our TBCD/α-tubulin/β-tubulin trimer, which in Bhamidipati, *et al*. (Bhamidipati et al., 2000) is partially converted to the TBCD/ARL2/β-tubulin trimer, the extra band they see in excess ARL2.

Our ability to purify the TBCD/α-tubulin/β-tubulin trimer, even though not mono-disperse, is compelling evidence of a specific interaction between TBCD and tubulin heterodimers. This specific trimer of TBCD/α-tubulin/β-tubulin might result in cells from (1) residual TBCD binding to recently folded αβ-tubulin based upon the Cowan model of folding (*i.e.*, slow release or resolution of a larger complex involved in the final step of folding), (2) TBCD binding to previously folded, native αβ-tubulin (perhaps the "tubulin destruction" pathway), or (3) TBCD binding to microtubules with resulting loss of microtubule integrity and at least a quasi-stable trimer. We cannot currently distinguish between these possibilities. However, because overexpression of TBCD results in the loss of microtubules in cells (Bhamidipati et al., 2000; Martin et al., 2000; Cunningham and Kahn, 2008) we believe option 3 to be the most likely source of this trimer from cells. More work is clearly needed to provide stronger testing of these models.

Prior to this study, there have been two different complexes of ARL2 and TBCD that have been purified. One of these complexes was identified in a previous study from our lab by following ARL2 through several chromatographic steps using bovine tissues as the source (Shern et al., 2003). This produced a complex of ARL2, TBCD, and the protein phosphatase 2A, though we now believe this to be coincidental co-purification of PP2A. Notably, there was no evidence of tubulin in this preparation. A recent study by Nithianantham, et al (Nithianantham et al., 2015) showed that co-expression and purification of yeast orthologs of TBCD, TBCE and ARL2 (CIN1p/PAC2p/CIN4p) from bacteria resulted in the formation of the orthologous TBCD/TBCE/ARL2 complex. As this complex was purified from bacteria, there was no opportunity for co-purification of tubulin. However, they showed that purified tubulin heterodimer could bind the complex *in vitro*. Though both of these approaches to purifying TBCD/ARL2 complexes have merit and are predicted to produce biologically active complexes, the methods used in this current study allowed us to identify the predominant form of ARL2 and TBCD in many mammalian cells (*i.e.*, TBCD/ARL2/β-tubulin) and generate mg amounts of the purified complex. Based on the ability to add other tubulin cofactors to this complex, namely TBCE, and its predominance in a number of tissues and cell

lines, we posit that the TBCD/ARL2/β-tubulin trimer is a key scaffold onto which other proteins bind in the tubulin biogenesis pathway. Admittedly, further characterization of these ARL2/cofactor complexes will be required to continue the development of a more complete model of tubulin folding and the effects of TBCD and ARL2 on tubulin pools and microtubule arrays.

The identification of ARL2 mutants that disrupt interaction with TBCD, and thus formation of the TBCD/ARL2/β-tubulin complex, has allowed us to test the biological relevance of the ARL2-TBCD interaction, using a cell-based assay in correlation with a novel ARL2-TBCD binding assay. Combining these mutants (L3A, I6R, and F50A) with the dominant activating ARL2[Q70L], which causes wholesale loss of microtubules, revealed a good correlation between loss of TBCD binding and loss of effects on microtubules. ARL2[Q70L] is considered constitutively active due to its inability to hydrolyze GTP. As the relative binding assay shows, this mutant binds to TBCD at similar levels to wild-type ARL2. Thus, when ARL2[Q70L] is expressed in cells, at several fold higher levels than endogenous ARL2, we believe that the ARL2[Q70L] is incorporated into the TBCD complex in place of the endogenous protein. The resulting loss of polymerized microtubules may then result from the inability of ARL2[Q70L] to cycle between GTP- and GDP-bound conformational states as a result of the absence of the glutamine that is directly involved in hydrolysis of the gamma phosphate. This interesting, but unproven model, clearly places conformational changes occurring in ARL2 as an important component in the effects on microtubules in cells and should be examined further in later studies. When the loss-of-binding double mutants (L3A or F50A with Q70L) are expressed, they are unable to cause the loss of microtubules, presumably due to their relative inability to complex with TBCD. Therefore, it seems that not only the binding of ARL2 to TBCD/β-tubulin is important, but that the hydrolysis of guanine nucleotide on the bound ARL2 is required for proper microtubule regulation. Indeed, in a related study (Francis, et al; manuscript in preparation) we show that ARL2, but not β-tubulin, binds guanine nucleotides in the TBCD/ARL2/β-tubulin trimer.

The use of second site mutations combined with dominant activating (Q70L) mutation of ARL2 has also proven to be invaluable in cleanly dissecting the roles of ARL2 in tubulin folding/microtubule density from those inside mitochondria; *i.e.*, regulating mitochondrial fusion from the intermembrane space (Newman, et al; manuscript submitted). Though not important to the current study, about 5-10% of cellular ARL2 is found inside mitochondria (Sharer and Kahn, 1999), and when the ARL2[Q70L] mutant is expressed, mitochondria become hyperfused/elongated (Newman, et al; manuscript submitted). When the additional mutations used here were tested for effects on mitochondria, we found that ARL2[L3A, Q70L], ARL2[I6R, Q70L], and ARL2[F50A, Q70L] each retained full activity in mitochondrial fusion, despite the complete or nearly complete loss of binding to TBCD (Figure 6) or effects on microtubules (Figure 7). Due to its multiple cellular functions, such mutational analyses are predicted to be increasingly important in deconvoluting the complexities of signaling by this one essential, regulatory GTPase. Because the design of the ARL2 mutants was based on crystal structures of ARL2 bound to other effectors, it is almost certain that expression of these mutants in cells may also disrupt other ARL2 interactions. However, of the known ARL2 binding proteins, TBCD is the only one that has an integrated role in the production of αβ-tubulin heterodimer and in the regulation of microtubule stability. Thus, we conclude that the effect of the ARL2 mutants on polymerized microtubules is specifically due to the interaction between ARL2 and TBCD, and ultimately the formation of the TBCD/ARL2/β-tubulin complex.

Further evidence of the importance of the TBCD/ARL2/β-tubulin complex has been recently highlighted by Flex, *et al*. (Flex et al., 2016), in which several point mutations in TBCD were described that lead to neurodegenerative disorders in humans. When a subset of the identified TBCD mutants were co-expressed with ARL2 in our HEK cell system, they result in a reduced amount of β-tubulin in the TBCD/ARL2/β-tubulin complex. Additionally, the purified complexes each have reduced stability (lower melting point, $T_m$) in a thermal denaturation assay (Flex et al., 2016). The study also analyzed patient cells in an *in vivo* tubulin polymerization (nocodazole

washout) assay. The TBCD mutants that had reduced binding to β-tubulin showed an increase in the rate of tubulin polymerization, compared to control cells. Similar studies have recently added to our appreciation of the importance of TBCD and its binding to ARL2 and β-tubulin in related neurological syndromes (Edvardson et al., 2016; Ikeda et al., 2016; Miyake et al., 2016; Pode-Shakked et al., 2016). Together these findings argue that the TBCD/ARL2/β-tubulin complex is vital for proper homeostasis that is required in microtubule dynamics and human health.

In addition to the very stable trimer of TBCD/ARL2/β-tubulin, we also purified from HEK cells the tetramer of TBCD/ARL2/β-tubulin/TBCE, though the stoichiometry of the TBCE in the complex was more variable and lower than the other three components. The functional significance of this complex is difficult to evaluate at this point but could be used to identify sites in the other three proteins to which TBCE binds. It also suggests that α-tubulin is not required for binding of TBCE to TBCD-containing complexes, though it is possible that its presence may increase the affinity. The finding that the HEK cell system could also confirm the formation in mammalian cells of a different trimer, consisting of TBCE/TBCB/α-tubulin, structurally analyzed by Serna, et al (Serna et al., 2015), we interpret as yet further evidence that this expression system will be of tremendous value in the further testing of models of tubulin folding. We hope it will also allow researchers to reconstitute the folding of tubulins in milligram amounts for a variety of uses.

Thus, we conclude that ARL2 plays an essential role in the cellular actions of TBCD, but rather than competing with the binding of β-tubulin, facilitates it. As a consequence, we propose the TBCD/ARL2/β-tubulin complex to be a key player in the folding process and potentially separately in regulating the lifetime or stability of the microtubule array. Finally, the studies by Flex, et al (Flex et al., 2016) and others (Edvardson et al., 2016; Ikeda et al., 2016; Miyake et al., 2016; Pode-Shakked et al., 2016) highlight the clinical significance of the TBCD/ARL2/β-tubulin trimer, and suggest that continued study of this complex will prove beneficial to both the scientific and clinical communities.

**Experimental Procedures**

*Cell Culture:* Human cervical carcinoma (HeLa), human embryonic kidney (HEK293T/17), mouse Neuro2A (N2A) neuroblastoma, mouse embryonic fibroblast (NIH-3T3), and human neuroblastoma (SH-SY5Y) cells were obtained from the ATCC and grown in DMEM (Invitrogen, Carlsbad, CA) supplemented with 10% fetal bovine serum and 2 mM glutamine at 37°C in the presence of 5% $CO_2$. Cells were screened for mycoplasma regularly by staining with Hoechst 33342 DNA dye, usually in conjunction with immunofluorescence experiments (described below).

*Plasmids:* Plasmids directing expression of human ARL2, ARL2[T30N], or ARL2[Q70L] used pcDNA3.1 as vector, as described previously (Zhou et al., 2006), and were used as starting points to generate plasmids used for expression of the following mutants through PCR-based mutagenesis: ARL2[L3A], ARL2[I6R], ARL2[F50A], ARL2[L3A, Q70L], ARL2[I6R, Q70L], ARL2[F50A, Q70L], ARL2-HA, and HA-ARL2. A plasmid containing human TBCD (NP_005984.3) was obtained from the ATCC (clone MGC-1583) and the full length open reading frame was moved into the pLEXm-GST vector (gift from James Hurley, NIH) at NotI and XhoI sites to generate an N-terminal, GST-tagged construct (GST-TBCD). Full length bovine TBCD was cloned into the same sites. The construct has a TEV protease cleavage site between the GST and TBCD, which results in a 12 amino acid residual extension at the N-terminus of TBCD after cleavage. A plasmid containing the full length open reading frame of human TBCE was purchased from ATCC (Cat. MGC-8912, Lot 61980096) and directs expression of isoform A (NP_003184.1). TBCE was also cloned into the pLEXm vector using SacI and SphI sites, inserted with PCR, to generate pLEXm-GST-TBCE. Plasmids directing expression of human TBCB or TBCC were the generous gift of Juan Carlos Zabala (Univ. of Cantabria, Madrid, Spain) and were both in pcDNA3.1.

*Antibodies:* Affinity-purified rabbit polyclonal ARL2 (R-86336) antibodies were prepared as described in Sharer and Kahn (Sharer and Kahn, 1999). Affinity-purified rabbit polyclonal

TBCD antibodies were prepared as described in Cunningham and Kahn (Cunningham and Kahn, 2008). As these two rabbit polyclonal antibodies were generated in our lab and purified whole protein antigens are readily available, we routinely perform antigen competition experiments to confirm specificity of signals in both immunoblot and immunofluorescence experiments. Other antibodies used in this study included a rabbit polyclonal GST (Sigma, Cat. G7781), mouse monoclonal actin (Sigma, Cat. A3853), mouse monoclonal α-tubulin (Sigma, clone DM1A, Cat. T9026), and mouse monoclonal β-tubulin (Developmental Studies Hybridoma Bank, Univ. of Iowa, Cat. E7-c).

*Cell transfections:* For immunofluorescence experiments, cells were transfected at ≥90% density in 6-well plates. The numbers given here are for transfection of a single well. The amount of DNA and Lipofectamine were separately optimized for ARL2 expression in HeLa cells. A ratio of 2 µg:1 µg (Lipofectamine:DNA) yielded the highest transfection efficiency. ARL2 plasmids (2 µg) were diluted in 250 µL Optimem (Invitrogen). Lipofectamine 2000 (4 µg; Invitrogen) was diluted in a separate tube containing 250 µL Optimem, vortexed briefly, and incubated at room temperature for 5 minutes. The tubes were mixed and incubated for 20 minutes at room temperature. Cell culture medium was changed to 1 mL of fresh growth medium (DMEM + 10% FBS), and transfection complexes (500 µL) were added dropwise to the cells. After 24 hours, cells were trypsinized and re-plated onto coverslips, typically at a 1:4 split. Cells were allowed to attach overnight before fixation. This transfection typically resulted in ~70% of cells expressing exogenous ARL2 and ~50% expressing ARL2[T30N] or ARL2[Q70L] when assayed 48 hours after the start of transfection.

For recombinant protein purifications, HEK cells were transfected at 70-90% density using polyethyleneimine (PEI; Polysciences, Cat. 24765-2) at a 1:3 ratio (DNA:PEI). In all transfections and co-transfections, plasmids were used at 1 µg DNA/mL medium and scaled accordingly for larger/smaller transfections. Prior to transfection, the DNA and PEI were mixed in 1 mL serum free medium and incubated at room temperature for 15 minutes. Cell culture medium was changed to 9

mL of a reduced serum medium (DMEM + 2% FBS), and the transfection mixture was added dropwise to the cells (10 mL final volume). After 48 hours, cells were harvested and the pellets either lysed immediately for purification or flash frozen in liquid nitrogen and stored at -80°C for later use.

*Preparation of cell/tissue lysates:* Cells were grown to confluence before collecting in PBS (140 mM NaCl, 2.7 mM KCl, 10 mM $Na_2HPO_4$, 1.8 mM $KH_2PO_4$, pH 7.4). Cell pellets were resuspended in lysis buffer (0.5 mL/~$10^7$ cells; 25 mM HEPES, 100 mM NaCl, 1 mM DTT, 1% CHAPS, pH 7.4) and incubated at 4ºC for 15 minutes with gentle rotation. The lysates were clarified by centrifugation at 100,000x*g* for 1 hour at 4ºC, and the resulting supernatant (S100) was collected. Mouse tissues were harvested from freshly euthanized animals, minced with a razor blade, resuspended in lysis buffer, and cells were lysed using a Dounce homogenizer, prior to centrifugation to generate the soluble fraction (S100). Bovine and human brain samples were obtained from frozen tissue stocks and similarly prepared to generate the S100.

*Gel electrophoresis:* Blue-Native Polyacrylamide Gel Electrophoresis (BN-PAGE) was performed using 4-16% Novex Bis-Tris gels (Invitrogen, Cat. BN1002) according to manufacturer's instructions. Native Mark protein standards (Invitrogen, Cat. LC0725) were used as references and to estimate sizes of protein complexes. Denaturing SDS-PAGE was performed using 13% or 4-20% (Bio-Rad, Cat. 4561096) acrylamide gels with Precision Plus Protein All Blue Standards (Bio-Rad, Cat. 1610373).

*Protein purification:* For purification of GST-tagged proteins, HEK cell pellets were resuspended in 0.5 mL (per 10 cm plate/~$10^7$ cells) of lysis buffer (25 mM HEPES, 100 mM NaCl, 1 mM DTT, 1% CHAPS, pH 7.4, supplemented with protease inhibitor cocktail (Sigma, Cat. P2714)) and incubated at 4°C for 15 minutes with gentle rotation. For large pellets, a Dounce homogenizer was used to aid in resuspension/lysis. The lysate was clarified at 14,000x*g* for 30 minutes at 4ºC and the resulting supernatant (S14) was collected. Glutathione-conjugated Sepharose beads (GE, Cat. 17075601) were equilibrated with lysis buffer, and 100 µL slurry (~50

µL beads)/10 cm plate was added to the S14 and incubated overnight at 4°C with gentle rotation. The sample was then added to a Poly-Prep chromatography column (Bio-Rad, Cat. 7311550) and filtered by gravity. The column was washed with five column volumes of wash buffer (25 mM HEPES, 100 mM NaCl, 1 mM DTT, pH 7.4). The beads were then resuspended in 1 column volume of elution buffer (25 mM HEPES, 100 mM NaCl, 1 mM DTT, 20 mM glutathione, pH 8.0) and incubated at 4°C for 20 minutes before elution of the sample. Another column volume of elution buffer was added to the beads and immediately collected to maximize recovery. Eluted protein concentration was determined using a Bradford assay. In some instances, TEV protease was added to the sample at 1% (w/w) the amount of purified protein and allowed to incubate at 4°C for at least 4 hours and up to overnight. The cleaved sample was further purified by gel filtration over a Superdex 200 column (Pharmacia) and the fractions analyzed in SDS-PAGE gels. Appropriate fractions were pooled and concentrated by ultrafiltration as needed for use.

Alternatively, small-scale batch purifications of GST-tagged proteins was performed to allow analyses of protein complexes to be performed in a more high-throughput manner. Cells were transfected using PEI, as described above, in a 6-well plate and cell pellets resuspended in 200 µL of lysis buffer per well (~$10^6$ cells). After equilibration, 10 µL of glutathione-conjugated Sepharose beads (20 µL slurry) was added to the S14 of each sample and incubated overnight at 4°C with gentle rotation. The samples were spun at 14,000x*g* for 30 seconds to pellet the beads, and the supernatant was removed by careful aspiration. The beads were washed 3 times by adding 500 µL wash buffer and immediately spinning at 14,000x*g* for 30 seconds. After aspiration of the last wash, 20 µL of 2X SDS sample buffer was added directly to the beads and samples were heated at 95°C for 5 minutes. For Coomassie staining, 15 µL of each sample was loaded onto the gel. For immunoblotting, the samples were diluted 1:10 in 1X SDS sample buffer and 15 µL loaded onto the gel.

*Relative Binding Assay*: To quantify the effects of ARL2 mutants on interaction with TBCD, a relative binding assay was developed. GST-TBCD was co-expressed in HEK cells with

a C-terminally tagged ARL2-HA and an untagged ARL2 mutant. Batch purification was performed, as described above. During purification, a sample of S14 was collected, diluted 1:10 in wash buffer, and then diluted again (1:1) in 2X SDS sample buffer. For each ARL2 mutant tested, the S14 sample (15 µL) was loaded adjacent to the final product of the pulldown (PD; 15 µl, as described above). The samples were resolved by SDS-PAGE (4-20% acrylamide) and immunoblotted with ARL2 antibodies. A fluorescent secondary antibody (Invitrogen, Cat. A11374) was used, and the blots were imaged with an Odyssey imaging system (LI-COR). To account for differing levels of expression in the assay, the level of expression of ARL2-HA, as determined by densitometry, was compared to the expression level of the ARL2 mutant by taking the ratio of ARL2-HA:ARL2 mutant in the S14 sample ($R_{exp}$). The relative levels of ARL2-HA and ARL2 mutant co-purifying with GST-TBCD was similarly determined in the pulldown (PD) sample ($R_{pur}$). The ratio of expression levels was then divided by the ratio of co-purification levels ($R_{exp}/R_{pur}$), and these results were normalized to those obtained for ARL2-HA and wild-type ARL2 expression and co-purification with GST-TBCD. A final result greater than 1 indicates that the ARL2 mutant co-purified with GST-TBCD better than wild-type ARL2. A value less than 1 indicates that the mutant co-purified worse than wild-type, and a value equal to 1 implies that the mutant bound and co-purified similar to wild-type.

*Immunofluorescence:* Cells were grown on matrigel (BD Biosciences, Cat. 356231) coated coverslips. Cells were fixed in a pre-warmed (37°C) solution of 4% paraformaldehyde in PBS (v/v) and permeabilized with 0.1% (v/v) Triton X-100 in PBS for 10 minutes at room temperature. Incubation with primary antibodies was carried out in filtered PBS containing 1% (w/v) bovine serum albumin at 4°C overnight, followed by 4 x 5 minute washes in PBS. Secondary antibodies (1:500; Alexa fluorophores, Invitrogen) were incubated in the same buffer for 1 hour at room temperature, followed by 2 x 5 minute washes in PBS. DNA was stained with Hoechst 33342 for 4 minutes, followed by 2 x 5 minute washes in PBS, prior to mounting onto slides using Prolong Antifade (Invitrogen). Images were acquired using an Olympus FV1000 microscope and Olympus

Fluoview v1.7 software, using 488 and 543 laser excitation and a 100x oil objective (1.45 NA). Z-stacks were acquired with a step size of 0.37 μm, which were converted to average image intensity projections using ImageJ, where indicated.

Effects of protein expression on microtubule morphology were scored by visual inspection of fixed, stained HeLa cells. To quantify consequences of protein expression on microtubule density, we used the following categories, as previously described (Zhou et al., 2006): 1) complete loss = near or complete loss of microtubules, 2) intermediate loss = microtubule density is obviously lower than untransfected cells in the same field, 3) normal = transfected cell cannot be readily distinguished from untransfected cell in terms of microtubule density. A cell was excluded from analysis if it appeared to be dying, as defined by cell rounding with membrane blebs and fragmented nuclear staining; these cells typically had the highest levels of expression in the cell population. Only transfected cells were scored, which were identified by ARL2 immunofluorescence signal (ARL2 signal obviously brighter than surrounding cells in the field).

*Reproducibility and statistical analyses:* Every experiment described has been independently repeated at least twice. Protein preparations were performed multiple times and variations in composition or relative abundance of components are indicated in the text. For quantification of immunofluorescence assays experiments were independently repeated at least three times, and at least 200 cells per condition were analyzed per experiment. For quantification of the relative binding assay (see above), averages are the result of three independent experiments. Error bars for both sets of quantified data represent one standard deviation.

**Acknowledgements:** We would like to thank Dr. Juan Carlos Zabala (University of Cantabria, Spain) for the gift of the TBCB plasmid. We thank Dr. James Hurley (NIH) for the gift of the pLEXm vectors. We are also grateful to Drs. Alyssa Bushey Long and Tamara Caspary (Emory University) for the gifts of the mouse tissues, and thank the Emory Proteomics Core for the human tissue samples. This work was supported by grants from the National Institutes of Health

5R01GM090158 to RAK, 1F31CA189672 to JWF, and 1F31GM111047 to LEN, and an American Heart Association pre-doctoral fellowship 14PRE18840040 to LEN. This research was supported in part by the Emory University Integrated Cellular Imaging Microscopy Core and Proteomics Core of the Emory Neuroscience NINDS Core Facilities grant, P30NS055077. This study was also supported in part by the Emory Integrated Genomics Core (EIGC), which is subsidized by the Emory University School of Medicine and is one of the Emory Integrated Core Facilities. Additional support was provided by the National Center for Advancing Translational Sciences of the National Institutes of Health under Award Number UL1TR000454.

**Conflict of Interest:** The authors declare that they have no conflicts of interest with the contents of this article.

**Author Contributions:** JWF conducted most of the experiments, analyzed the data, and wrote the paper. LEN designed, performed and analyzed the experiments shown in Figure 7A, B and D. LAC designed, performed and analyzed the experiments shown in Figure 1. RAK coordinated the study and wrote the paper with JWF.

**References**

Antoshechkin, I. and Han, M. (2002). The C. elegans evl-20 gene is a homolog of the small GTPase ARL2 and regulates cytoskeleton dynamics during cytokinesis and morphogenesis. Dev Cell 2, 579-591.

Bhamidipati, A., Lewis, S.A. and Cowan, N.J. (2000). ADP ribosylation factor-like protein 2 (Arl2) regulates the interaction of tubulin-folding cofactor D with native tubulin. J Cell Biol 149, 1087-1096.

Bichet, P., Mollat, P., Capdevila, C. and Sarubbi, E. (2000). Endogenous glutathione-binding proteins of insect cell lines: characterization and removal from glutathione S-transferase (GST) fusion proteins. Protein Expr Purif 19, 197-201.

Chen, K., Koe, C.T., Xing, Z.B., Tian, X., Rossi, F., Wang, C., Tang, Q., Zong, W., Hong, W.J., Taneja, R., Yu, F., Gonzalez, C., Wu, C., Endow, S. and Wang, H. (2016). Arl2- and Msps-dependent microtubule growth governs asymmetric division. J Cell Biol 212, 661-676.

Clark, J., Moore, L., Krasinskas, A., Way, J., Battey, J., Tamkun, J. and Kahn, R.A. (1993). Selective amplification of additional members of the ADP-ribosylation factor (ARF) family: cloning of additional human and Drosophila ARF-like genes. Proc Natl Acad Sci U S A 90, 8952-8956.

Cunningham, L.A. and Kahn, R.A. (2008). Cofactor D functions as a centrosomal protein and is required for the recruitment of the gamma-tubulin ring complex at centrosomes and organization of the mitotic spindle. J Biol Chem 283, 7155-7165.

Edvardson, S., Tian, G., Cullen, H., Vanyai, H., Ngo, L., Bhat, S., Aran, A., Daana, M., Da'amseh, N., Abu-Libdeh, B., Cowan, N.J., Heng, J. and Elpeleg, O. (2016). Infantile Neurodegenerative Disorder Associated with Mutations in TBCD, an Essential Gene in the Tubulin Heterodimer Assembly Pathway. Human Molecular Genetics.

Edvardson, S., Tian, G., Cullen, H., Vanyai, H., Ngo, L., Bhat, S., Aran, A., Daana, M., Da'amseh, N., Abu-Libdeh, B., Cowan, N.J., Heng, J. and Elpeleg, O. (2016). Infantile

Neurodegenerative Disorder Associated with Mutations in TBCD, an Essential Gene in the Tubulin Heterodimer Assembly Pathway. Hum Mol Genet.

Fanarraga, M.L., Bellido, J., Jaen, C., Villegas, J.C. and Zabala, J.C. (2010). TBCD links centriologenesis, spindle microtubule dynamics, and midbody abscission in human cells. PLoS One 5, e8846.

Fanarraga, M.L., Carranza, G., Castano, R., Nolasco, S., Avila, J. and Zabala, J.C. (2010). Nondenaturing electrophoresis as a tool to investigate tubulin complexes. Methods Cell Biol 95, 59-75.

Fedyanina, O.S., Mardanov, P.V., Tokareva, E.M., McIntosh, J.R. and Grishchuk, E.L. (2006). Chromosome segregation in fission yeast with mutations in the tubulin folding cofactor D. Curr Genet 50, 281-294.

Flex, E., Niceta, M., Cecchetti, S., Thiffault, I., Au, M.G., Capuano, A., Piermarini, E., Ivanova, A.A., Francis, J.W., Chillemi, G., Chandramouli, B., Carpentieri, G., Haaxma, C.A., Ciolfi, A., Pizzi, S., Douglas, G.V., Levine, K., Sferra, A., Dentici, M.L., Pfundt, R.R., Le Pichon, J.B., Farrow, E., Baas, F., Piemonte, F., Dallapiccola, B., Graham, J.M., Jr., Saunders, C.J., Bertini, E., Kahn, R.A., Koolen, D.A. and Tartaglia, M. (2016). Biallelic Mutations in TBCD, Encoding the Tubulin Folding Cofactor D, Perturb Microtubule Dynamics and Cause Early-Onset Encephalopathy. Am J Hum Genet 99, 962-973.

Francis, J.W., Turn, R.E., Newman, L.E., Schiavon, C. and Kahn, R.A. (2016). Higher order signaling: ARL2 as regulator of both mitochondrial fusion and microtubule dynamics allows integration of two essential cell functions. Small GTPases, 0.

Gao, Y., Vainberg, I.E., Chow, R.L. and Cowan, N.J. (1993). Two cofactors and cytoplasmic chaperonin are required for the folding of alpha- and beta-tubulin. Mol Cell Biol 13, 2478-2485.

Hanzal-Bayer, M., Renault, L., Roversi, P., Wittinghofer, A. and Hillig, R.C. (2002). The complex of Arl2-GTP and PDE delta: from structure to function. EMBO J 21, 2095-2106.

Hirata, D., Masuda, H., Eddison, M. and Toda, T. (1998). Essential role of tubulin-folding cofactor D in microtubule assembly and its association with microtubules in fission yeast. EMBO J 17, 658-666.

Hoyt, M.A., Stearns, T. and Botstein, D. (1990). Chromosome instability mutants of Saccharomyces cerevisiae that are defective in microtubule-mediated processes. Mol Cell Biol 10, 223-234.

Ikeda, T., Nakahara, A., Nagano, R., Utoyama, M., Obara, M., Moritake, H., Uechi, T., Mitsui, J., Ishiura, H., Yoshimura, J., Doi, K., Kenmochi, N., Morishita, S., Nishino, I., Tsuji, S. and Nunoi, H. (2016). TBCD may be a causal gene in progressive neurodegenerative encephalopathy with atypical infantile spinal muscular atrophy. J Hum Genet.

Jordan, M.A. and Wilson, L. (2004). Microtubules as a target for anticancer drugs. Nat Rev Cancer 4, 253-265.

Lewis, S.A., Gu, W. and Cowan, N.J. (1987). Free intermingling of mammalian beta-tubulin isotypes among functionally distinct microtubules. Cell 49, 539-548.

Martin, L., Fanarraga, M.L., Aloria, K. and Zabala, J.C. (2000). Tubulin folding cofactor D is a microtubule destabilizing protein. FEBS Lett 470, 93-95.

Miyake, N., Fukai, R., Ohba, C., Chihara, T., Miura, M., Shimizu, H., Kakita, A., Imagawa, E., Shiina, M., Ogata, K., Okuno-Yuguchi, J., Fueki, N., Ogiso, Y., Suzumura, H., Watabe, Y., Imataka, G., Leong, H.Y., Fattal-Valevski, A., Kramer, U., Miyatake, S., Kato, M., Okamoto, N., Sato, Y., Mitsuhashi, S., Nishino, I., Kaneko, N., Nishiyama, A., Tamura, T., Mizuguchi, T., Nakashima, M., Tanaka, F., Saitsu, H. and Matsumoto, N. (2016). Biallelic TBCD Mutations Cause Early-Onset Neurodegenerative Encephalopathy. Am J Hum Genet 99, 950-961.

Montecinos-Franjola, F., Schuck, P. and Sackett, D.L. (2016). Tubulin Dimer Reversible Dissociation: AFFINITY, KINETICS, AND DEMONSTRATION OF A STABLE MONOMER. J Biol Chem 291, 9281-9294.

Nithianantham, S., Le, S., Seto, E., Jia, W., Leary, J., Corbett, K.D., Moore, J.K. and Al-Bassam, J. (2015). Tubulin cofactors and Arl2 are cage-like chaperones that regulate the soluble alphabeta-tubulin pool for microtubule dynamics. Elife 4.

Okumura, M., Sakuma, C., Miura, M. and Chihara, T. (2015). Linking cell surface receptors to microtubules: tubulin folding cofactor D mediates Dscam functions during neuronal morphogenesis. J Neurosci 35, 1979-1990.

Pode-Shakked, B., Barash, H., Ziv, L., Gripp, K.W., Flex, E., Barel, O., Carvalho, K.S., Scavina, M., Chillemi, G., Niceta, M., Eyal, E., Kol, N., Ben-Zeev, B., Bar-Yosef, O., Marek-Yagel, D., Bertini, E., Duker, A.L., Anikster, Y., Tartaglia, M. and Raas-Rothschild, A. (2016). Microcephaly, intractable seizures and developmental delay caused by biallelic variants in TBCD: Further delineation of a new chaperone-mediated tubulinopathy. Clin Genet.

Price, H.P., Peltan, A., Stark, M. and Smith, D.F. (2010). The small GTPase ARL2 is required for cytokinesis in Trypanosoma brucei. Mol Biochem Parasitol 173, 123-131.

Radcliffe, P.A., Hirata, D., Vardy, L. and Toda, T. (1999). Functional dissection and hierarchy of tubulin-folding cofactor homologues in fission yeast. Mol Biol Cell 10, 2987-3001.

Serna, M., Carranza, G., Martin-Benito, J., Janowski, R., Canals, A., Coll, M., Zabala, J.C. and Valpuesta, J.M. (2015). The structure of the complex between alpha-tubulin, TBCE and TBCB reveals a tubulin dimer dissociation mechanism. J Cell Sci 128, 1824-1834.

Sharer, J.D. and Kahn, R.A. (1999). The ARF-like 2 (ARL2)-binding protein, BART. Purification, cloning, and initial characterization. J Biol Chem 274, 27553-27561.

Shern, J.F., Sharer, J.D., Pallas, D.C., Bartolini, F., Cowan, N.J., Reed, M.S., Pohl, J. and Kahn, R.A. (2003). Cytosolic Arl2 is complexed with cofactor D and protein phosphatase 2A. J Biol Chem 278, 40829-40836.

Shultz, T., Shmuel, M., Hyman, T. and Altschuler, Y. (2008). Beta-tubulin cofactor D and ARL2 take part in apical junctional complex disassembly and abrogate epithelial structure. FASEB J 22, 168-182.

Spiess, C., Meyer, A.S., Reissmann, S. and Frydman, J. (2004). Mechanism of the eukaryotic chaperonin: protein folding in the chamber of secrets. Trends in cell biology 14, 598-604.

Stearns, T., Hoyt, M.A. and Botstein, D. (1990). Yeast mutants sensitive to antimicrotubule drugs define three genes that affect microtubule function. Genetics 124, 251-262.

Tian, G. and Cowan, N.J. (2013). Tubulin-specific chaperones: components of a molecular machine that assembles the alpha/beta heterodimer. Methods Cell Biol 115, 155-171.

Tian, G., Huang, Y., Rommelaere, H., Vandekerckhove, J., Ampe, C. and Cowan, N.J. (1996). Pathway leading to correctly folded beta-tubulin. Cell 86, 287-296.

Tian, G., Lewis, S.A., Feierbach, B., Stearns, T., Rommelaere, H., Ampe, C. and Cowan, N.J. (1997). Tubulin subunits exist in an activated conformational state generated and maintained by protein cofactors. J Cell Biol 138, 821-832.

Tian, G., Thomas, S. and Cowan, N.J. (2010). Effect of TBCD and its regulatory interactor Arl2 on tubulin and microtubule integrity. Cytoskeleton (Hoboken) 67, 706-714.

Zhang, T., Li, S., Zhang, Y., Zhong, C., Lai, Z. and Ding, J. (2009). Crystal structure of the ARL2-GTP-BART complex reveals a novel recognition and binding mode of small GTPase with effector. Structure 17, 602-610.

Zhou, C., Cunningham, L., Marcus, A.I., Li, Y. and Kahn, R.A. (2006). Arl2 and Arl3 regulate different microtubule-dependent processes. Mol Biol Cell 17, 2476-2487.

# CHAPTER 3

## Nucleotide binding to ARL2 in the TBCD/ARL2/β-tubulin complex drives conformational changes in β-tubulin

Joshua W. Francis*, Devrishi Goswami†, Scott J. Novick†, Bruce D. Pascal†, Emily R. Weikum*, Eric A. Ortlund*, Patrick R. Griffin† and Richard A. Kahn*

*Department of Biochemistry, Emory University School of Medicine, Atlanta, GA 30322

†Department of Molecular Medicine, The Scripps Research Institute, Jupiter, FL 33458

This research has been submitted and is under review at

The Journal of Biological Chemistry.

**Abstract**

Microtubules are highly dynamic tubulin polymers that are required for a variety of basic cellular functions, including cell division, intracellular traffic, and formation of cilia/flagella. The continual assembly and disassembly of microtubules is a highly regulated process, termed dynamic instability, which is largely regulated by the polymerization and depolymerization of αβ-tubulin dimers. Despite the obvious importance of a stable cellular population of tubulin dimers, we have incomplete information about the mechanisms involved in the biogenesis of native αβ-tubulin heterodimers. In addition to prefoldin and the TCP-1 Ring Complex, several tubulin-specific chaperones, termed cofactors A-E, are required for the proper folding of α- and β-tubulin subunits and the ultimate production of nascent tubulin dimers. We propose a novel role for the regulatory GTPase, ARL2, in this process of tubulin folding and dimer formation. We recently described a novel trimer, TBCD/ARL2/β-tubulin, and its potential role in maintaining the microtubule network. Here we characterize the nucleotide-binding properties of the purified TBCD/ARL2/β-tubulin complex and show that it is ARL2, and not β-tubulin, that is responsible for binding guanine nucleotide in the trimer. Using hydrogen/deuterium exchange (HDX) coupled with mass spectrometry, we also show that nucleotide binding to ARL2 shifts the conformational equilibrium of TBCD and β-tubulin subunits of the complex. We conclude that the TBCD/ARL2/β-tubulin complex represents a functional intermediate in the β-tubulin folding pathway whose activity is regulated by the cycling of nucleotides on ARL2.

**Introduction**

Microtubules are polymers of αβ-tubulin heterodimers, which can be highly dynamic or stable ultrastructural components, and are present in all eukaryotic cells. They are essential during cell division, forming mitotic spindles that resolve chromosomes to mother and daughter cells. In other parts of the cell cycle, microtubules serve as tracks along which organelles traffic, which is particularly important in highly polarized cells such as neurons. They are also core to the axonemes

present in both sensory and motile cilia and flagella. Several genes encode each α- or β-tubulin subunit (*e.g.*, see Lewis et al., 1987) resulting in diversity in composition, with functional consequences that are incompletely understood. Tubulins can also be post-translationally modified to alter the dynamics of microtubules (*e.g.*, acetylation, phosphorylation, tyrosination). Because of their central role in cell division/proliferation and other aspects of cell biology, tubulins/microtubules are also the target of several anti-tumor agents, *e.g.*, the taxanes and Vinca alkaloids (Jordan and Wilson, 2004). Despite their importance to cells and in the clinic, we lack a detailed understanding of the mechanisms regulating the formation of the key component, the αβ-tubulin heterodimer.

Tubulins are among the most abundant proteins in every cell, often reaching levels of ~5% of total cell protein. Despite, or perhaps because of, that abundance a complex series of biosynthetic steps is required to support tubulin folding and dimer assembly. Many proteins, particularly abundant ones like α- and β-tubulin, first interact with the hexameric chaperone complex, termed prefoldin, upon exiting the ribosome (Vainberg et al., 1998). These proteins are then handed off to the cytosolic chaperonin, TCP-1 Ring Complex (TriC or CCT), as the next step in the folding process (Gao et al., 1993; Spiess et al., 2004). Then tubulins uniquely interact with five tubulin-specific co-chaperones, termed cofactors A-E, in a series of interactions first described by Tian et al. (Tian et al., 1996; Tian et al., 1997), using native gels to monitor the formation of different inferred complexes of *in vitro* translated tubulin. This foundational work from the Cowan lab provided the first model for all steps in the tubulin-folding pathway, but aspects of it are challenged by more recent studies. A detailed model for tubulin folding that withstands rigorous testing would include the roles played by each of the required components, allow the generation of key biochemical reagents for multiple studies, and generate novel opportunities for therapeutic development. Such a model requires the ability to generate each component in a functional state that would then allow reconstitution of the formation of the αβ-tubulin dimer. One roadblock to this goal has been the lack of a soluble, stable preparation of the largest component in the folding

pathway, tubulin-specific chaperone D (TBCD, also termed Cofactor D), as it is insoluble in bacteria and poorly expressed or unstable in other expression systems. This is in marked contrast to the other four cofactors, A-C and E (Tian and Cowan, 2013). We recently described the use of human embryonic kidney (HEK293T/17) cells to overexpress and purify human or bovine TBCD and showed it to be soluble and stable (Francis et al., 2017). That study identified a number of novel complexes containing TBCD and strong physical connection to the regulatory GTPase, ARL2.

The use of model genetic systems and screens to investigate aspects of microtubule biology repeatedly identified both TBCD and ARL2. Screening *S. cerevisiae* for altered sensitivity to benomyl, a microtubule poison, identified the yeast orthologs of TBCD and ARL2, *CIN1* and *CIN4*, respectively (Hoyt et al., 1990; Stearns et al., 1990). Similar screens pulled out *Alp1 and Alp41* in *S. pombe* (Hirata et al., 1998; Radcliffe et al., 1999), and *TTN1* and *TTN5* in *A. thaliana* (Liu and Meinke, 1998; McElver et al., 2000), encoding orthologs of TBCD and ARL2, respectively. When combined with the results from the Cowan lab showing direct effects on tubulin folding, there is compelling evidence for TBCD in this pathway. Other screens found mutations in ARL2 orthologs in *C. elegans* (Antoshechkin and Han, 2002), *T. brucei* (Price et al., 2010), and *D. melanogaster* (Chen et al., 2016) that further support a role for this regulatory GTPase in tubulin biology. There are also data that reveal roles for TBCD and ARL2 acting at distinct sites and pathways. TBCD has been implicated in actions at centrosomes (Fedyanina et al., 2006; Cunningham and Kahn, 2008; Fanarraga et al., 2010) and at the cell surface (Shultz et al., 2008; Okumura et al., 2015). Additionally, a spate of recent reports describe a number of point mutations in TBCD found in patients with links to early-onset encephalopathy (Edvardson et al., 2016; Flex et al., 2016; Ikeda et al., 2016; Miyake et al., 2016) and intractable seizures (Pode-Shakked et al., 2016). A subset of these mutations were specifically shown to disrupt formation and stability of the TBCD/ARL2/β-tubulin complex (Flex et al., 2016), which we have recently purified and characterized (Francis et al., 2017).

ARF family GTPases are in the RAS superfamily, and as such are typically found as monomers in cytosol. But we found the vast majority of ARL2 to fractionate with an apparent molecular weight of ~200 kDa (Shern et al., 2003; Francis et al., 2017). Although first purified from bovine tissues as a dimer of TBCD/ARL2 (Shern et al., 2003), we later showed that in most cells and tissues a species of ~200 kDa is comprised of the TBCD/ARL2/β-tubulin trimer (Francis et al., 2017). The TBCD/ARL2 dimer purified from bovine brain was inactive in the tubulin folding assay and displayed the unique property of binding GDP but not GTP (Shern et al., 2003). Because the TBCD/ARL2 heterodimer purified from bovine brain is inactive in key respects and is only available in small amounts, we developed an expression system in mammalian cells capable of generating milligram amounts of TBCD complexes (Francis et al., 2017). This study found that only when co-expressed with ARL2 does TBCD purify as a monodisperse complex, which appears to be a 1:1:1 complex of TBCD/ARL2/β-tubulin. The presence of β-tubulin in the novel TBCD/ARL2/β-tubulin trimer clearly distinguishes it from the TBCD/ARL2 dimer and strongly implicates it playing a role in tubulin folding. In the current study, we focused initially on the nucleotide-binding properties of this trimer as this was a distinguishing feature of the TBCD/ARL2 dimer.

Small GTPases are single domain proteins that bind and hydrolyze GTP in a highly regulated fashion to alter signaling through transient interactions with effectors, modulators, and often membranes. The binding of guanine nucleotides typically stabilize the folded structures of the GTPase such that the apoproteins are unstable and rarely found. This is not true of ARL2 as it purifies from mammalian or bacterial sources free of nucleotides and is relatively stable as the apoprotein. Thus, ARL2 provides an unusual opportunity to compare structural features of the apoprotein to the liganded forms.

A common feature of RAS superfamily GTPases is the presence of a highly conserved set of motifs, termed G motifs, which provide direct sites of interaction with bound nucleotides (Wittinghofer and Vetter, 2011). For example, the G1 motif (aka Walker A motif) is the consensus

GXXXXGK(S/T) and interacts with phosphates of the bound nucleotide. The G3 motif (DXXGQ) includes the glutamine that is critical to GTP hydrolysis. Another distinguishing feature of regulatory GTPases are the two switches, I and II, as the conformation of each of these altered upon exchange of GTP for GDP, resulting in increased affinity for effectors and modulators. ARL2 contains the canonical G motifs and switches I/II, but unlike other families within the RAS superfamily, ARF family members, including ARL2, have an N-terminal extension that forms an amphipathic α-helix that is also critical to function. The N termini are commonly found to serve as a functional switch III in that the conformation is sensitive to the bound nucleotide and residues within it make direct contacts with effectors and modulatory proteins (Hanzal-Bayer et al., 2002; Bailey et al., 2009; Zhang et al., 2009). In contrast, β-tubulin is considered an atypical GTPase as it does not share many of the common motifs that are highly conserved among guanine nucleotide binding proteins (Saraste et al., 1990). However, there is a high level of conservation of the residues involved in nucleotide binding among tubulin isoforms, as well as between α- and β-tubulin subunits (Lowe et al., 2001). GTPase cascades (*i.e.*, increased activity of one GTPase leading to activation of another GTPase in the same pathway) are increasingly common, particularly in membrane traffic (Jones et al., 1999; Christis and Munro, 2012; Mizuno-Yamasaki et al., 2012; D'Souza et al., 2014). However, it is very uncommon, perhaps unique, for a regulatory GTPase, like ARL2, to play a fundamental role in the folding or biogenesis of another GTPase.

The final stage in the Cowan model for tubulin folding (Tian et al., 1996; Lewis et al., 1997) proposes that the TBCD/TBCE/α-tubulin/β-tubulin tetramer binds TBCC, resulting in release of the folded αβ-tubulin heterodimer and disassembly of other components. Due to its large size (133 kDa) and predicted, predominantly α-helical structure (Grynberg et al., 2003), TBCD is proposed to act as a scaffold onto which other components assemble. A challenge to the early Cowan model has come from studies in which co-expression in bacteria of the yeast orthologs revealed the formation of a trimer of TBCD(CIN1p)-ARL2(CIN4p)-TBCE(PAC2p) (Nithianantham et al., 2015). Our studies using human proteins purified from HEK cells failed to

identify the homologous complex, though we did report the co-purification of our TBCD/ARL2/β-tubulin trimer with sub-stoichiometric amounts of TBCE only after overexpression of the GST-TBCD, ARL2, and TBCE. Thus, differences between yeast and mammals likely exist in the affinities for different subunit interactions resulting in the formation or stability of different protein complexes. In the current study, we again focused on the TBCD/ARL2/β-tubulin trimer in efforts to better understand the role(s) of the regulatory GTPase and of GTP binding to the processes of tubulin folding and protein complex assembly/disassembly.

To accomplish these goals, we characterized the nucleotide-binding properties of the TBCD/ARL2/β-tubulin complex and compared them to those of the ARL2 monomer, using *in vitro* binding assays. We also used hydrogen/deuterium exchange, coupled with mass spectrometry (HDX-MS), to analyze the effects of nucleotide binding on the conformational dynamics of each subunit of the trimer. HDX-MS is a technique that measures the levels of solvent exchange of backbone amide hydrogens throughout a protein in solution. Using this technique, we were able to determine direct and allosteric effects of nucleotide binding on the conformational flexibility, or stability, of regions within each protein in the TBCD/ARL2/β-tubulin complex, from which we propose a role for nucleotide binding to ARL2 in the trimer in regulating β-tubulin folding.

## Results

### *The TBCD/ARL2/β-tubulin complex binds both GDP and GTP*

We recently described the identification and purification of a trimeric complex of TBCD/ARL2/β-tubulin (Francis et al., 2017). We purify this trimer by affinity chromatography, using glutathione-conjugated Sepharose beads, following co-expression of human GST-TBCD and ARL2 in human embryonic kidney (HEK) cells. The GST tag is removed using the engineered TEV protease cleavage site, and the trimer is further purified by gel filtration in a Superdex 200 column to remove the TEV, GST and any minor contaminants. The complex elutes as a symmetrical peak off this column and at the appropriate position for a ~200 kDa complex. The

trimeric complex is stable at 4 °C for at least one week, remains soluble after freezing and thawing, and runs as a sharp band of ~200 kDa in blue native gels. All of this is consistent with the TBCD/ARL2/β-tubulin trimer being a well-behaved, stable species amenable for biochemical studies.

Because the TBCD/ARL2 dimer purified from bovine brain had the unique property of binding GDP indistinguishably from human ARL2 monomer but differed in being unable to bind GTP or GTPγS, we assessed the nucleotide binding properties of the trimer. We first used the classical filter trapping assay, as described under Experimental Procedures, to determine its guanine-nucleotide binding properties. The trimer was incubated with the slowly hydrolysable GTP analog, [$^{35}$S]GTPγS, at 30 °C and at various times the reaction was stopped by dilution into ice cold buffer containing 10 mM $MgCl_2$, to slow nucleotide dissociation (Bowzard et al., 2005). Rapid filtration on BA85 nitrocellulose filters that retain protein and bound nucleotides allowed determination of radioligand binding by scintillation counting (Figure 1). The TBCD/ARL2/β-tubulin trimer binds GTPγS rapidly, reaching a plateau within 5-10 min that is stable for at least 30 min. Human ARL2 monomer, exogenously expressed and purified from *E. coli* (Figure 1) or HEK cells, bound GTPγS to similar stoichiometries, ranging between 0.15-0.25 pmol GTPγS bound/pmol protein in different replicates. The finding that equimolar concentrations of ARL2 monomer and TBCD/ARL2/β-tubulin trimer bind equal amounts of GTPγS is consistent with the trimer being a 1:1:1 complex, though small differences would go undetected using this metric.

As differences have been noted between the human and bovine orthologs of TBCD (Cunningham and Kahn, 2008; Tian et al., 2010), we also co-expressed bovine GST-TBCD with human ARL2 in HEK cells (bovine and human ARL2 are 98% identical in primary sequence, with only 3 conservative differences). Bovine TBCD behaves comparably to the human ortholog and was purified from HEK cells as the trimer upon co-expression with ARL2 (Francis et al., 2017). We found no clear differences between the two trimers, made up of bovine or human TBCD, in their ability to bind [$^{35}$S]GTPγS in the filter trapping assay (Figure 1).

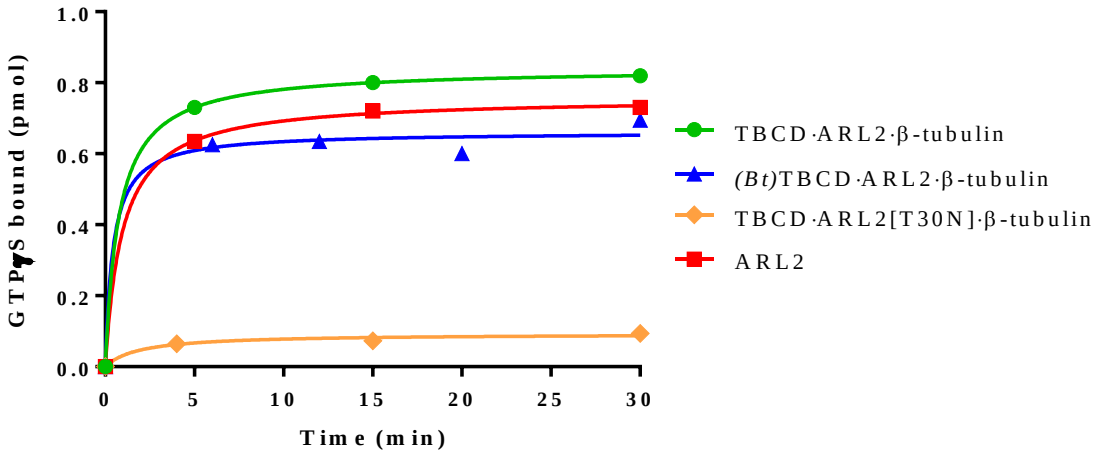


**Figure 3-1. TBCD/ARL2/β-tubulin trimer and ARL2 monomer bind GTP**. Human GST-TBCD was co-expressed with human ARL2 (green circles) or ARL2[T30N] (orange diamonds) in HEK cells and affinity purified as trimers, as described under Experimental Procedures. Bovine GST-TBCD/ARL2/β-tubulin was similarly purified (blue triangles) for assay. We expressed and purified ARL2 monomer (red boxes) from BL21(DE3) cells. TBCD complexes and ARL2 monomer (1 μM each) were incubated with 10 μM [$^{35}$S]GTPγS at 30 °C and nucleotide binding was determined at various time points, using the filter trapping assay. *Bt, Bos taurus.*

human ARL2 in HEK cells (bovine and human ARL2 are 98% identical in primary sequence, with only 3 conservative differences). Bovine TBCD behaves comparably to the human ortholog and was purified from HEK cells as the trimer upon co-expression with ARL2 (Francis et al., 2017). We found no clear differences between the two trimers, made up of bovine or human TBCD, in their ability to bind [$^{35}$S]GTPγS in the filter trapping assay (Figure 1).

We interpret these data as evidence that the trimer is capable of binding GTPγS, but it is also possible that the ARL2 or β-tubulin is dissociating under the conditions used in the binding assay and is binding nucleotide as a monomer. To test this we pre-incubated the trimer with GDP or GTPγS, using the same reaction conditions described above, and attempted to resolve subunits in each of two different ways: blue native PAGE or ultrafiltration. The former showed that the trimer remained an intact complex with all three components migrating to the same position in the gel after incubation with GDP or GTPγS, though nucleotide dissociation could have occurred during electrophoresis. More convincingly, we found that continual exposure to GDP or GTPγS before and during ultrafiltration was able to completely resolve a ~24 kDa contaminant that co-purifies on glutathione-Sepharose beads (predicted to be an endogenous HEK cell GST (Bichet et al., 2000)) but resulted in no losses in ARL2.

Should subunit dissociation be occurring upon binding of a guanine nucleotide, it is expected to alter the stability of one or more of the proteins. Thus, we also analyzed effects of nucleotide binding on the stability of the TBCD/ARL2/β-tubulin complex using a Thermofluor assay (Figure 2). We incubated the purified trimer with a 10-fold molar excess of GDP, GTPγS or no nucleotide and then added to each solution the fluorescent dye, SYPRO Orange. The dye binds to hydrophobic regions and alters its fluorescent properties upon doing so. We varied the temperature and determined the fluorescence under each condition to determine the melting points, defined as the half-maximal change in fluorescence (Figure 2). In each case we observed curves displaying a single, gradual change in fluorescence, consistent with coordinated unfolding/denaturation. We found no apparent difference in the melting temperature when the

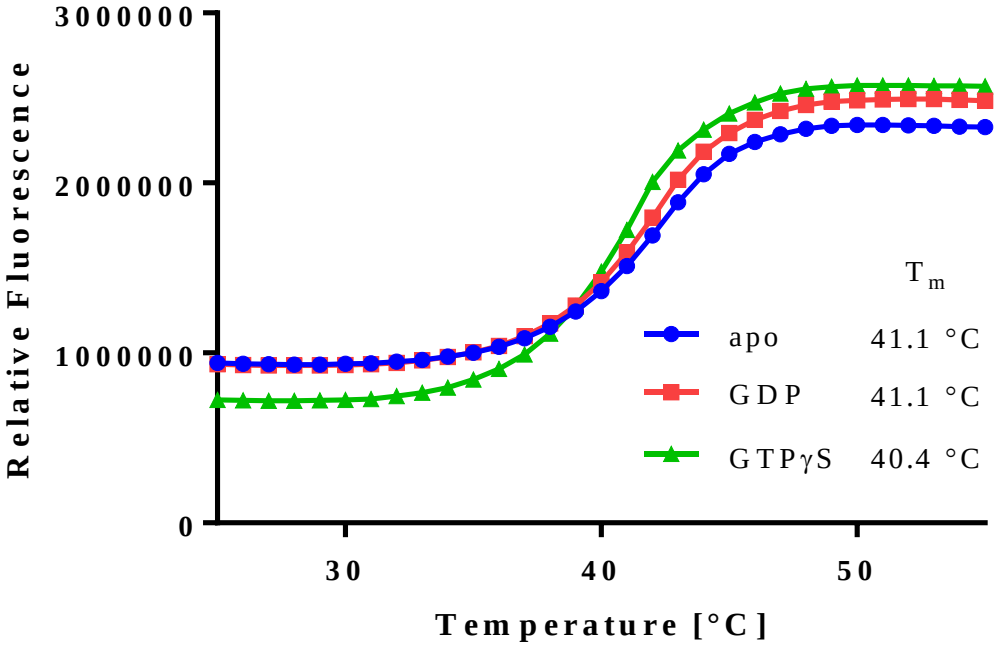


**Figure 3-2. Nucleotide binding does not alter the thermal stability of the TBCD/ARL2/β-tubulin complex.** We used the Thermofluor assay to determine the thermal stability of purified TBCD/ARL2/β-tubulin after the addition of GDP (red squares), GTPγS (green triangles) or no nucleotide (apo; blue circles). Samples were mixed with SYPRO Orange dye and the fluorescence was measured every 2 min for 1 hr, while the temperature was increased 0.5 °C/min. Melting points ($T_m$) were determined as the half-maximal change in fluorescence.

TBCD/ARL2/β-tubulin trimer was pre-incubated without nucleotide, with GDP, or with GTPγS (41.1 °C, 41.1 °C, and 40.4 °C, respectively). Thus, the trimeric complex is capable of binding GDP or GTPγS stably, and doing so does not result in substantial dissociation of subunits.

We next performed real-time nucleotide binding assays using GDP or the non-hydrolyzable GTP analog, 5′-[β, γ-imido]triphosphate (Gpp(NH)p), each labeled with the *N*-methylanthraniloyl (mant) fluorophore. We incubated TBCD/ARL2/β-tubulin or ARL2 (2 μM each) with 1 μM mant-Gpp(NH)p or mant-GDP and changes in fluorescence were measured at room temperature using a BioTek Synergy 4 plate reader equipped with an injector system to allow monitoring of rapid kinetics. After 20 min, excess (100 μM) unlabeled nucleotide was added to the reaction mixture, and the fluorescence intensity was measured for an additional 20 min to allow determination of off-rates (Figure 3). We normalized the resulting data to the percentage of maximal signal to allow ready comparisons of the binding curves. The TBCD/ARL2/β-tubulin trimer clearly binds mant-Gpp(NH)p more rapidly than does the monomer (Figure 3A, C). In order to determine kinetic rate constants and calculate apparent affinities, we fit the data to mathematical models using GraphPad Prism software, as described in Experimental Procedures. Though TBCD/ARL2/β-tubulin and ARL2 show similar dissociation rates ($k_{off}$ = 0.046 $min^{-1}$ and 0.062 $min^{-1}$, respectively), the trimer has a ~10-fold increase in the rate of association, compared to ARL2 ($k_{on}$ = 1.4x$10^6$ $M^{-1}{\cdot}min^{-1}$ and 1.4x$10^5$ $M^{-1}{\cdot}min^{-1}$, respectively). Together, these data yield a ~13-fold difference in the apparent affinities of TBCD/ARL2/β-tubulin and ARL2 for mant-Gpp(NH)p ($K_{D(app)}$ = 33 nM and 433 nM, respectively).

Differences between the trimer and monomer were also observed when GDP binding was assessed, using mant-GDP (Figure 3B, C). TBCD/ARL2/β-tubulin bound mant-GDP at a ~8-fold faster rate than monomeric ARL2 ($k_{on}$ = 3.2x$10^5$ $M^{-1}{\cdot}min^{-1}$ and 3.9x$10^4$ $M^{-1}{\cdot}min^{-1}$, respectively). Unlike mant-Gpp(NH)p, however, the rate of dissociation of mant-GDP from TBCD/ARL2/β-tubulin was also faster than from ARL2 ($k_{off}$ = 0.51 $min^{-1}$ and 0.15 $min^{-1}$, respectively). These rates

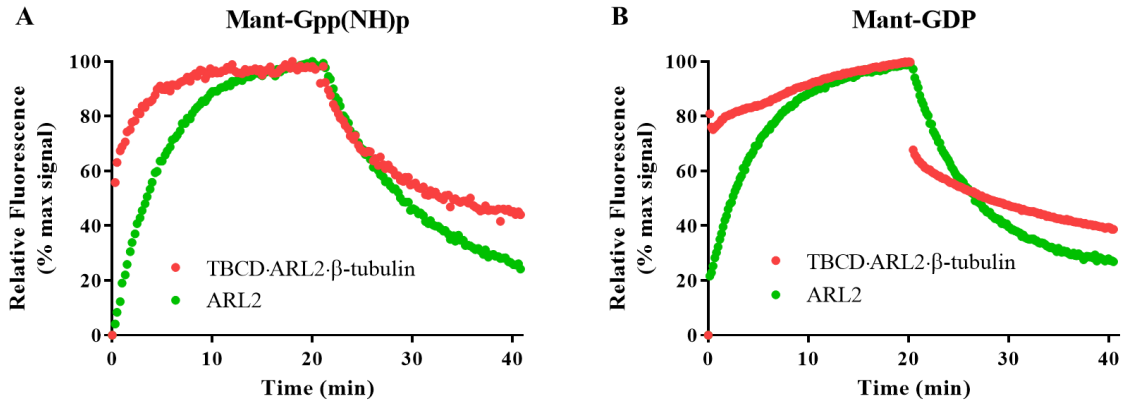


C

| | $k_{on}$ ($M^{-1}·min^{-1}$) | $k_{off}$ ($min^{-1}$) | $K_{D(app)}$ |
|---|---|---|---|
| TBCD·ARL2·β-tubulin (mant-Gpp(NH)p) | $1.4x10^6$ | 0.046 | 33 nM |
| ARL2 (mant-Gpp(NH)p) | $1.4x10^5$ | 0.062 | 433 nM |
| TBCD·ARL2·β-tubulin (mant-GDP) | $3.2x10^5$ | 0.51 | 1.6 μM |
| ARL2 (mant-GDP) | $3.9x10^4$ | 0.15 | 3.9 μM |

**Figure 3-3. The TBCD/ARL2/β-tubulin trimer has a higher affinity than ARL2 for guanine nucleotides.** Kinetics of nucleotide binding to TBCD/ARL2/β-tubulin (red circles) or ARL2 monomer (green circles) were determined by monitoring changes in fluorescence of mant-labeled nucleotides in a solution-based assay. We incubated TBCD/ARL2/β-tubulin trimer or ARL2 (2 μM each) with 1 μM (**A**) mant-Gpp(NH)p or (**B**) mant-GDP and the fluorescence intensity was measured at room temperature for 20 min, at which point excess (100 μM) unlabeled Gpp(NH)p or GDP, respectively, was added and monitoring of fluorescence continued for another 20 min. Data were normalized to percent maximal signal and (**C**) mathematical models generated in GraphPad Prism software were used to determine on- and off-rates and apparent affinities.

reveal that the TBCD/ARL2/β-tubulin trimer has a higher apparent affinity for mant-GDP than does ARL2 ($K_{D(app)}$ = 1.6 μM and 3.9 μM, respectively). We note that due to the very fast rates of nucleotide binding and release, particularly for the trimer, the numbers shown here are likely underestimates of the true association/dissociation constants.

While these data support the conclusion that the TBCD/ARL2/β-tubulin complex readily binds GDP and GTP, further interpretation of these results is confounded by the presence of two guanine-nucleotide binding proteins within the complex. To determine if the ARL2 and/or β-tubulin is responsible for binding nucleotide, we first used the filter trapping assay described above to analyze purified trimer that included a point mutant of ARL2, ARL2[T30N], that has been shown to be deficient in binding guanine nucleotides, compared to the wild type protein (Hanzal-Bayer et al., 2005). By analogy to ARF1[T31N] (Dascher and Balch, 1994; Szul et al., 2005) and RAS[S17N] (Feig and Cooper, 1988; Farnsworth and Feig, 1991; Jung et al., 1994; Nassar et al., 2010), ARL2[T30N] is thought to act as an apoprotein in a dominant negative fashion in cells by mimicking the transition state while bound to its guanine-nucleotide exchange factor (GEF), to prevent activation of endogenous ARL2. Co-expression of human GST-TBCD and ARL2[T30N] allowed us to purify the GST-TBCD/ARL2[T30N]/β-tubulin trimer with comparable purity and abundance as when the wild type ARL2 was used (Francis et al., 2017). However, in contrast to the wild type, TBCD/ARL2[T30N]/β-tubulin has almost completely lost the ability to bind GTPγS (Figure 1). We interpret these results as being most consistent with ARL2 being the species that binds guanine nucleotides in our trimer, but other explanations are possible. To definitively address this and related issues, we used hydrogen/deuterium exchange coupled with mass spectrometry (HDX-MS) to monitor solvent exchange of amide hydrogens of each protein in the trimer and compared results after the complex was pre-incubated with saturating amounts of GDP or GTPγS, or when no nucleotide was added. Alterations in HDX reflect changes in the environment of the corresponding amides within the folded protein. Increased protection to exchange suggests an increased number or strength of hydrogen bonds, often characterized as a decrease in solvent

accessibility, whereas decreased protection would suggest a decrease in hydrogen bonding (*i.e.*, increased solvent accessibility). We used the same approach to compare ARL2 monomer to ARL2 in the trimer, again under different nucleotide-bound states. This allowed additional comparisons to be made and, because ARL2 is among the very few regulatory GTPases that are stable in solution as an apoprotein, allowed us to monitor effects of nucleotide binding.

*Molecular dynamics of TBCD in the TBCD/ARL2/β-tubulin complex are only minimally affected by the binding of guanine nucleotides*

Current models of tubulin folding portray TBCD as a scaffold onto which other components bind, based more on its relatively large size (133 kDa) than on any functional data. With the exception of *in silico* predictions (Grynberg et al., 2003) and low-resolution electron microscopy data (Nithianantham et al., 2015), there are almost no structural data to support this proposed role for TBCD. A large roadblock to structural studies of TBCD has been the lack a recombinant expression system capable of producing large amounts of soluble, stable TBCD. We have recently described the purification of three novel TBCD complexes (Francis et al., 2017), with TBCD/ARL2/β-tubulin being the most stable. To date, neither our lab nor others has achieved high level purification of monomeric TBCD and our analyses of the protein in cell and tissue lysates (Francis et al., 2017) suggest it may only be stable in cells when complexed with other proteins.

While TBCD itself does not bind guanine nucleotides, we applied differential HDX-MS to assess changes in TBCD solvent exchange that may result from the binding of GDP or GTPγS to other components in the trimer. Purified TBCD/ARL2/β-tubulin (10 μM) was incubated with a 10-fold molar excess (100 μM) of GDP, GTPγS, or no nucleotide for at least 1 hour on ice before analysis by HDX-MS. Radioligand binding data confirm that maximal nucleotide binding was achieved under these conditions. We incubated the samples in $D_2O$ and collected six time points over the course of an hour (10 s, 30 s, 60 s, 300 s, 900 s, and 3600 s). For each time point, solvent exchange was slowed by addition of low pH buffer and each sample was then subjected to on-line

pepsin digestion. The peptic peptides were separated by RP-HPLC, coupled to an ESI source and the ions for each peptide were mass measured using a high resolution, high mass accuracy mass spectrometer, as described under Experimental Procedures. HDX Workbench software (Pascal et al., 2012) was used to calculate the deuterium uptake over time for each peptide. TBCD sequence coverage was ~92% for all experiments, with data generated for many overlapping peptides throughout the protein. The average percent deuterium uptake was calculated for all peptides whose sequence was verified by tandem mass spectrometry. To directly compare the effect that the addition of nucleotide had on TBCD solvent exchange, the uptake profiles for the apo, GDP, and GTPγS samples were subtracted from one another to generate three differential HDX datasets that portray the *change* in average deuterium uptake between the different nucleotide-bound states. For example, to determine the effect that addition of GDP had on TBCD deuterium exchange, we subtracted the data for the apoprotein from that of the sample incubated with GDP and plotted the differences. Thus, a region of the protein that has reduced deuterium exchange after addition of GDP yields a negative value, and this region would be considered stabilized in terms of conformational mobility. Conversely, a positive value indicates an increase in the rate of deuterium exchange, or increased conformational mobility, occurred after addition of the nucleotide. To extract putative single amide resolution of the HDX data, average values were determined for each residue of the protein; *e.g.*, those for TBCD are shown in the graph in Figure 4. Dotted lines indicate regions of the protein that were not covered in the MSMS analysis. It is apparent that only quite modest changes in the levels of deuterium exchange were observed for TBCD when comparing the three nucleotide-bound states. However, we observe a few localized regions that exhibit moderate changes (± 15%) in deuterium exchange. When comparing the apo and GDP samples (apo→GDP; blue line), the tendency is a slight increase in solvent exchange upon binding GDP, indicative of an increase in the conformational flexibility of the protein. In contrast, the apo→GTPγS (red line)

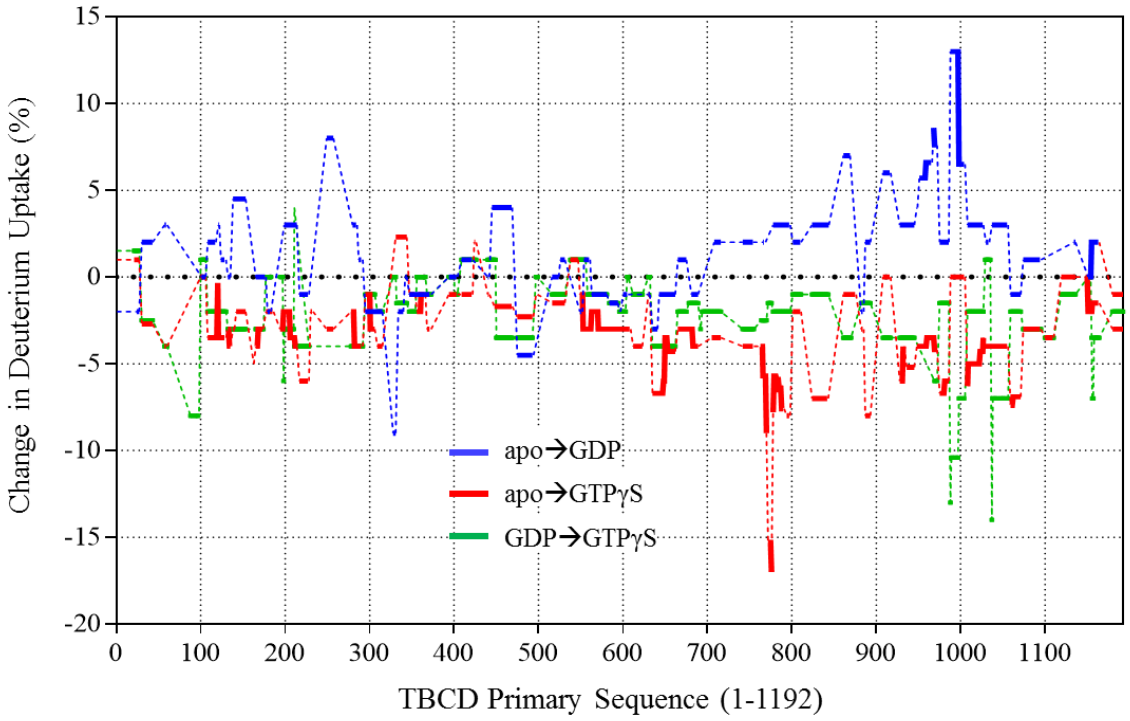


**Figure 3-4. The molecular dynamics of TBCD in the TBCD/ARL2/β-tubulin complex are minimally affected by nucleotide binding to the trimer.** We analyzed purified TBCD/ARL2/β-tubulin (10 μM) by HDX-MS before (apo) and after pre-incubation with GDP or GTPγS (100 μM each). The average percent of deuterium exchange over 1 hr was determined for each sample, and datasets were then compared to determine the change in deuterium uptake between each of the nucleotide-bound states. For each of the comparisons, the average percent change in deuterium uptake was determined and plotted for each residue in the TBCD sequence. Blue lines show the result of subtracting values from the apo-trimer from those of the GDP-bound trimer. Red lines show differential data of GTPγS minus the apo-complex and green lines for the GTPγS minus GDP data. Dotted lines indicate regions of the protein not covered in the mass spectrometry analysis. Positive values indicate an increase in deuterium uptake and negative values indicate a decrease in uptake.

and GDP→GTPγS (green line) comparisons show a general decrease in solvent exchange, indicative of stabilization of the protein. While the changes observed are subtle, they are statistically significant, and these data indicate that the addition of GDP or GTPγS has opposing effects on the molecular dynamics (*i.e.,* backbone mobility) of TBCD in the TBCD/ARL2/β-tubulin complex. We interpret these results to indicate that there are modest conformational changes within TBCD induced by nucleotide binding to the complex. As it is improbable that TBCD is interacting directly with the nucleotide, the observed changes are allosteric (*i.e.*, driven by nucleotide binding to one or both of the other proteins).

*Addition of guanine nucleotides to the TBCD/ARL2/β-tubulin complex results in conformational changes in β-tubulin that do not map onto regions involved in guanine-nucleotide binding*

We hypothesize that the TBCD/ARL2/β-tubulin complex serves as a folding intermediate for β-tubulin in the tubulin biogenesis pathway. As such, we predict that the β-tubulin in this complex has an underdeveloped nucleotide-binding pocket and does not contribute to the nucleotide binding that we observe in our binding assays (Figures 1, 2). To test this model, we performed differential HDX analyses of β-tubulin in the TBCD/ARL2/β-tubulin complex after the addition of GDP, GTPγS, or no nucleotide. The graphical representation of the differential HDX data describing the transitions between the three nucleotide-bound states are shown in Figure 5A. Upon binding GDP, there was a moderate increase in deuterium exchange throughout the entire β-tubulin sequence, indicating a decrease in the conformational stability of the protein (Figure 5A, blue line). In stark contrast, addition of GTPγS to the complex resulted in almost no changes in the levels of deuterium exchange seen in β-tubulin (Figure 5A, red line), suggesting that the conformational dynamics of β-tubulin are very similar between the apo and GTPγS-bound states. These findings are further highlighted in Figure 5B, where the differential HDX data were converted to a heat map and overlaid onto a three-dimensional representation of β-tubulin.

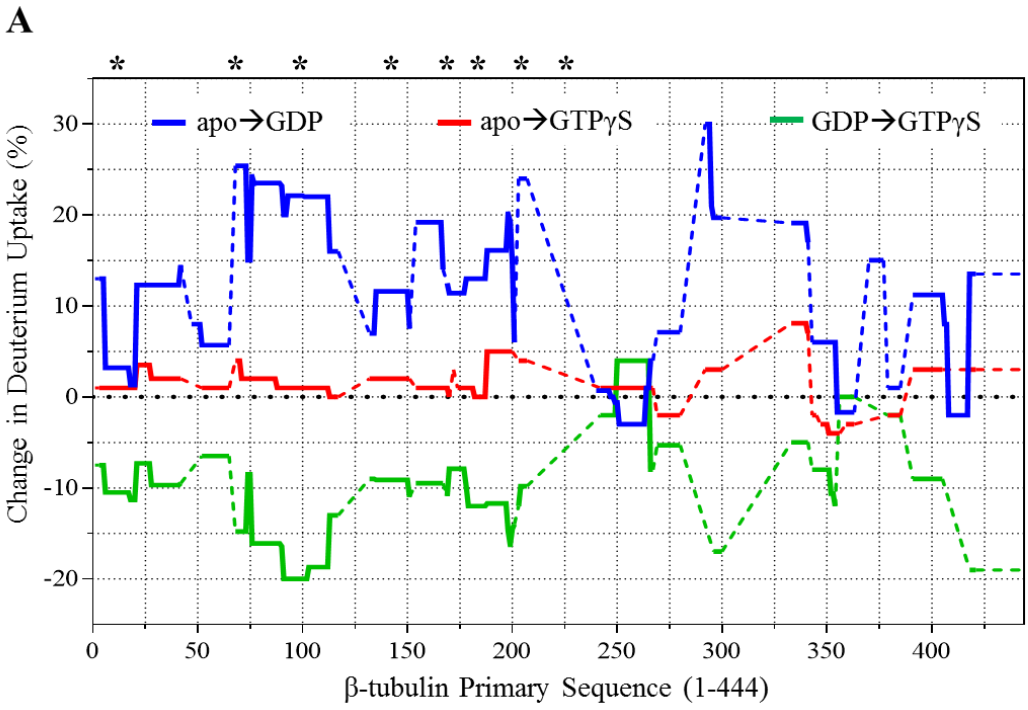
A
apo→GDP
apo→GTPγS
GDP→GTPγS
Change in Deuterium Uptake (%)
β-tubulin Primary Sequence (1-444)

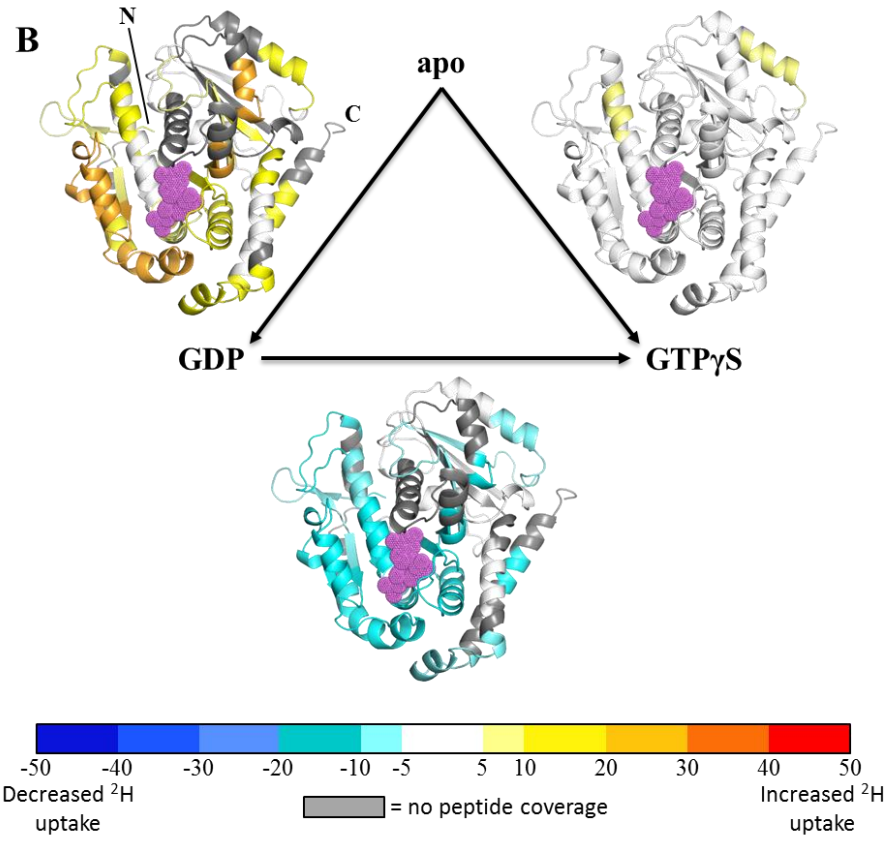
B
N
C
apo
GDP
GTPγS
-50 -40 -30 -20 -10 -5 5 10 20 30 40 50
Decreased ²H uptake
= no peptide coverage
Increased ²H uptake

**Figure 3-5. The binding of guanine nucleotides to TBCD/ARL2/β-tubulin causes moderate changes throughout the β-tubulin protein.** Purified TBCD/ARL2/β-tubulin (10 μM) was pre-incubated with a 10-fold molar excess of GDP, GTPγS or no nucleotide and analyzed by HDX-MS, as described in the legend to Figure 4. (**A**) The change in the average percent of deuterium uptake among the three samples was determined per residue of β-tubulin. Asterisks above the graph indicate regions of the protein involved in direct interaction with nucleotide, based upon published structures. Dotted lines indicate regions of the protein not covered by MSMS. (**B**) Differential data were converted to heap map form and overlaid onto a homology model for human β-tubulin (based on PDB ID: 3RYC). The nucleotide-binding pocket is shown in magenta. Gray represents regions not sequenced by mass spectrometry. N, amino terminus. C, carboxyl terminus.

Decreases in deuterium exchange are represented in shades of blue, increases in yellow/red, and no significant change (±5%) in white, as indicated in the scale below the structures. Areas shaded grey are indicative of regions of the protein that were not covered by the MSMS analysis (~86% sequence coverage of β-tubulin in all assays). As clearly shown by the HDX perturbation map, the addition of GDP or GTPγS causes no observable decrease in solvent exchange around the nucleotide-binding pocket of β-tubulin (bound GDP is shown in magenta). As ligand binding typically leads to a localized decrease in deuterium exchange (protection to solvent exchange), specifically around the ligand-binding pocket (*e.g.*, see below), these results indicate that β-tubulin is not the species binding GDP or GTPγS in the TBCD/ARL2/β-tubulin trimer. Interestingly, when we compared the GDP- and GTPγS-bound states (GDP→GTPγS), there was an overall decrease in deuterium exchange observed throughout β-tubulin. This shows that when GTPγS replaces GDP in the TBCD/ARL2/β-tubulin complex, we see a decrease in solvent exchange, or an increase in protein stability, for β-tubulin. As we hypothesize that the β-tubulin is not binding nucleotide in the trimer, we interpret these results as evidence of an allosteric effect on the conformation of β-tubulin that is differentially altered by the binding of GDP or GTPγS to the only other protein capable of doing so, ARL2.

*HDX-MS analysis of ARL2 monomer reveals large changes, particularly at consensus GTP-binding motifs*

ARL2 is distinct among the ARF family GTPases as it has relatively low affinity for guanine nucleotides, is stable as an apoprotein, and purifies from tissues or recombinant sources without bound GDP. These characteristics allow us to study effects of binding either GDP or GTPγS without interference from pre-bound GDP. We overexpressed and then purified human ARL2 from HEK cell lysates using anion-exchange and size exclusion chromatography, as described previously (Bowzard et al., 2005) and in Experimental Procedures.

To determine the effects of nucleotide binding on the conformational dynamics of ARL2, we again performed differential HDX-MS analyses comparing the three nucleotide-bound states and graphed the average change in deuterium uptake per residue (Figure 6A), as described above. The addition of GDP to ARL2 (apo→GDP) resulted in large protection to deuterium uptake at the conserved nucleotide-binding motifs G1 and G3 (defined here as residues 23-30 and 125-128, respectively; see Figure 6A, blue line). These results are consistent with the well-established roles that these motifs play in nucleotide binding. Adding GTPγS to ARL2 (apo→GTPγS) showed similar changes in the G1 and G3 motifs to those seen in the apo→GDP comparison (Figure 6A, red line). The addition of GDP or GTPγS also caused increased solvent exchange around the effector binding loops, switches I and II (residues 40-53 and 70-81, respectively). Because these switches are directly involved in binding to effectors and/or modulators of the GTPase, it is expected that they become more conformationally mobile upon binding GTPγS. The binding of GTPγS also caused a stabilization, not seen in apo→GDP, around the G2 motif (residues 66-70), which is responsible for interactions with the gamma phosphate of GTP and contains the glutamine residue required for hydrolysis.

The GDP→GTPγS comparison is relevant to the actions of this GTPase in biology as it represents the activation process. This comparison (Figure 6A, green line) reveals that the largest increase in protein stabilization (*i.e.*, decrease in deuterium uptake, protection to solvent exchange) was localized around the G2 motif. We again generated a heat map that we then overlaid onto a previously published crystal structure of ARL2 (Zhang et al., 2009). The heat map data corresponding to the changes in deuterium uptake between each of the three comparisons made (apo→GDP, apo→GTPγS, and GDP→GTPγS) are shown in Figure 6B. As highlighted in these HDX perturbation map structures, addition of GDP or GTPγS to ARL2 results in the stabilization of the protein in regions concentrated around the nucleotide binding pocket (bound GTP shown in magenta), consistent with a typical protein-ligand interaction. Using these data as a baseline for the

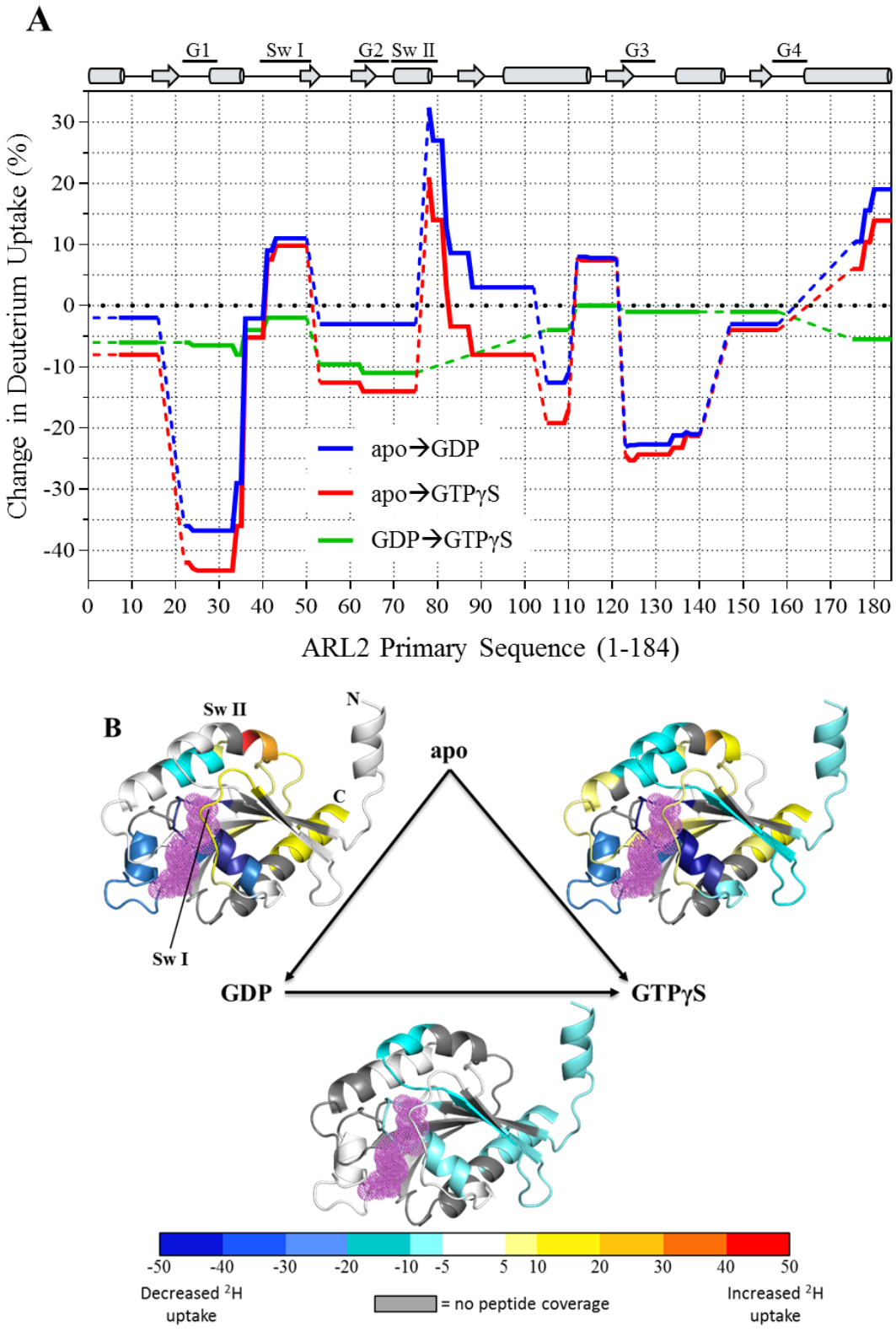
A
G1
Sw I
G2
Sw II
G3
G4
Change in Deuterium Uptake (%)
30
20
10
0
-10
-20
-30
-40
0 10 20 30 40 50 60 70 80 90 100 110 120 130 140 150 160 170 180
ARL2 Primary Sequence (1-184)
apo→GDP
apo→GTPγS
GDP→GTPγS
B
Sw II
N
C
Sw I
apo
GDP
GTPγS
-50 -40 -30 -20 -10 -5 5 10 20 30 40 50
Decreased ²H uptake
= no peptide coverage
Increased ²H uptake

**Figure 3-6. Nucleotide binding to ARL2 monomer results in distinct changes to the G motifs and switch regions of the protein.** ARL2 monomer was overexpressed and purified from HEK cells, as described in Experimental Procedures. Purified ARL2 (10 μM) was pre-incubated with 100 μM GDP, GTPγS or no nucleotide before analysis by HDX-MS. (**A**) The change in average percent of deuterium uptake was determined among the three samples at each residue. Dotted lines indicate regions not covered by mass spectrometry. Shown above the graph are the locations of conserved nucleotide binding motifs, G1-G4, the two canonical switches (Sw I/II), and α-helices and β-strands, based upon published structures. (**B**) We converted the differential deuterium exchange data to a heat map and overlaid it onto a previously published crystal structure of ARL2 (PDB ID: 3DOE). The nucleotide-binding site is shown in magenta. Gray indicates regions not sequenced by mass spectrometry. N, amino terminus. C, carboxyl terminus.

structural changes observed in ARL2 upon nucleotide binding, we proceeded to analyze effects of nucleotide binding to ARL2 in the TBCD/ARL2/β-tubulin complex.

*Formation of the TBCD/ARL2/β-tubulin complex results in distinct changes in the molecular dynamics of ARL2*

Comprehensive HDX analysis of protein-protein interactions can identify putative sites of interaction between two species. This requires the ability to compare the bound and unbound states of the protein in order to generate a differential deuterium exchange profile. A protein-protein interaction interface will result in increased intermolecular hydrogen bond formation, overall stabilization of the complex, and reduced solvent accessibility, all resulting in decreased solvent exchange. Unfortunately, ARL2 is the only component of our TBCD/ARL2/β-tubulin trimer that we can purify as a monomer in sufficient quantities to make such a comparison. Thus, we began our analysis of ARL2 in the TBCD/ARL2/β-tubulin complex by comparing ARL2 monomer and ARL2 in the trimer. We separately made comparisons to monitor the effects of nucleotide binding on ARL2 in the trimer (see below), but it is important to note that, unlike previously, in this section we are looking at differences in solvent accessibility of different regions/residues of ARL2 between monomer and trimer, primarily with a goal of identifying regions/residues involved in protein-protein interactions.

We compared the changes in deuterium uptake by ARL2 between the monomeric and trimeric species for each of the three forms (apo-ARL2, ARL2-GDP, and ARL2-GTPγS) and the average values per residue are shown in Figure 7A. Though the magnitude of the effects differed, the differential uptake profiles for ARL2 in the trimer were largely conserved between the different liganded states. This can be seen in the overall similarities in the three graphs in Figure 7A, or when the differences are mapped onto the three-dimensional model of ARL2-GTP (Figure 7B). Note that because no atomic structures are available for apo-ARL2 or ARL2-GDP the structure shown in

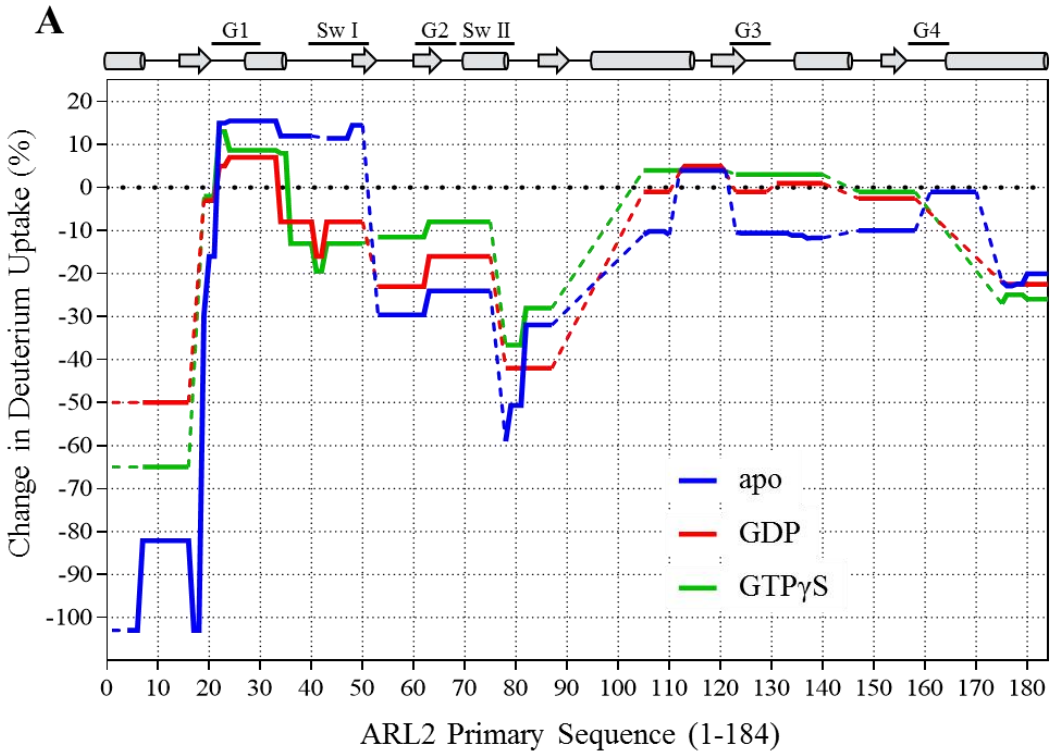
A
G1
Sw I
G2
Sw II
G3
G4
Change in Deuterium Uptake (%)
ARL2 Primary Sequence (1-184)
apo
GDP
GTPγS

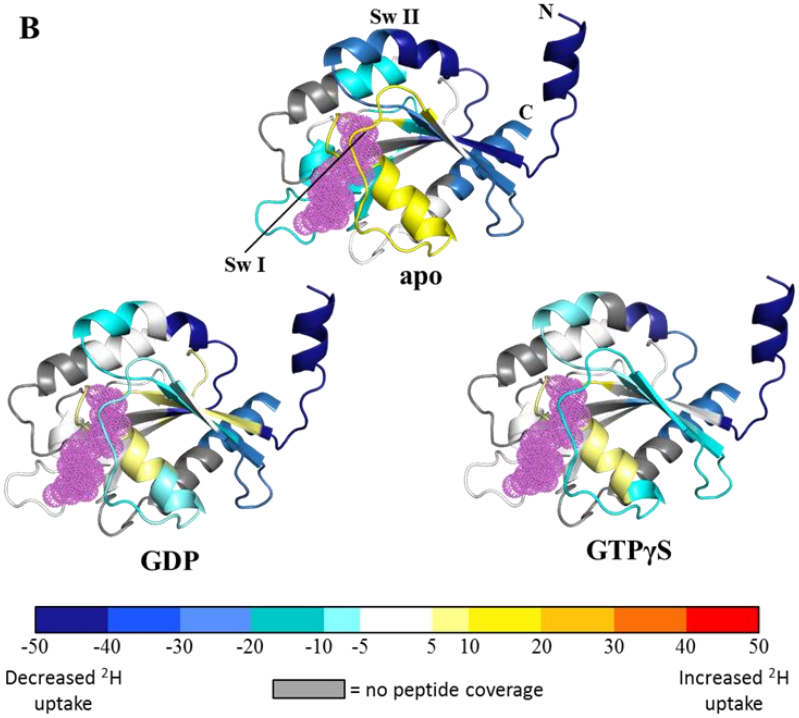
B
Sw II
N
C
Sw I
apo
GDP
GTPγS
Decreased ²H uptake
= no peptide coverage
Increased ²H uptake

**Figure 3-7. Comparing ARL2 monomer to the TBCD/ARL2/β-tubulin trimer reveals putative sites of protein-protein interaction**. ARL2 monomer or TBCD/ARL2/β-tubulin trimer were prepared and analyzed by HDX-MS, as described in previous legends and under Experimental Procedures. (**A**) The changes in deuterium exchange were determined per residue for ARL2 by subtracting the average rate of deuterium exchange at each residue in the monomer from the same residue in the trimer after incubation with no nucleotide (apo; blue line), GDP (red line), or GTPγS (green line). Dotted lines indicate regions not sequenced by mass spectrometry. (**B**) The differential exchange data were overlaid onto an ARL2 crystal structure (PDB ID: 3DOE) to highlight the localized changes in deuterium uptake. The nucleotide binding pocket is highlighted in magenta. Gray indicates regions not covered by mass spectrometry sequencing. N, amino terminus. C, carboxyl terminus.

every case is that of ARL2 bound to GTP and an effector (not shown), and thus are not intended to represent the actual structures of monomer or ARL2 in the trimer. Rather, we show them to highlight where in the folded protein the differences are occurring. Most obviously, there was a complete protection to deuterium exchange at the N terminus of ARL2 in the trimer compared to the monomer. This is interpreted as strong evidence that the N terminus is involved in binding to TBCD/β-tubulin. The N-terminal, amphipathic helix of ARF family members are known to act like a third switch region and, specifically, structures of ARL2 bound to effectors document such a role in effector interactions (Hanzal-Bayer et al., 2002; Zhang et al., 2009). As highlighted by the structural overlay of the HDX perturbation map data (Figure 7B), the N-terminal helix is positioned away from the main body of the protein, making it readily available for interaction with effector proteins. The next most altered regions of ARL2 in this comparison are switch II and the C terminus. While switch II is also known to be directly involved in binding to protein partners, no such role has previously been identified for the C terminus. In contrast, residues 21-50 had increased solvent exchange in the trimer, in comparison to the monomer. This region includes both the G1 motif and switch I, with the effect on the latter reversed upon binding of GDP or GTPγS. Thus, the only destabilization seen in all three liganded states was localized to the G1 region, indicating that ARL2 interaction with TBCD/β-tubulin causes this conserved nucleotide binding motif to become more conformationally flexible.

*ARL2 binds guanine nucleotide in the TBCD/ARL2/β-tubulin complex*

While in the previous experiment we compared solvent exchange of ARL2 residues in monomer vs trimer, here we compare the changes seen in ARL2 only in the trimer (*i.e.*, trimer vs trimer), but comparing the different liganded states. We incubated purified TBCD/ARL2/β-tubulin in a 10-fold molar excess of GDP, GTPγS, or no nucleotide before performing HDX-MS. As described above, we analyzed the changes in deuterium uptake for ARL2 in the trimer by plotting

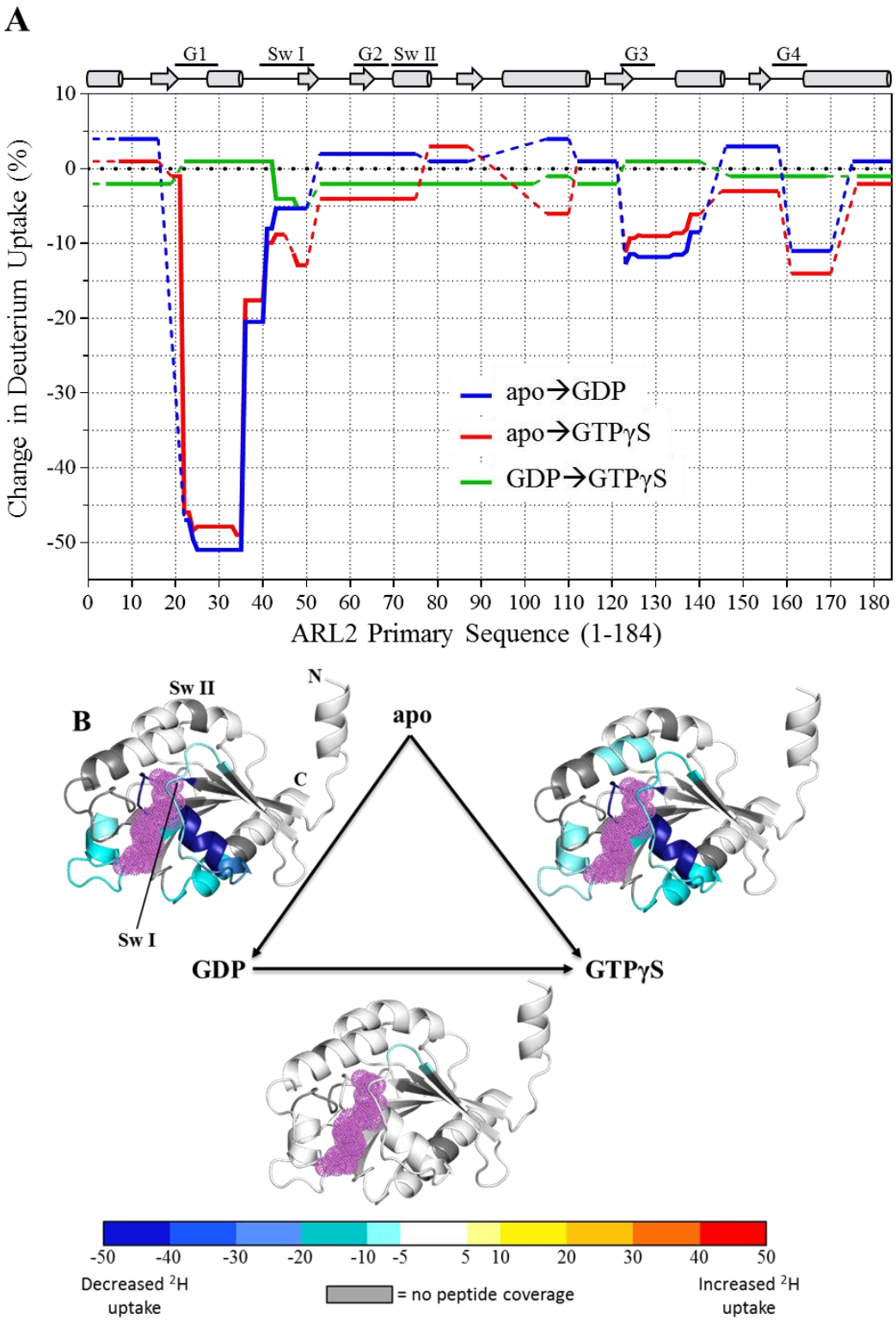
A
G1
Sw I
G2
Sw II
G3
G4
Change in Deuterium Uptake (%)
ARL2 Primary Sequence (1-184)
apo→GDP
apo→GTPγS
GDP→GTPγS
B
Sw II
N
C
Sw I
apo
GDP
GTPγS
Decreased ²H uptake
= no peptide coverage
Increased ²H uptake

**Figure 3-8. Binding of guanine nucleotides by the TBCD/ARL2/β-tubulin trimer results in highly localized changes in deuterium uptake around the nucleotide binding pocket of ARL2.** Purified trimer (10 μM) was pre-incubated with 100 μM GDP, GTPγS or no nucleotide before being analyzed by HDX-MS. (**A**) The changes in deuterium uptake at each residue of ARL2 were compared among the three samples. Dotted lines indicate regions not covered by MSMS. (**B**) The differential deuterium exchange data were overlaid onto an ARL2 structure (PDB ID: 3DOE). The nucleotide binding site is highlighted in magenta. Gray indicates regions not covered by mass spectrometry sequencing. N, amino terminus. C, carboxyl terminus.

the average values per residue (Figure 8A) and showing a structural overlay of the corresponding heat map data (Figure 8B). The addition of GDP (apo→GDP) or GTPγS (apo→GTPγS) to the TBCD/ARL2/β-tubulin trimer resulted in localized stabilizations, or decreased exchange, of ARL2 at the conserved nucleotide binding motifs G1 and G3. In contrast to the results obtained for the ARL2 monomer, we also observed a decrease in exchange at the G4 motif (residues 158-162), though this is possibly a result of better sequence coverage for this specific region in the trimer analysis. Interestingly, we did not see a change in solvent exchange around the G2 motif after the addition of GTPγS, or in the comparison of GDP→GTPγS, which we saw for the ARL2 monomer. We believe this to be due to the strong stabilization of the G2 and switch II regions of ARL2 that result from interaction with TBCD/β-tubulin (Figure 7). As can be clearly seen in Figure 8B, the addition of nucleotide to the TBCD/ARL2/β-tubulin complex results in highly localized decreases in deuterium exchange that are centered around the nucleotide binding pocket of ARL2. These results are consistent with the nucleotide binding data (Figure 1) and strongly support the conclusion that ARL2 binds nucleotide in the TBCD/ARL2/β-tubulin trimeric complex.

**Discussion**

We recently described the use of HEK cells to express human or bovine TBCD, either alone or with co-expression of other components of the tubulin-folding pathway, and purified three novel protein complexes that each contained TBCD (Francis et al., 2017). Only one of those appeared to be a monodisperse complex with stoichiometric components, the TBCD/ARL2/β-tubulin trimer. The binding of ARL2 to TBCD is highly specific in that other ARF family members, specifically the closest paralog ARL3, could not bind to TBCD under these conditions, in contrast to previously reported results (Veltel et al., 2008). Additionally, no α-tubulin was present in the trimer (Francis et al., 2017). Here we describe the characterization of the guanine-nucleotide binding properties of this trimer, in comparison to the ARL2 monomer. We found fairly large

changes in both on- and off-rates when ARL2 is bound to TBCD/β-tubulin that result in higher apparent affinities for guanine nucleotides. We also used HDX assays to monitor effects of nucleotide binding on the conformational dynamics of each component in the complex. Despite TBCD being the largest component in the trimer, it displayed the smallest conformational changes overall. The β-tubulin in the trimer displayed larger changes in deuterium uptake than those seen in TBCD, with GDP binding causing an increase in solvent exchange (decreased stability) and GTPγS a decrease in exchange (increased stability) as compared to the GDP-bound state. We conclude that the folding, or conformational stability, of β-tubulin in the trimer is sensitive to the binding of guanine nucleotides by the trimer. However, the observed changes in solvent exchange of residues in β-tubulin, upon the trimer binding to GDP or GTPγS, did not map onto the nucleotide binding pocket, suggesting that β-tubulin is not the species that binds nucleotides in our assays. In contrast, the largest changes in solvent exchange seen in any of the three proteins in the trimer, resulting from nucleotide binding, were those seen in ARL2, and were all in the canonical nucleotide binding motifs, G1, G3, and G4. Therefore, we propose that the binding, and cycling, of guanine nucleotides on ARL2 in the TBCD/ARL2/β-tubulin trimer regulates the conformational dynamics, or folded state, of β-tubulin in the complex. HDX data were also used to identify residues/regions of ARL2 that are involved in its binding to TBCD/β-tubulin, and we found those to be similar to previously reported effector binding residues. We discuss the implications of these findings further below.

The fact that our trimer bound both GDP and GTPγS, in contrast to the previously characterized TBCD/ARL2 dimer purified from bovine brain (Shern et al., 2003), allowed us to make comparisons between the ligands and the different quaternary states of ARL2. The trimer displayed higher apparent affinities (lower $K_D$'s) for both nucleotides than did the monomer, with the highest affinity for Gpp(NH)p. As ARL2 remains a stable part of the trimer regardless of whether either nucleotide is bound, the binding of ARL2 in the trimer is not consistent with TBCD/β-tubulin acting as a classical effector of ARL2. Rather, TBCD/β-tubulin may serve a role

as a non-canonical GEF for ARL2 in that it binds stably to the apo-GTPase, it increases the off-rate of GDP, and its binding increases the apparent affinity for GTP. However, in contrast to the canonical actions of a GEF, the ARL2 is not released upon binding the activating ligand, GTPγS. We speculate that ARL2 may not be acting in the trimer, and by extension in tubulin folding, as a classical regulatory GTPase that activates a downstream signaling pathway upon binding GTP. Rather, the rapid binding and exchange of guanine nucleotides may be required for its actions, which include promoting changes in the tertiary structure of β-tubulin. Because ARL2 has other essential actions in other parts of the cell, notably effects on mitochondrial morphology, motility and ATP production (Sharer et al., 2002; Nishi et al., 2010; Newman et al., 2014; Francis et al., 2016; Newman et al., 2017), it is interesting that the vast majority of it is complexed with TBCD and not readily released upon nucleotide exchange. We speculate that release of ARL2 from the trimer will be found to be a regulated process with the potential to link its disparate functions in cells.

We began here by analyzing the nucleotide binding properties of TBCD/ARL2/β-tubulin using a filter trapping assay, a classical binding assay that was also used in characterization of the TBCD/ARL2 dimer, purified from bovine tissue (Shern et al., 2003). In contrast to that TBCD/ARL2 dimer, the TBCD/ARL2/β-tubulin trimer bound GTPγS to similar stoichiometries as ARL2 monomer. This comparison leads to the implication that it is the β-tubulin that, when bound to TBCD/ARL2, promotes the binding of GTP to ARL2. If true, this would have clear implications to models of tubulin folding and the roles of ARL2 in this process, as described below. However, we caution that comparisons between results obtained from studies of the bovine brain TBCD/ARL2 dimer to those from the trimer purified from HEK cells, after overexpression of two of the three components, may be complicated by a number of factors. These include potential differences in post-translational modifications on any of the proteins involved, and that those may change over the time required (>1 week) to purify the dimer from bovine tissue. However, we do

not believe species differences play an important role as the human and bovine TBCD behave indistinguishably in our assays.

Characterization of the nucleotide-binding properties of the TBCD/ARL2/β-tubulin complex is inherently confounded by the presence of two nucleotide-binding proteins. We began to address this by showing that when we form the complex using the dominant-negative ARL2 mutant (*i.e.*, TBCD/ARL2[T30N]/β-tubulin), the trimer loses the ability to bind GTP in the filter trapping assay. This result strongly suggests that the nucleotide binding is on ARL2. This was further strongly supported by HDX data, as the other potential nucleotide binder, β-tubulin, displayed no protection from solvent exchange in its nucleotide binding pocket residues upon addition of guanine nucleotides. In contrast, ARL2 had quite large, localized decreases in solvent exchange centered around the consensus binding motifs, G1, G3, and G4. Thus, we conclude that β-tubulin in the trimer is not binding guanine nucleotides in either of our *in vitro* binding assays and that any nucleotide-induced changes in solvent exchange, of residues in any of the three proteins analyzed, result from binding of the ligand to ARL2.

Though we conclude that the β-tubulin is not binding guanine nucleotides, we do believe its structure is altered in response to the ARL2 binding ligands. The binding of GTP caused moderate decreases in deuterium exchange across nearly the entire β-tubulin sequence, as compared to the GDP-bound state. The increased solvent protection is not localized to specific regions of the protein, suggesting perhaps a concerted conformational change of the β-tubulin while still bound in the complex. The predominant factor in decreased, or slowed, hydrogen/deuterium exchange is the hydrogen bond, specifically the strengthening of existing H-bonds or the formation of new H-bonds. Because we see a decrease in solvent exchange (*i.e.*, increased hydrogen bonding) throughout β-tubulin, we conclude that exchange of GDP for GTP on ARL2 causes an increase in the stability of β-tubulin, consistent with its progression toward folding into a more native state.

The 133 kDa TBCD in the trimer did not display large changes in deuterium exchange upon incubation with nucleotides. There were a few localized changes that occurred after the

addition of GDP or GTP, suggesting that nucleotide binding (to ARL2) can induce conformational changes that result in altered molecular dynamics of TBCD. It also appears that the conformational changes are nucleotide-specific as the addition of GDP or GTP had generally opposing effects, with GDP causing a few moderate increases in deuterium exchange and GTP causing slight decreases in exchange. We believe that these changes in TBCD structure are consistent with it playing a scaffolding role in binding ARL2 and β-tubulin, allowing nucleotide binding and promoting a more stable conformation, respectively; though more work is needed to confirm such a role.

In addition to the effects of nucleotide binding, a stable preparation of ARL2 monomer permitted comparisons of the protein monomer vs in the trimer, which is not currently feasible for the other components of the complex. Mammalian ARL2 can be readily purified from bacteria as a soluble, stable and active monomer (Clark et al., 1993; Bowzard et al., 2005). However, in efforts to minimize potential differences resulting from bacterial expression, we also purified ARL2 monomer from HEK cells after overexpression of the human protein. ARL2 has a relatively low affinity for nucleotide (Hanzal-Bayer et al., 2005) and is assumed to purify in the nucleotide-free state, unlike most other regulatory GTPases that purify with GDP bound and are unstable as apoproteins. This allowed us to directly compare the apo and nucleotide-bound states in our HDX studies, which to our knowledge has not been reported previously for a regulatory GTPase. When ARL2 was incubated with either GDP or GTP, there were distinct decreases in deuterium exchange localized around the conserved G1 and G3 motifs, each of which contain residues that directly interact with the bound nucleotide. Decreased solvent exchange in the G2 motif was also observed with the addition of GTP or the comparison of GDP to GTP, which is consistent with the role this motif plays in interacting with the γ-phosphate. The G4 motif was the only conserved nucleotide-binding region that did not show a decrease in deuterium exchange, though this could possibly be due to a lack of MS coverage near this region. Also interesting are the changes in switch I and switch II, the nucleotide-sensitive regions involved in effector binding, which both show a significant increase in deuterium exchange after the addition of either GDP or GTP. Although

perhaps surprising that the comparison of GDP- and GTP-bound states did not result in larger changes in the switch regions, these loops may be inherently conformationally flexible in each ligand-bound state, with more subtle differences promoting association with effectors or modulators of the GTPase.

By comparing the deuterium exchange profiles of ARL2 monomer and ARL2 in the trimer, we were able to identify regions of ARL2 that we propose to be involved in the binding of ARL2 to TBCD/β-tubulin. The N-terminal, amphipathic helix of ARF family members has been proposed to function as a third switch region as a result of its dramatic changes in structure associated with activation of the protein. In some family members (including the ARFs and ARL1) the N terminus is myristoylated and GTP binding results in increased translocation onto membranes, with the N terminus being directly involved in membrane insertion (Kahn et al., 1988; Tamkun et al., 1991; Randazzo and Kahn, 1995; Liu et al., 2009). Though ARL2 is not acylated, its N terminus is directly involved in interaction with downstream effectors, based upon both detailed structural studies of protein complexes and the loss of interactions and functions resulting from its deletion (Hanzal-Bayer et al., 2002; Zhang et al., 2009; Francis et al., 2017). Consistently, the N terminus shows the most dramatic decrease in deuterium exchange when comparing the monomer and trimer forms of ARL2, strongly indicating a direct role in protein-protein interaction. The HDX data also suggest that switch II, and possibly the C terminus, are involved in direct interaction with TBCD/β-tubulin. We previously showed that a mutation in switch I, ARL2[F50A], had a severe effect on the ability of ARL2 to co-purify with TBCD/β-tubulin (Francis et al., 2017). However, the data shown here only show a moderate protection to solvent exchange around switch I. Interestingly, switch I is the only region of ARL2 that shows a difference between nucleotide-bound and apo states, perhaps further indication of different nucleotide-dependent conformations of the TBCD/ARL2/β-tubulin complex.

By way of summary, we offer our current, putative model of the role of ARL2 in tubulin folding. Modeling the actions of the different components in our trimer leads us to speculate that

nascent β-tubulin, presumably presented in the form of TBCA/β-tubulin, based upon Tian, et al (Tian et al., 1996), binds to the TBCD/ARL2 dimer, with release of TBCA and formation of the TBCD/ARL2/β-tubulin trimer. As a consequence, the binding of GTP to ARL2 is promoted, which in turn promotes the folding of β-tubulin toward a more stable/native state. Again based upon previous work (Lewis et al., 1997), we further speculate that α-tubulin, likely the TBCE/α-tubulin dimer, is introduced at that point to form the penultimate complex: the TBCD/ARL2/TBCE/α-tubulin/β-tubulin pentamer. It has been proposed that αβ-tubulin heterodimer formation is completed and this penultimate complex resolved upon hydrolysis of GTP, by association of TBCC (Lewis et al., 1997; Tian et al., 1999). In our model of tubulin folding, and consistent with our purification of TBCD/ARL2 from bovine brain and of the trimer purified from HEK cells, TBCD and ARL2 are very stably bound and are modeled as not dissociating at any point during the cycle of tubulin folding. It is each cycle of GTP binding, GTP hydrolysis, and release of GDP (all proposed now to be on ARL2) that promote a round of increased folding of β-tubulin into a form that associates with α-tubulin. Of course, this larger model goes well beyond our current studies but is based upon previous studies and is intended to highlight the proposed impact of our findings on the model of tubulin folding. Further testing of aspects of this, and other, models of tubulin folding are planned and made more feasible by the availability of recombinant complexes in milligram amounts.

**Experimental Procedures**

*Cell Culture:* Human embryonic kidney (HEK293T/17) cells were obtained from the ATCC and grown in DMEM (Invitrogen, Carlsbad, CA) supplemented with 10% fetal bovine serum and 2 mM glutamine at 37 °C in the presence of 5% $CO_2$.

*Plasmids:* Plasmids directing expression of human ARL2 and ARL2[T30N] in pcDNA3.1 (Zhou et al., 2006) and pET3C (Clark et al., 1993) vectors were described previously. We obtained a

plasmid containing human TBCD (NP_005984.3) from ATCC (clone MGC-1583) and the full-length open reading frame was moved into the pLEXm-GST vector (gift from James Hurley, NIH) using NotI and XhoI sites to generate an N-terminal, GST-tagged construct (GST-TBCD). We also cloned full-length bovine TBCD (NP_776619.1; Source Biosciences) into the same sites. The human and bovine constructs have a TEV protease cleavage site between the GST and TBCD, which results in a 12 amino acid residual extension at the N terminus of TBCD after cleavage.

*Recombinant Protein Expression/Purification:* Human ARL2 was expressed in BL21(DE3) *E. coli* and purified as previously described (Bowzard et al., 2005). For recombinant mammalian expression of GST-TBCD and ARL2, HEK293T/17 (HEK) cells were transfected as previously described (Francis et al., 2017). Briefly, HEK cells were transfected at 70-90% density using polyethyleneimine (PEI; Polysciences, catalog no. 24765-2) at a 1:3 ratio (DNA:PEI). In all transfections and co-transfections, plasmids were used at 1 µg DNA/mL medium. After 48 hours, cells were harvested and the pellets either lysed immediately for purification or flash frozen in liquid nitrogen and stored at -80 °C for later use. GST-TBCD complexes were purified from HEK cell lysates as previously described (Francis et al., 2017). Briefly, HEK cell pellets were resuspended in lysis buffer (25 mM HEPES, 100 mM NaCl, 1 mM DTT, 1% CHAPS, pH 7.4, supplemented with protease inhibitor cocktail (Sigma, catalog no. P2714)) and incubated at 4 °C for 15 min, with gentle rotation. Lysates were clarified by centrifugation at 14,000×*g* for 30 min (S14). For recombinant purification of untagged human ARL2 from HEK cells, lysates were further clarified as previously described (Bowzard et al., 2005). For purification of GST-TBCD complexes, we incubated the S14 with glutathione-conjugated Sepharose beads (GE, catalog no. 17075601) overnight at 4 °C, with gentle rotation. The sample was poured onto a chromatography column (Bio-Rad, catalog no. 7311550), washed with 5 column volumes of wash buffer (25 mM HEPES, 100 mM NaCl, 1 mM DTT, pH 7.4), and eluted in wash buffer supplemented with 20 mM glutathione (EMD Millipore, catalog no. 3541), adjusted to pH 8.0. For removal of the GST tag,

1% (w/w) TEV protease was added to the sample and incubated overnight at 4 °C. We further purified the sample by size exclusion chromatography (Superdex 200), and then pooled and concentrated the appropriate fractions.

*Nucleotide Binding Assays:* Binding of [$^{35}$S]GTPγS to ARL2 or TBCD complexes was assayed using the nitrocellulose filter trapping method, as previously described (Bowzard et al., 2005). Nucleotide binding kinetics were determined in a solution-based assay using GDP and 5′-[β,γ-imido]triphosphate (Gpp(NH)p), each fluorescently labeled with *N*-methylanthraniloyl (mant). Using an automatic injector, mant-GDP or mant-Gpp(NH)p (1 μM each) was added to purified proteins (2 μM) diluted in binding buffer (25 mM HEPES, 100 mM NaCl, 1 mM EDTA, 2.5 mM $MgCl_2$, pH 7.4), and fluorescence intensity (Ex 340, Em 460) was measured every 10 s at room temperature using a BioTek Synergy 4 plate reader. After 20 min, excess (100 μM) unlabeled GDP or Gpp(NH)p was added to the reaction and the fluorescence intensity was again measured every 10 s. For each individual assay, we obtained a baseline measurement for 2 min prior to injection of nucleotide to account for intrinsic fluorescence of the protein; the average value of the baseline signal was subtracted from every point measured throughout the assay. A no protein control was included in each assay and subtracted to account for the background fluorescence of the mant-labeled nucleotides. We imported the resulting datasets into GraphPad Prism software for graphing and kinetics analyses. Nonlinear regression was used to fit an association/dissociation model to the data, from which on- and off-rates, and corresponding apparent affinities, were determined. All binding assays (radioligand and mant) were performed at least twice for each of the proteins and protein complexes shown and typically with independently prepared protein preparations.

*Thermal Denaturation (Thermofluor) Assay:* Purified TBCD/ARL2/β-tubulin (5 μM) was pre-incubated with a 10-fold molar excess of GDP, GTPγS or no nucleotide for one hr on ice. $MgCl_2$ was included at a final concentration of 1 mM to facilitate nucleotide binding. Immediately prior

to analysis, 2 µL of a 1:100 dilution of SYPRO Orange dye (Sigma, catalog no. S5692) was added to 20 µL of each sample. Fluorescence intensity (Ex 488 nm, Em 603 nm) was monitored, as a measure of thermal denaturation, using a StepOnePlus Real-Time PCR System (ThermoFisher, catalog no. 4376600) every 2 min over the range of 25-55 °C (0.5 °C/min temperature gradient). We fit the resulting curves to a Boltzmann sigmoidal equation using GraphPad Prism software to determine the melting temperature (inflection point) for each sample. Data represent the averages of two experiments for each sample.

*Hydrogen/Deuterium Exchange Coupled with Mass Spectrometry (HDX-MS):* TBCD/ARL2/β-tubulin and ARL2 monomer were purified from HEK cells, as described above. Purified proteins (10 µM) were pre-incubated in 100 µM GDP, GTPγS or no nucleotide with 1 mM $MgCl_2$ for at least 1 hr on ice prior to HDX analyses. Solution phase amide HDX was performed with a fully automated system as previously described (Goswami et al., 2013). Briefly, 5 µl of 10 µM sample (monomer or trimer) was diluted to 25 µl with $D_2O$-containing wash buffer (described above) and incubated at 4 °C for 10, 30, 60, 300, 900, or 3600 s. Following on-exchange, back-exchange was minimized and the protein denatured by dilution to 50 µl in a low pH and low temperature buffer containing 0.1% (v/v) TFA in 3 M urea (held at 1 °C). Samples were then passed across an immobilized pepsin column (prepared in house) at 50 µl/min (0.1% (v/v) TFA, 15 °C). The resulting peptides were trapped on a C8 trap cartridge (Hypersil Gold, Thermo Fisher). Peptides were then gradient eluted from 4% (w/v) $CH_3CN$ to 40% (w/v) $CH_3CN$, 0.3% (w/v) formic acid over 5 min at 2 °C across a 1 X 50-mm C18 HPLC column (Hypersil Gold, Thermo Fisher) and electrosprayed directly into an Exactive hybrid quadrupole-Orbitrap mass spectrometer (Thermo Fisher). Peptide ion signals were confirmed if they had a MASCOT score of 20 or greater and had no ambiguous hits using a decoy (reverse) sequence in a separate experiment using a 60 min gradient. The intensity-weighted average m/z value (centroid) of each peptide's isotopic envelope was calculated with software developed in house (Pascal et al., 2012) and corrected for back-

exchange on an estimated 70% recovery and accounting for the known deuterium content of the on-exchange buffer. In order to visualize the differential exchange data for each of the comparisons made, we calculated the average percentage of deuterium uptake for each sequenced peptide following 10, 30, 60, 300, 900, and 3600 s of on-exchange, and then we subtracted the average percentage of deuterium uptake for the corresponding sample (*i.e.*, GDP – apo, GTPγS – apo, GTPγS – GDP, and trimer – monomer). We then used a residue averaging approach to obtain better resolution of the data. For each residue, the deuterium incorporation values and peptide lengths from all overlapping peptides were assembled. A weighting function was applied in which shorter peptides were weighted more heavily and longer peptides were weighted less. Each of the weighted deuterium incorporation values were then averaged to produce a single value for each amino acid. The initial two residues of each peptide, as well as prolines, were omitted from the calculations. This approach is similar to that previously described (Keppel and Weis, 2015). These single residue values were plotted using GraphPad Prism software. The data were also color coded based on magnitude and direction, and the resulting heat map data were overlaid onto crystal structures of the proteins, where available. A previously published structure for ARL2 (PDB ID: 3DOE (Zhang et al., 2009)) and a homology model for human β-tubulin (based on PDB ID: 3RYC (Nawrotek et al., 2011)) were used. For each of these structures, the bound nucleotide (GTP for ARL2 and GDP for β-tubulin) was included in the figure (shown in magenta) to highlight the nucleotide-binding pocket of each protein.

*Reproducibility and Statistical Analyses:* All nucleotide binding and thermal denaturation assays described have been independently repeated at least twice. HDX analyses were performed in triplicate, with single preparations of each purified protein/complex. Statistical significance for the differential HDX data is determined by t test for each time point, and is integrated into the HDX Workbench software (Pascal et al., 2012).

**Acknowledgements:** We would like to thank Dr. James Hurley (NIH) for the gift of the pLEXm vectors. This work was supported by grants from the National Institutes of Health 5R01GM090158 to RAK, 1F31CA189672 to JWF, R01DK095750 to EAO, and 1F31GM113397-01A1 to ERW.

**Conflict of Interest:** The authors declare that they have no conflicts of interest with the contents of this article.

**Author Contributions:** JWF conducted many of the experiments, analyzed all data, and wrote the paper. DG and SJN designed, performed and, along with BDP, analyzed the HDX experiments. PRG coordinated HDX analyses and contributed to writing of the manuscript. ERW designed, performed and analyzed data shown in Figure 2. EAO provided critical analysis of HDX data and manuscript. RAK coordinated the study and wrote the paper with JWF.

**References**

Antoshechkin, I. and Han, M. (2002). The C. elegans evl-20 gene is a homolog of the small GTPase ARL2 and regulates cytoskeleton dynamics during cytokinesis and morphogenesis. Dev Cell 2, 579-591.

Bailey, L.K., Campbell, L.J., Evetts, K.A., Littlefield, K., Rajendra, E., Nietlispach, D., Owen, D. and Mott, H.R. (2009). The structure of binder of Arl2 (BART) reveals a novel G protein binding domain: implications for function. J Biol Chem 284, 992-999.

Bichet, P., Mollat, P., Capdevila, C. and Sarubbi, E. (2000). Endogenous glutathione-binding proteins of insect cell lines: characterization and removal from glutathione S-transferase (GST) fusion proteins. Protein Expr Purif 19, 197-201.

Bowzard, J.B., Sharer, J.D. and Kahn, R.A. (2005). Assays used in the analysis of Arl2 and its binding partners. Methods Enzymol 404, 453-467.

Chen, K., Koe, C.T., Xing, Z.B., Tian, X., Rossi, F., Wang, C., Tang, Q., Zong, W., Hong, W.J., Taneja, R., Yu, F., Gonzalez, C., Wu, C., Endow, S. and Wang, H. (2016). Arl2- and Msps-dependent microtubule growth governs asymmetric division. J Cell Biol 212, 661-676.

Christis, C. and Munro, S. (2012). The small G protein Arl1 directs the trans-Golgi-specific targeting of the Arf1 exchange factors BIG1 and BIG2. J Cell Biol 196, 327-335.

Clark, J., Moore, L., Krasinskas, A., Way, J., Battey, J., Tamkun, J. and Kahn, R.A. (1993). Selective amplification of additional members of the ADP-ribosylation factor (ARF) family: cloning of additional human and Drosophila ARF-like genes. Proc Natl Acad Sci U S A 90, 8952-8956.

Cunningham, L.A. and Kahn, R.A. (2008). Cofactor D functions as a centrosomal protein and is required for the recruitment of the gamma-tubulin ring complex at centrosomes and organization of the mitotic spindle. J Biol Chem 283, 7155-7165.

D'Souza, R.S., Semus, R., Billings, E.A., Meyer, C.B., Conger, K. and Casanova, J.E. (2014). Rab4 orchestrates a small GTPase cascade for recruitment of adaptor proteins to early endosomes. Curr Biol 24, 1187-1198.

Dascher, C. and Balch, W.E. (1994). Dominant inhibitory mutants of ARF1 block endoplasmic reticulum to Golgi transport and trigger disassembly of the Golgi apparatus. J Biol Chem 269, 1437-1448.

Edvardson, S., Tian, G., Cullen, H., Vanyai, H., Ngo, L., Bhat, S., Aran, A., Daana, M., Da'amseh, N., Abu-Libdeh, B., Cowan, N.J., Heng, J. and Elpeleg, O. (2016). Infantile Neurodegenerative Disorder Associated with Mutations in TBCD, an Essential Gene in the Tubulin Heterodimer Assembly Pathway. Hum Mol Genet.

Fanarraga, M.L., Bellido, J., Jaen, C., Villegas, J.C. and Zabala, J.C. (2010). TBCD links centriologenesis, spindle microtubule dynamics, and midbody abscission in human cells. PLoS One 5, e8846.

Farnsworth, C.L. and Feig, L.A. (1991). Dominant inhibitory mutations in the Mg(2+)-binding site of RasH prevent its activation by GTP. Mol Cell Biol 11, 4822-4829.

Fedyanina, O.S., Mardanov, P.V., Tokareva, E.M., McIntosh, J.R. and Grishchuk, E.L. (2006). Chromosome segregation in fission yeast with mutations in the tubulin folding cofactor D. Curr Genet 50, 281-294.

Feig, L.A. and Cooper, G.M. (1988). Inhibition of NIH 3T3 cell proliferation by a mutant ras protein with preferential affinity for GDP. Mol Cell Biol 8, 3235-3243.

Flex, E., Niceta, M., Cecchetti, S., Thiffault, I., Au, M.G., Capuano, A., Piermarini, E., Ivanova, A.A., Francis, J.W., Chillemi, G., Chandramouli, B., Carpentieri, G., Haaxma, C.A., Ciolfi, A., Pizzi, S., Douglas, G.V., Levine, K., Sferra, A., Dentici, M.L., Pfundt, R.R., Le Pichon, J.B., Farrow, E., Baas, F., Piemonte, F., Dallapiccola, B., Graham, J.M., Jr., Saunders, C.J., Bertini, E., Kahn, R.A., Koolen, D.A. and Tartaglia, M. (2016). Biallelic Mutations in

TBCD, Encoding the Tubulin Folding Cofactor D, Perturb Microtubule Dynamics and Cause Early-Onset Encephalopathy. Am J Hum Genet 99, 962-973.

Francis, J.W., Newman, L.E., Cunningham, L.A. and Kahn, R.A. (2017). A Trimer Consisting of the Tubulin-specific Chaperone D (TBCD), Regulatory GTPase ARL2, and beta-Tubulin Is Required for Maintaining the Microtubule Network. J Biol Chem 292, 4336-4349.

Francis, J.W., Turn, R.E., Newman, L.E., Schiavon, C. and Kahn, R.A. (2016). Higher order signaling: ARL2 as regulator of both mitochondrial fusion and microtubule dynamics allows integration of 2 essential cell functions. Small GTPases 7, 188-196.

Gao, Y., Vainberg, I.E., Chow, R.L. and Cowan, N.J. (1993). Two cofactors and cytoplasmic chaperonin are required for the folding of alpha- and beta-tubulin. Mol Cell Biol 13, 2478-2485.

Goswami, D., Devarakonda, S., Chalmers, M.J., Pascal, B.D., Spiegelman, B.M. and Griffin, P.R. (2013). Time window expansion for HDX analysis of an intrinsically disordered protein. J Am Soc Mass Spectrom 24, 1584-1592.

Grynberg, M., Jaroszewski, L. and Godzik, A. (2003). Domain analysis of the tubulin cofactor system: a model for tubulin folding and dimerization. BMC Bioinformatics 4, 46.

Hanzal-Bayer, M., Linari, M. and Wittinghofer, A. (2005). Properties of the interaction of Arf-like protein 2 with PDEdelta. J Mol Biol 350, 1074-1082.

Hanzal-Bayer, M., Renault, L., Roversi, P., Wittinghofer, A. and Hillig, R.C. (2002). The complex of Arl2-GTP and PDE delta: from structure to function. EMBO J 21, 2095-2106.

Hirata, D., Masuda, H., Eddison, M. and Toda, T. (1998). Essential role of tubulin-folding cofactor D in microtubule assembly and its association with microtubules in fission yeast. EMBO J 17, 658-666.

Hoyt, M.A., Stearns, T. and Botstein, D. (1990). Chromosome instability mutants of Saccharomyces cerevisiae that are defective in microtubule-mediated processes. Mol Cell Biol 10, 223-234.

Ikeda, T., Nakahara, A., Nagano, R., Utoyama, M., Obara, M., Moritake, H., Uechi, T., Mitsui, J., Ishiura, H., Yoshimura, J., Doi, K., Kenmochi, N., Morishita, S., Nishino, I., Tsuji, S. and Nunoi, H. (2016). TBCD may be a causal gene in progressive neurodegenerative encephalopathy with atypical infantile spinal muscular atrophy. J Hum Genet.

Jones, S., Jedd, G., Kahn, R.A., Franzusoff, A., Bartolini, F. and Segev, N. (1999). Genetic interactions in yeast between Ypt GTPases and Arf guanine nucleotide exchangers. Genetics 152, 1543-1556.

Jordan, M.A. and Wilson, L. (2004). Microtubules as a target for anticancer drugs. Nat Rev Cancer 4, 253-265.

Jung, V., Wei, W., Ballester, R., Camonis, J., Mi, S., Van Aelst, L., Wigler, M. and Broek, D. (1994). Two types of RAS mutants that dominantly interfere with activators of RAS. Mol Cell Biol 14, 3707-3718.

Kahn, R.A., Goddard, C. and Newkirk, M. (1988). Chemical and immunological characterization of the 21-kDa ADP-ribosylation factor of adenylate cyclase. J Biol Chem 263, 8282-8287.

Keppel, T.R. and Weis, D.D. (2015). Mapping residual structure in intrinsically disordered proteins at residue resolution using millisecond hydrogen/deuterium exchange and residue averaging. J Am Soc Mass Spectrom 26, 547-554.

Lewis, S.A., Gu, W. and Cowan, N.J. (1987). Free intermingling of mammalian beta-tubulin isotypes among functionally distinct microtubules. Cell 49, 539-548.

Lewis, S.A., Tian, G. and Cowan, N.J. (1997). The alpha- and beta-tubulin folding pathways. Trends Cell Biol 7, 479-484.

Liu, C.M. and Meinke, D.W. (1998). The titan mutants of Arabidopsis are disrupted in mitosis and cell cycle control during seed development. Plant J 16, 21-31.

Liu, Y., Kahn, R.A. and Prestegard, J.H. (2009). Structure and membrane interaction of myristoylated ARF1. Structure 17, 79-87.

Lowe, J., Li, H., Downing, K.H. and Nogales, E. (2001). Refined structure of alpha beta-tubulin at 3.5 A resolution. J Mol Biol 313, 1045-1057.

McElver, J., Patton, D., Rumbaugh, M., Liu, C., Yang, L.J. and Meinke, D. (2000). The TITAN5 gene of Arabidopsis encodes a protein related to the ADP ribosylation factor family of GTP binding proteins. Plant Cell 12, 1379-1392.

Miyake, N., Fukai, R., Ohba, C., Chihara, T., Miura, M., Shimizu, H., Kakita, A., Imagawa, E., Shiina, M., Ogata, K., Okuno-Yuguchi, J., Fueki, N., Ogiso, Y., Suzumura, H., Watabe, Y., Imataka, G., Leong, H.Y., Fattal-Valevski, A., Kramer, U., Miyatake, S., Kato, M., Okamoto, N., Sato, Y., Mitsuhashi, S., Nishino, I., Kaneko, N., Nishiyama, A., Tamura, T., Mizuguchi, T., Nakashima, M., Tanaka, F., Saitsu, H. and Matsumoto, N. (2016). Biallelic TBCD Mutations Cause Early-Onset Neurodegenerative Encephalopathy. Am J Hum Genet 99, 950-961.

Mizuno-Yamasaki, E., Rivera-Molina, F. and Novick, P. (2012). GTPase networks in membrane traffic. Annu Rev Biochem 81, 637-659.

Nassar, N., Singh, K. and Garcia-Diaz, M. (2010). Structure of the dominant negative S17N mutant of Ras. Biochemistry 49, 1970-1974.

Nawrotek, A., Knossow, M. and Gigant, B. (2011). The determinants that govern microtubule assembly from the atomic structure of GTP-tubulin. J Mol Biol 412, 35-42.

Newman, L.E., Schiavon, C.R., Zhou, C. and Kahn, R.A. (2017). The abundance of the ARL2 GTPase and its GAP, ELMOD2, at mitochondria are modulated by the fusogenic activity of mitofusins and stressors. PLoS One 12, e0175164.

Newman, L.E., Zhou, C.J., Mudigonda, S., Mattheyses, A.L., Paradies, E., Marobbio, C.M. and Kahn, R.A. (2014). The ARL2 GTPase is required for mitochondrial morphology, motility, and maintenance of ATP levels. PLoS One 9, e99270.

Nishi, H., Ono, K., Iwanaga, Y., Horie, T., Nagao, K., Takemura, G., Kinoshita, M., Kuwabara, Y., Mori, R.T., Hasegawa, K., Kita, T. and Kimura, T. (2010). MicroRNA-15b modulates

cellular ATP levels and degenerates mitochondria via Arl2 in neonatal rat cardiac myocytes. J Biol Chem 285, 4920-4930.

Nithianantham, S., Le, S., Seto, E., Jia, W., Leary, J., Corbett, K.D., Moore, J.K. and Al-Bassam, J. (2015). Tubulin cofactors and Arl2 are cage-like chaperones that regulate the soluble alphabeta-tubulin pool for microtubule dynamics. Elife 4.

Okumura, M., Sakuma, C., Miura, M. and Chihara, T. (2015). Linking cell surface receptors to microtubules: tubulin folding cofactor D mediates Dscam functions during neuronal morphogenesis. J Neurosci 35, 1979-1990.

Pascal, B.D., Willis, S., Lauer, J.L., Landgraf, R.R., West, G.M., Marciano, D., Novick, S., Goswami, D., Chalmers, M.J. and Griffin, P.R. (2012). HDX workbench: software for the analysis of H/D exchange MS data. J Am Soc Mass Spectrom 23, 1512-1521.

Pode-Shakked, B., Barash, H., Ziv, L., Gripp, K.W., Flex, E., Barel, O., Carvalho, K.S., Scavina, M., Chillemi, G., Niceta, M., Eyal, E., Kol, N., Ben-Zeev, B., Bar-Yosef, O., Marek-Yagel, D., Bertini, E., Duker, A.L., Anikster, Y., Tartaglia, M. and Raas-Rothschild, A. (2016). Microcephaly, intractable seizures and developmental delay caused by biallelic variants in TBCD: Further delineation of a new chaperone-mediated tubulinopathy. Clin Genet.

Price, H.P., Peltan, A., Stark, M. and Smith, D.F. (2010). The small GTPase ARL2 is required for cytokinesis in Trypanosoma brucei. Mol Biochem Parasitol 173, 123-131.

Radcliffe, P.A., Hirata, D., Vardy, L. and Toda, T. (1999). Functional dissection and hierarchy of tubulin-folding cofactor homologues in fission yeast. Mol Biol Cell 10, 2987-3001.

Randazzo, P.A. and Kahn, R.A. (1995). Myristoylation and ADP-ribosylation factor function. Methods Enzymol 250, 394-405.

Saraste, M., Sibbald, P.R. and Wittinghofer, A. (1990). The P-loop--a common motif in ATP- and GTP-binding proteins. Trends Biochem Sci 15, 430-434.

Sharer, J.D., Shern, J.F., Van Valkenburgh, H., Wallace, D.C. and Kahn, R.A. (2002). ARL2 and BART enter mitochondria and bind the adenine nucleotide transporter. Mol Biol Cell 13, 71-83.

Shern, J.F., Sharer, J.D., Pallas, D.C., Bartolini, F., Cowan, N.J., Reed, M.S., Pohl, J. and Kahn, R.A. (2003). Cytosolic Arl2 is complexed with cofactor D and protein phosphatase 2A. J Biol Chem 278, 40829-40836.

Shultz, T., Shmuel, M., Hyman, T. and Altschuler, Y. (2008). Beta-tubulin cofactor D and ARL2 take part in apical junctional complex disassembly and abrogate epithelial structure. FASEB J 22, 168-182.

Spiess, C., Meyer, A.S., Reissmann, S. and Frydman, J. (2004). Mechanism of the eukaryotic chaperonin: protein folding in the chamber of secrets. Trends Cell Biol 14, 598-604.

Stearns, T., Hoyt, M.A. and Botstein, D. (1990). Yeast mutants sensitive to antimicrotubule drugs define three genes that affect microtubule function. Genetics 124, 251-262.

Szul, T., Garcia-Mata, R., Brandon, E., Shestopal, S., Alvarez, C. and Sztul, E. (2005). Dissection of membrane dynamics of the ARF-guanine nucleotide exchange factor GBF1. Traffic 6, 374-385.

Tamkun, J.W., Kahn, R.A., Kissinger, M., Brizuela, B.J., Rulka, C., Scott, M.P. and Kennison, J.A. (1991). The arflike gene encodes an essential GTP-binding protein in Drosophila. Proc Natl Acad Sci U S A 88, 3120-3124.

Tian, G., Bhamidipati, A., Cowan, N.J. and Lewis, S.A. (1999). Tubulin folding cofactors as GTPase-activating proteins. GTP hydrolysis and the assembly of the alpha/beta-tubulin heterodimer. J Biol Chem 274, 24054-24058.

Tian, G. and Cowan, N.J. (2013). Tubulin-specific chaperones: components of a molecular machine that assembles the alpha/beta heterodimer. Methods Cell Biol 115, 155-171.

Tian, G., Huang, Y., Rommelaere, H., Vandekerckhove, J., Ampe, C. and Cowan, N.J. (1996). Pathway leading to correctly folded beta-tubulin. Cell 86, 287-296.

Tian, G., Lewis, S.A., Feierbach, B., Stearns, T., Rommelaere, H., Ampe, C. and Cowan, N.J. (1997). Tubulin subunits exist in an activated conformational state generated and maintained by protein cofactors. J Cell Biol 138, 821-832.

Tian, G., Thomas, S. and Cowan, N.J. (2010). Effect of TBCD and its regulatory interactor Arl2 on tubulin and microtubule integrity. Cytoskeleton (Hoboken) 67, 706-714.

Vainberg, I.E., Lewis, S.A., Rommelaere, H., Ampe, C., Vandekerckhove, J., Klein, H.L. and Cowan, N.J. (1998). Prefoldin, a chaperone that delivers unfolded proteins to cytosolic chaperonin. Cell 93, 863-873.

Veltel, S., Kravchenko, A., Ismail, S. and Wittinghofer, A. (2008). Specificity of Arl2/Arl3 signaling is mediated by a ternary Arl3-effector-GAP complex. FEBS Lett 582, 2501-2507.

Wittinghofer, A. and Vetter, I.R. (2011). Structure-function relationships of the G domain, a canonical switch motif. Annu Rev Biochem 80, 943-971.

Zhang, T., Li, S., Zhang, Y., Zhong, C., Lai, Z. and Ding, J. (2009). Crystal structure of the ARL2-GTP-BART complex reveals a novel recognition and binding mode of small GTPase with effector. Structure 17, 602-610.

Zhou, C., Cunningham, L., Marcus, A.I., Li, Y. and Kahn, R.A. (2006). Arl2 and Arl3 regulate different microtubule-dependent processes. Mol Biol Cell 17, 2476-2487.

# CHAPTER 4

## Discussion

**Summary**

The molecular mechanisms underlying tubulin folding and assembly of the αβ-tubulin heterodimer are a key aspect of microtubule/tubulin biology that is incompletely understood. Much of our current understanding stems from the pioneering work of Cowan and colleagues, who first purified the tubulin-specific chaperones and described their role in transitioning nascent α- and β-tubulin polypeptides into native, polymerization-competent tubulin dimers (Figure1-1). Of particular importance to this dissertation are the purported roles of TBCD and ARL2 as they pertain to tubulin folding, as well as other aspects of microtubule regulation. In addition to the folding of β-tubulin and assembly of the αβ-dimer, Cowan proposes that TBCD can act to reverse dimer formation by interacting with, and dissociating, αβ-tubulin (Bhamidipati et al., 2000). This is referred to as the back-reaction, which leads to the loss of polymerized microtubules and is proposed to be part of a tubulin destruction pathway. According to Cowan's model, the primary function of ARL2 is to inhibit TBCD interaction with αβ-tubulin, preventing dimer dissociation and eventual loss of microtubules. However, the work described herein provides some of the first direct challenges to the Cowan model, which has been the cornerstone of our understanding of tubulin folding for close to twenty years. The previous chapters describe the purification and biochemical characterization of novel TBCD/ARL2 complexes, which provide insights into the molecular mechanisms underlying tubulin folding and the importance of TBCD/ARL2 interaction in regulating microtubule dynamics. Thus, a close re-examination of the available information is necessary in order to advance the existing models in context of our recent work. As a result, our findings suggest a direct role for ARL2 in the tubulin folding pathway, and argue that the cycling and hydrolysis of guanine nucleotide on TBCD-bound ARL2 is critical for the proper regulation of microtubules.

**Challenging the Status Quo**

The rigorous study of TBCD has largely been limited by the inability to express and purify a soluble, active preparation. In Chapter 2, I described the use of HEK cells as a mammalian expression system as a means of purifying soluble, stable TBCD complexes; notably, the TBCD/ARL2/β-tubulin trimer. The quaternary states of TBCD and ARL2 were also examined in several different mammalian cell lines and tissues and were both found to predominantly exist as ~200 kDa species, consistent with the size of the TBCD/ARL2/β-tubulin trimer (208 kDa). The purification of this stable, trimeric complex directly challenges one key aspect of the Cowan model: that ARL2 and β-tubulin compete for binding to TBCD. The use of the co-purification of TBCD/ARL2/β-tubulin complexes in a novel "relative binding assay" was also explained in Chapter 2 as a means to identify ARL2 mutants with decreased affinity for TBCD. Combining these mutants with the dominant-active ARL2[Q70L], which prevents GTP hydrolysis, allowed us to show a strong correlation between interaction with TBCD and integrity of the microtubule network. The interesting point here is that not only do these data suggest a requirement for ARL2/TBCD interaction in regulating microtubules but also that the hydrolysis of guanine nucleotide on ARL2 is specifically important to this mechanism, consistent with ARL2 acting as a canonical regulatory GTPase. This conclusion is further strengthened by the observation that expression of the dominant-inactive ARL2[T30N] results in the same microtubule loss phenotype caused by ARL2[Q70L] expression, indicating that the cycling, and not just hydrolysis, of nucleotide on ARL2 (while bound to TBCD) is also essential for proper microtubule stability. Taken together, these findings point toward a more direct and active role for ARL2 in the regulation of microtubule/tubulin dynamics.

In Chapter 3, I describe the characterization of the nucleotide-binding properties of the TBCD/ARL2/β-tubulin complex, which are quite distinct from both the ARL2 monomer and other ARL2 complexes. As compared to ARL2 monomer, the TBCD/ARL2/β-tubulin trimer has higher apparent affinities for both GDP and GTP, with a faster off-rate for GDP and faster on-rates for

both nucleotides. These data suggest that TBCD is not acting as an ARL2 effector, as interactions between GTPases and effectors are typically GTP-dependent. The nucleotide-binding properties of the trimer also differ greatly from a previously purified TBCD/ARL2 complex, which was isolated from bovine tissues using several chromatographic steps (Shern et al., 2003). The bovine-derived complex also co-purified with protein phosphatase 2A (PP2A) subunits, though this is now believed to have been coincidental as there has been no further evidence of any interaction among these proteins. The purified TBCD/ARL2 dimer was able to bind GDP indistinguishably from ARL2 monomer, but was incapable of binding GTP. While also considering that almost all cytosolic ARL2 is found in a complex with TBCD, these data led to the early hypothesis that TBCD served as a depot for inactive, cytosolic ARL2 and the release of the GTPase from TBCD was required for it to become activated (*i.e.*, bind GTP) and perform its many cellular functions. However, the more recently purified TBCD/ARL2/β-tubulin trimer very readily binds GTP. Furthermore, HDX analyses (described in Chapter 3) confirm that it is ARL2, and not β-tubulin, that is binding nucleotide in our *in vitro* binding assays. Thus, ARL2 is capable of becoming activated (in the canonical GTPase sense) while bound to TBCD, though association with β-tubulin is perhaps required for this activity. These data also suggest a potential GEF-like role for β-tubulin in the trimer, in that it seems required for ARL2 to bind GTP and also increases the rate at which nucleotide dissociates from ARL2 in the complex. However, this would be an atypical GEF as the binding of GTP does not cause β-tubulin to be released from the complex; hence, GEF-like activity.

In light of the work detailed in the previous chapters, and in context of all other available data, a new model is proposed here describing an integral role for ARL2 in the cofactor-mediated tubulin folding and αβ-tubulin dimer assembly pathway (Figure 4-1). As opposed to a linear pathway, this model portrays tubulin assembly as a cycle that is regulated by the exchange and hydrolysis of guanine nucleotides on ARL2. First, β-tubulin polypeptides are transferred from TBCA to generate TBCD/ARL2-GDP. Interaction with β-tubulin facilitates the exchange of GTP for ARL2-bound GDP. The binding of GTP also causes a conformational shift in the complex that

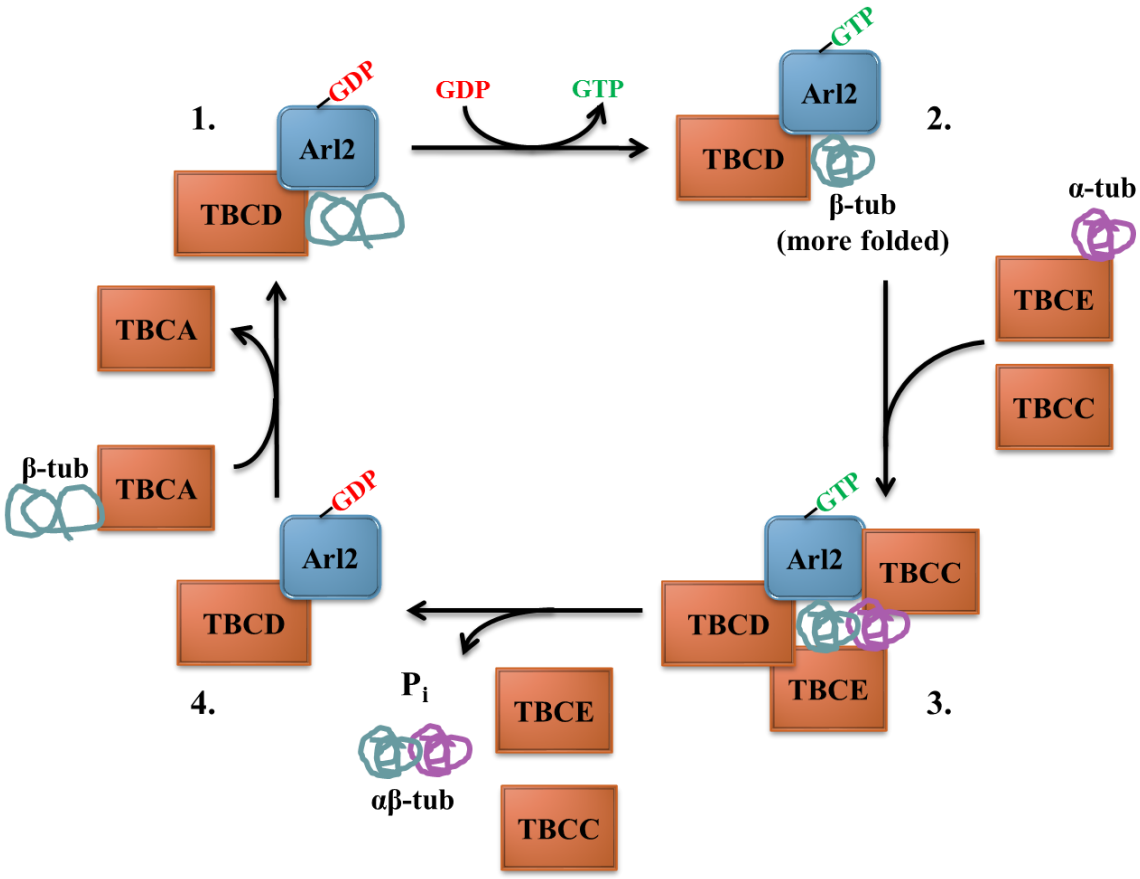


**Figure 4-1. A novel role for ARL2 in the cofactor-mediated tubulin folding and αβ-tubulin heterodimer assembly pathway.** ARL2 is proposed to play an integral role in regulating the folding and production of native tubulin dimers. **1.** Partially folded β-tubulin polypeptides are transferred from TBCA to a complex of TBCD/ARL2-GDP. **2.** The binding of β-tubulin promotes exchange of GTP for bound GDP on ARL2, which in turn facilitates the progression of β-tubulin to a more folded state. **3.** Association of TBCE/α-tubulin and TBCC brings the tubulin subunits together and results in formation of the cofactor supercomplex. **4.** TBCC-stimulated GTP hydrolysis on ARL2 causes dissociation of TBCE and TBCC and production of the native αβ-tubulin heterodimer. The TBCD/ARL2-GDP complex remains intact and ready to accept another β-tubulin polypeptide for continuation through the folding cycle.

results in the progression of β-tubulin to a more folded tertiary structure. Next, the tubulin subunits are brought together by association of TBCE/α-tubulin, and the subsequent binding of TBCC results in formation of the ultimate cofactor supercomplex (analogous to Cowan's model). TBCC then stimulates GTP hydrolysis by ARL2, resulting in the release of TBCE and TBCC and the production of native αβ-tubulin heterodimer. TBCD/ARL2-GDP remains intact and is poised to cycle back through the pathway by accepting another β-tubulin polypeptide. This model accounts for much of the seemingly disparate data concerning TBCD and ARL2 activities. It accounts for the purification of a TBCD/ARL2 dimer that is incapable of binding GTP. It incorporates the distinct nucleotide-binding properties of the TBCD/ARL2/β-tubulin complex, as well as the HDX data indicating nucleotide-dependent changes in β-tubulin folding/stability (Chapter 3). The model also provides an explanation for why expression of either ARL2[Q70L] or ARL2[T30N] leads to the loss of polymerized microtubules; *i.e.*, preventing the exchange or hydrolysis of nucleotide on ARL2 in this pathway would stop progression of the cycle and halt the production of αβ-tubulin. With limited availability of polymerization-competent tubulin, the process of dynamic instability dictates that microtubules would ultimately shift toward states of depolymerization. The current model also has overlapping characteristics with another recently proposed model describing a more essential role for ARL2 in the cofactor-mediated regulation of tubulin (Nithianantham et al., 2015). This study used yeast orthologs expressed in bacteria to form a different, stable trimer, TBCD/TBCE/ARL2, which was argued to be the basal complex upon which tubulin subunits are assembled and αβ-tubulin dimers produced. However, there have been functional differences described between even the human and bovine orthologs of TBCD (Cunningham and Kahn, 2008; Tian et al., 2010), therefore I speculate that yeast and mammalian orthologs will likely exhibit differences in the pathway of tubulin dimer biogenesis. However, the differences between these two models are difficult to interpret without more information.

While the current model attempts to consolidate much of our understanding of TBCD and ARL2 biologies, there are still some apparent shortcomings with regards to other known activities

of these proteins. For example, the proposed model does not include the incompletely understood centrosomal activities of TBCD and ARL2. Both proteins localize to centrosomes, and have been shown to influence centrosomal dynamics (Zhou et al., 2006; Cunningham and Kahn, 2008). TBCD is also involved in the recruitment of centrosomal proteins, such as the γ-tubulin ring complex (Cunningham and Kahn, 2008), and has been proposed to function as a scaffold at the basal bodies of cilia (Fanarraga et al., 2010). There are also data that appear to be inconsistent with a role for TBCD in production of folded αβ-tubulin. For example, the overexpression of TBCD causes loss of polymerized microtubules (Bhamidipati et al., 2000; Tian et al., 2010), seeming to suggest a role for TBCD in either inhibiting microtubule polymerization or promoting depolymerization. Further evidence of this putative anti-microtubule activity is shown in studies of TBCD mutations found in human patients (Flex et al., 2016). The patient-derived TBCD mutants were used in our HEK cell expression system to determine their effect on formation of the TBCD/ARL2/β-tubulin complex. A select few of the mutations caused either reduced TBCD expression levels (*i.e.*, reduced protein stability) or decreased co-purification with β-tubulin (while ARL2 co-purified to normal levels). These same mutations led to increased rates of aster formation in nocodazole washout assays using patient-derived primary fibroblasts. These results suggest a correlation between reduced TBCD expression levels, or reduced interaction with β-tubulin, and increased rates of microtubule polymerization, which seems to indicate an inhibitory role for TBCD in microtubule polymerization. An alternative interpretation, and one that perhaps fits with the current model, is that the release of β-tubulin from TBCD is the rate-limiting step in production of native αβ-tubulin dimers, and that decreasing the affinity between TBCD and β-tubulin results in an increase in the rate at which tubulin dimers can be generated. It is our hope that, as understanding of TBCD and ARL2 activities becomes more complete, the current model can continue to be challenged and evolved to eventually encompass all aspects of microtubule-related processes.

**Future Directions**

The *in vitro* reconstitution of the complete tubulin folding pathway is a long-term goal that would allow the detailed dissection of each step of the process and a better understanding of the individual roles of each component involved in αβ-tubulin production. This knowledge would also likely give insight into the molecular basis underlying many diseases associated with mutations in the tubulin-specific chaperones. Additionally, the capability to produce isotype-specific tubulin, with the potential to control the incorporation of PTMs, would be an invaluable asset to understanding and "cracking" the tubulin code. Therefore, the future directions discussed here will focus on using the tools and information generated throughout the course of this project to further our knowledge of the molecular mechanisms of tubulin folding, as well as the involvement of TBCD and ARL2 in other microtubule-related functions.

Several recent studies have identified mutations in TBCD that lead to a host of neurological defects (Edvardson et al., 2016; Flex et al., 2016; Ikeda et al., 2016; Miyake et al., 2016; Pode-Shakked et al., 2017). A subset of these mutations have been tested in their capacity to form the TBCD/ARL2/β-tubulin complex using our recombinant HEK cell expression system, including the few published examples that resulted from collaboration (Flex et al., 2016). Thus far, 7 out of the 16 total mutations have been analyzed in this way (Figure 4-2). Some of the mutations, such as T374M, R377Q and T994M, show reduced co-purification with β-tubulin. Others, such as V1105M and P1122L, cause decreased expression levels of TBCD. As discussed previously, some of these mutations also cause changes in the rates of microtubule polymerization (Flex et al., 2016). An obvious, but likely fruitful, continuation to this line of study would be the complete analysis of all patient-derived TBCD mutations. It would be of particular interest to find a TBCD mutation that disrupted interaction with ARL2, as this would allow us to better understand the importance of the interaction between TBCD and ARL2 in regulating microtubule- and tubulin-related processes.

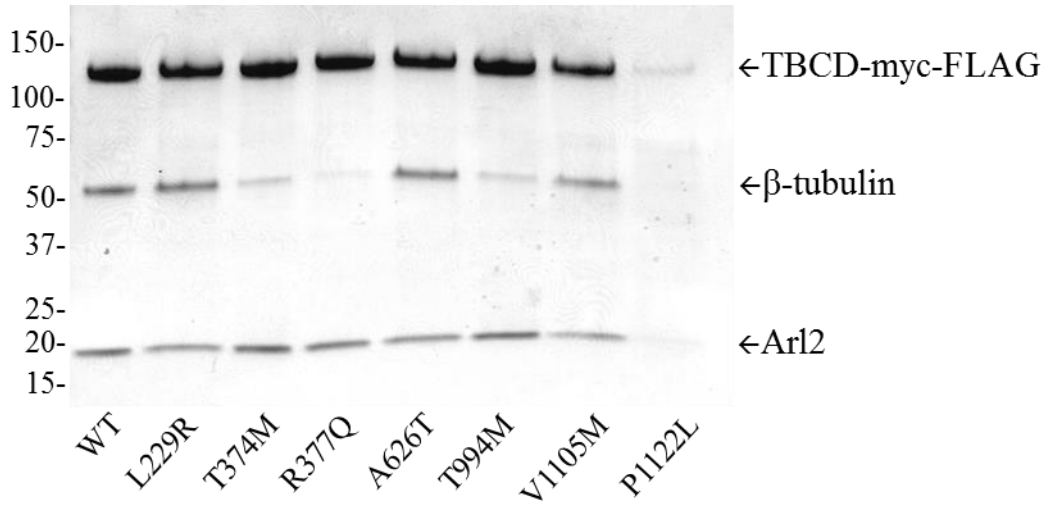


**Figure 4-2. Patient-derived TBCD mutations affect expression levels and interaction with β-tubulin.** HEK cells were co-transfected with plasmids directing expression of ARL2 and TBCD-myc-FLAG constructs with the indicated point mutation. After 2 days, FLAG affinity resin was used to affinity-purify the TBCD-myc-FLAG and associated proteins. Purified proteins (3 μg/lane) were analyzed by SDS-PAGE with Coomassie Blue staining.

Another key outstanding question is in regards to the activities of TBCD and ARL2 at centrosomes; specifically, do these proteins directly interact at centrosomes in order to regulate centrosomal dynamics? While it is known that both proteins localize to centrosomes and have very similar centrosomal phenotypes (Zhou et al., 2006; Cunningham and Kahn, 2008), there is still no direct evidence that TBCD and ARL2 physically interact at this cellular location. One way in which this could be tested is through utilizing the ARL2 mutants that have decreased affinity for TBCD (described in Chapter 2), as well as any TBCD mutants that are identified in the investigations described above. Another, perhaps simpler, approach would be to use the centrosome localization domains (CLDs) of TBCD that have been previously identified (Cunningham and Kahn, 2008). These CLDs were described as the minimal regions of TBCD that localize to centrosomes. Expression of these CLDs in cells resulted in a dominant effect, whereby the CLDs displace the endogenous TBCD at centrosomes. However, with only these minimal regions present, the TBCD fragments were unable to interact with any binding partners, which led to the results that TBCD is responsible for recruiting a variety of centrosomal proteins. In this way, this approach could also be used to determine if TBCD recruits ARL2 to centrosomes.

It has been proposed that unfolded tubulin subunits have a mature nucleotide-binding pocket as early as their interaction with the cytosolic chaperonin, CCT. This is largely presumed for β-tubulin and has only been specifically shown for α-tubulin, which irreversibly binds GTP throughout the folding process (Tian et al., 1995). In the purified TBCD/ARL2/β-tubulin trimer, nucleotide binding and HDX data indicate that only ARL2 is interacting with nucleotide in the *in vitro* binding assays. However, these data do not rule out the possibility that β-tubulin is co-purifying with GTP already bound in an irreversible fashion. Though this would be somewhat surprising based on the characterization of β-tubulin as the E-site in the tubulin dimer, which freely exchanges nucleotide. Regardless, some very preliminary data using HPLC analysis of the TBCD/ARL2/β-tubulin complex suggests that the timer is purifying with a mixture of GDP and GTP at a stoichiometry of 20-50%. These experiments need to be repeated, and it needs to be

determined whether the nucleotide is bound to ARL2 and/or β-tubulin. This could be accomplished through use of the dominant-inactive ARL2[T30N], which has a reduced affinity for guanine nucleotides (Hanzal-Bayer et al., 2005). If the β-tubulin in the trimer proves to purify with bound nucleotide(s), it would certainly alter the current interpretation of the data and prompt changes to the model. Specifically, we would need to further examine the role of GTP hydrolysis in tubulin dimer formation and determine if hydrolysis of ARL2-bound GTP is, in fact, regulating production of native αβ-tubulin, as suggested by my current model.

Even before the discovery of the tubulin-specific chaperones, it was shown that GTP hydrolysis is required for tubulin dimer formation (Fontalba et al., 1993). Cowan's work suggests that it is specifically the TBCC-induced hydrolysis of GTP on β-tubulin that is the rate-limiting step in cofactor release and αβ-tubulin dimer production (Tian et al., 1999). More recent studies propose that ARL2 is the actual target of TBCC GAP activity (Mori and Toda, 2013; Nithianantham et al., 2015). However, one of these studies does not actually perform any GAP assays, using only genetic analyses to draw conclusions (Mori and Toda, 2013), and the other study shows only very moderate increases in TBCC-stimulated rates of GTP hydrolysis (Nithianantham et al., 2015). Therefore, it would be a simple matter to utilize the novel TBCD/ARL2 complexes described in Chapter 2 (*i.e.*, TBCD/ARL2/β-tubulin and TBCD/TBCE/ARL2/β-tubulin) to determine the specific substrate for TBCC GAP activity. If, in fact, β-tubulin is co-purifying with GTP bound, it could also be determined if TBCC is stimulating GTP hydrolysis on ARL2 and/or β-tubulin.

**Concluding Remarks**

The long-term goal of this project is to understand the mechanism(s) by which ARL2 and TBCD function together to regulate tubulin- and microtubule-dependent processes. Gaining further insight into these activities will not only deepen our understanding of these basic cellular processes, but will undoubtedly provide tools for translational studies and the development of better

therapeutics. This effort also supports the larger goal of the lab, which is to ultimately understand how ARL2 regulates such a wide variety of essential cellular processes and how these processes are interconnected. The integral role of ARL2 in diverse cellular pathways positions the GTPase as a nexus for higher order signaling, providing a point at which inter-regulation of different cellular processes can occur. Although still lacking some key insight that would enable us to grasp how ARL2 functions in this capacity, the recent and ongoing work in the lab is continuing to advance our understanding and will eventually allow us to unravel this mystery.

**References**

Bhamidipati, A., Lewis, S.A. and Cowan, N.J. (2000). ADP ribosylation factor-like protein 2 (Arl2) regulates the interaction of tubulin-folding cofactor D with native tubulin. J Cell Biol 149, 1087-1096.

Cunningham, L.A. and Kahn, R.A. (2008). Cofactor D functions as a centrosomal protein and is required for the recruitment of the gamma-tubulin ring complex at centrosomes and organization of the mitotic spindle. J Biol Chem 283, 7155-7165.

Edvardson, S., Tian, G., Cullen, H., Vanyai, H., Ngo, L., Bhat, S., Aran, A., Daana, M., Da'amseh, N., Abu-Libdeh, B., Cowan, N.J., Heng, J.I. and Elpeleg, O. (2016). Infantile neurodegenerative disorder associated with mutations in TBCD, an essential gene in the tubulin heterodimer assembly pathway. Hum Mol Genet 25, 4635-4648.

Fanarraga, M.L., Bellido, J., Jaen, C., Villegas, J.C. and Zabala, J.C. (2010). TBCD links centriologenesis, spindle microtubule dynamics, and midbody abscission in human cells. PLoS One 5, e8846.

Flex, E., Niceta, M., Cecchetti, S., Thiffault, I., Au, M.G., Capuano, A., Piermarini, E., Ivanova, A.A., Francis, J.W., Chillemi, G., Chandramouli, B., Carpentieri, G., Haaxma, C.A., Ciolfi, A., Pizzi, S., Douglas, G.V., Levine, K., Sferra, A., Dentici, M.L., Pfundt, R.R., Le Pichon, J.B., Farrow, E., Baas, F., Piemonte, F., Dallapiccola, B., Graham, J.M., Jr., Saunders, C.J., Bertini, E., Kahn, R.A., Koolen, D.A. and Tartaglia, M. (2016). Biallelic Mutations in TBCD, Encoding the Tubulin Folding Cofactor D, Perturb Microtubule Dynamics and Cause Early-Onset Encephalopathy. Am J Hum Genet 99, 962-973.

Fontalba, A., Paciucci, R., Avila, J. and Zabala, J.C. (1993). Incorporation of tubulin subunits into dimers requires GTP hydrolysis. J Cell Sci 106 ( Pt 2), 627-632.

Hanzal-Bayer, M., Linari, M. and Wittinghofer, A. (2005). Properties of the interaction of Arf-like protein 2 with PDEdelta. J Mol Biol 350, 1074-1082.

Ikeda, T., Nakahara, A., Nagano, R., Utoyama, M., Obara, M., Moritake, H., Uechi, T., Mitsui, J., Ishiura, H., Yoshimura, J., Doi, K., Kenmochi, N., Morishita, S., Nishino, I., Tsuji, S. and Nunoi, H. (2016). TBCD may be a causal gene in progressive neurodegenerative encephalopathy with atypical infantile spinal muscular atrophy. J Hum Genet.

Miyake, N., Fukai, R., Ohba, C., Chihara, T., Miura, M., Shimizu, H., Kakita, A., Imagawa, E., Shiina, M., Ogata, K., Okuno-Yuguchi, J., Fueki, N., Ogiso, Y., Suzumura, H., Watabe, Y., Imataka, G., Leong, H.Y., Fattal-Valevski, A., Kramer, U., Miyatake, S., Kato, M., Okamoto, N., Sato, Y., Mitsuhashi, S., Nishino, I., Kaneko, N., Nishiyama, A., Tamura, T., Mizuguchi, T., Nakashima, M., Tanaka, F., Saitsu, H. and Matsumoto, N. (2016). Biallelic TBCD Mutations Cause Early-Onset Neurodegenerative Encephalopathy. Am J Hum Genet 99, 950-961.

Mori, R. and Toda, T. (2013). The dual role of fission yeast Tbc1/cofactor C orchestrates microtubule homeostasis in tubulin folding and acts as a GAP for GTPase Alp41/Arl2. Mol Biol Cell 24, 1713-1724, S1711-1718.

Nithianantham, S., Le, S., Seto, E., Jia, W., Leary, J., Corbett, K.D., Moore, J.K. and Al-Bassam, J. (2015). Tubulin cofactors and Arl2 are cage-like chaperones that regulate the soluble alphabeta-tubulin pool for microtubule dynamics. Elife 4.

Pode-Shakked, B., Barash, H., Ziv, L., Gripp, K.W., Flex, E., Barel, O., Carvalho, K.S., Scavina, M., Chillemi, G., Niceta, M., Eyal, E., Kol, N., Ben-Zeev, B., Bar-Yosef, O., Marek-Yagel, D., Bertini, E., Duker, A.L., Anikster, Y., Tartaglia, M. and Raas-Rothschild, A. (2017). Microcephaly, intractable seizures and developmental delay caused by biallelic variants in TBCD: further delineation of a new chaperone-mediated tubulinopathy. Clin Genet 91, 725-738.

Shern, J.F., Sharer, J.D., Pallas, D.C., Bartolini, F., Cowan, N.J., Reed, M.S., Pohl, J. and Kahn, R.A. (2003). Cytosolic Arl2 is complexed with cofactor D and protein phosphatase 2A. J Biol Chem 278, 40829-40836.

Tian, G., Bhamidipati, A., Cowan, N.J. and Lewis, S.A. (1999). Tubulin folding cofactors as GTPase-activating proteins. GTP hydrolysis and the assembly of the alpha/beta-tubulin heterodimer. J Biol Chem 274, 24054-24058.

Tian, G., Thomas, S. and Cowan, N.J. (2010). Effect of TBCD and its regulatory interactor Arl2 on tubulin and microtubule integrity. Cytoskeleton (Hoboken) 67, 706-714.

Tian, G., Vainberg, I.E., Tap, W.D., Lewis, S.A. and Cowan, N.J. (1995). Quasi-native chaperonin-bound intermediates in facilitated protein folding. J Biol Chem 270, 23910-23913.

Zhou, C., Cunningham, L., Marcus, A.I., Li, Y. and Kahn, R.A. (2006). Arl2 and Arl3 regulate different microtubule-dependent processes. Mol Biol Cell 17, 2476-2487.